NAS 12-2019
CR-86179

Honeywell

HIGH PRECISION ATTITUDE REFERENCE SYSTEM (HPARS)

FINAL REPORT

HIGH PRECISION ATTITUDE REFERENCE SYSTEM (HPARS)

FINAL REPORT

Submitted to
National Aeronautics and Space Administration
Electronics Research Center
Boston, Massachusetts

HONEYWELL Aerospace Division Minneapolis

Printed in U.S.A.

9 December 1968

HIGH PRECISION ATTITUDE REFERENCE SYSTEM

(HPARS)

FINAL REPORT

STUDY PERFORMED FOR NASA/ERC

CONTRACT NO. NAS 12-2019

Prepared by:

W. B. Fouts
S. G. Hummel
J. Lee
G. Matchett
A. Vilemsons

Approved by:

R. G. Woodle

R. G. Woodle

TABLE OF CONTENTS

REFERENCES

1) Kalman, R. E., "A New Approach to Linear Filtering and Prediction Problems", ASME Transactions, Journal of Basic Engineering, March, 1960.

2) Lee, Robert C. K., Optimal Estimation, Identification and Control, M. I. T. Research Monograph No 28, 1964.

3) LeMay, Dr. Joseph L., "Theory and Applications of Linear Estimation Theory", Preprint No. 3.2-i-65, Instrument Society of America 20th Conference, October, 1965.

4) Paulson, D. C., "SPARS Concept and Equations", Honeywell TM-20959-13, 15 March 1968.

5) Schlee, F. H., et al, "Divergence in the Kalman Filter", AIAA Journal, Vol. 5, No. 6, June, 1967.

6) Second Monthly Progress Report for Dr. Okubo-NASA/ERC, Project HPARS (9-15-68), Honeywell, Inc., Aero Division.

I. INTRODUCTION

The continuing trend toward production of more precise attitude pointing and inertial devices for space applications is beginning to yield devices with accuracy beyond the capability of existing test equipment. Factors which were previously somewhat secondary considerations such as seismic disturbances on the test slabs, and distortion of light waves in air are now primary factors which must be dealt with either actively or passively. The safety pad of test equipment an order ot magnitude better than the device under test has been continually squeezed down. Previously mystic numbers such as .01 arc sec pointing accuracy, are becoming goals.

Honeywell is acutely aware of this trend; and in fact has need today of laboratory test devices with greater accuracy and dynamic range than any available. Nor does it appear that any facilities are being developed either as commercial or laboratory devices to solve the problem of testing future (and some present) precision instruments for space applications.

One approach to this problem is to provide a test base composed of the most accurate inertial equipment available to measure all motions of the test base (including seismic disturbances). On the same test base would be mounted the equipment to be tested. The output of the reference inertial devices would be sent to a computer, the various outputs blended and filtered using extensive calibration data, and finally the unwanted disturbances would be subtracted from the output data of the device under test to provide "true attitude" reference. An extremely stable block between the inertial reference system and the device under test, or an active alignment system is also required of course. In the

case of an active alignment system this error would also be fed to the computer for compensation. Figure 1-1displays this approach.

This report describes and summarizes a four month study, using both hardware and software simulation, of a High Precision Attitude Reference System (HPARS) which could be used as the reference for the test base.

The features of this type of approach for a test facility are shown in Figure 1-2. The objectives of the HPARS study are shown in Figure 1-3.

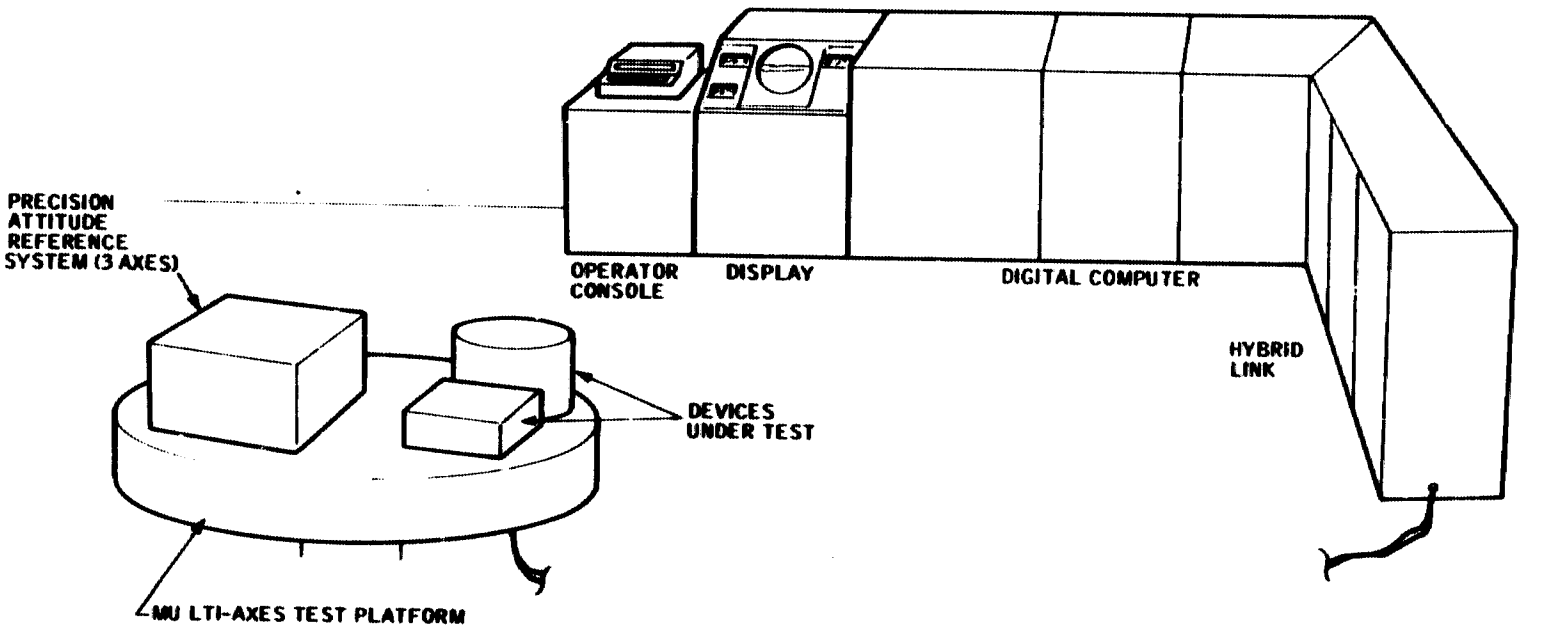

Figure 1-1. HPARS Test Facility Concept

- THE PRECISION ATTITUDE REFERENCE SENSORS MAY BE EASILY UPDATED OR REPLACED AS NEW LABORATORY UNITS BECOME AVAILABLE.
- THE TEST BASE AND COMPUTER WILL INHERENTLY ALLOW FURTHER STUDY OF THE HPARS SENSORS THEMSELVES.
- THE USE OF SCALE MODELING AND DIMENSIONAL ANALYSIS IS PROVIDED TO MOVE AHEAD OF THE STATE-OF-THE-ART DEVICES.
- REAL TIME PARAMETER CHANGES BY THE OPERATOR FOR COMPLETE ANALYSIS IS PROVIDED.

Figure 1-2. HPARS Approach Features

- TO INTEGRATE INDIVIDUAL PRECISION ATTITUDE REFERENCE DEVICES INTO A SINGLE SYSTEM TO STUDY A HIGH PRECISION ATTITUDE REFERENCE SYSTEM (3-AXIS) FOR THE ERC MULTI-AXIS TEST FACILITY

- TO DETERMINE THE PERFORMANCE OF THE HPARS VIA A SOFTWARE SIMULATION

- TO DEMONSTRATE THE PERFORMANCE OF THE HPARS VIA A SINGLE AXIS HARDWARE TEST

- BY VARYING CERTAIN PARAMETERS OF THE ABOVE SYSTEM DETERMINE WHAT THE HARDWARE AND SOFTWARE REQUIREMENTS ARE TO ACHIEVE ACCURACY IN THE .01 TO .1 ARC SEC RANGE AND WHAT THE OPERATIONAL LIMITS ON SUCH A SYSTEM MUST BE.

Figure 1-3. HPARS Study Objectives

II. SUMMARY

The study was very successful in meeting the primary objectives of determining what is achievable with existing hardware and what type of hardware is required for .01 arc sec pointing accuracy. The best that can be done with existing hardware, as described in this report, is approximately .1 arc sec. This is contingent upon updates to further compensate for gyro drift occurring every 10 sec. To achieve a .01 arc sec reference system will require preimarily a SDOF gyro with a noise level near .001°/hr in conjunction with an ESG to provide update information.

The Kalman filter approach proved very successful in compensating for bias drifts of the SDOF gyros. The non-linearities of the hardware, however, modify the "white noise" of the SDOF gyros sufficiently that the Kalman approach cannot compensate for more than 70-90% of the noise generated. In addition, the very low frequency drift of the ESG's selected is not suitable to Kalman filtering. It may be that the filter can be improved slightly by further analysis and reiterations using rms data in lieu of maximum error criteria.

Definite improvement to the system with regards to longer time between updates and holding accuracy for longer periods (such as days) can be made by considering a modified ESG system for update information. With regards to .1 or .01 arc sec the drift of the simulated ESG platforms becomes significant. Also the non-linearities of the gimbal readout system become a problem. A rather simple conceptual ESG system appears feasible which would greatly reduce both of these problems as well as providing a small system physically.

The design of the filter proved to be a formidable task even though the basic concept was pretty well laid out from the SPARS program. The problems came from the need for a very precise system and the interfacing of the specific hardware to the filter, and integrating the entire system. Once completed, however, the total concept proved quite flexible with regards to getting information fast as hardware and filter parameters were modified. With experience even the filter itself can now be readily changed to meet new hardware and new concepts.

Figures 2-1 and 2-2 further summarize some of the system performance.

- ATTITUDE ACCURACY OF .01 SEC APPEARS FEASIBLE WITH AN 18 BIT (.1 SEC) ESG, A GYRO OF .05°/HR DRIFT AND .001°/HR NOISE, AND GYRO UPDATES AT 10 SEC INTERVALS

- PRESENT FILTER CAN CORRECT FOR GYRO DRIFT BUT CANNOT REMOVE ALL OF THE ERROR DUE TO GYRO NOISE.

- AT LOW NOISE LEVELS (.001°/HR) THE ANALOG REBALANCE GYRO IS CONSIDERABLY SUPERIOR TO A PULSE REBALANCE GYRO WITH PULSE WEIGHTS OF .056 SEC/PULSE.

- A HARDWARE TEST WAS SUCCESSFUL IN DEMONSTRATING THE FILTER EFFECT BY BOUNDING THE GG287 GYRO (.3°/HR DRIFT AND .3°/HR NOISE) ERROR TO 1.5 SEC MAXIMUM.

Figure 2-1. Summary

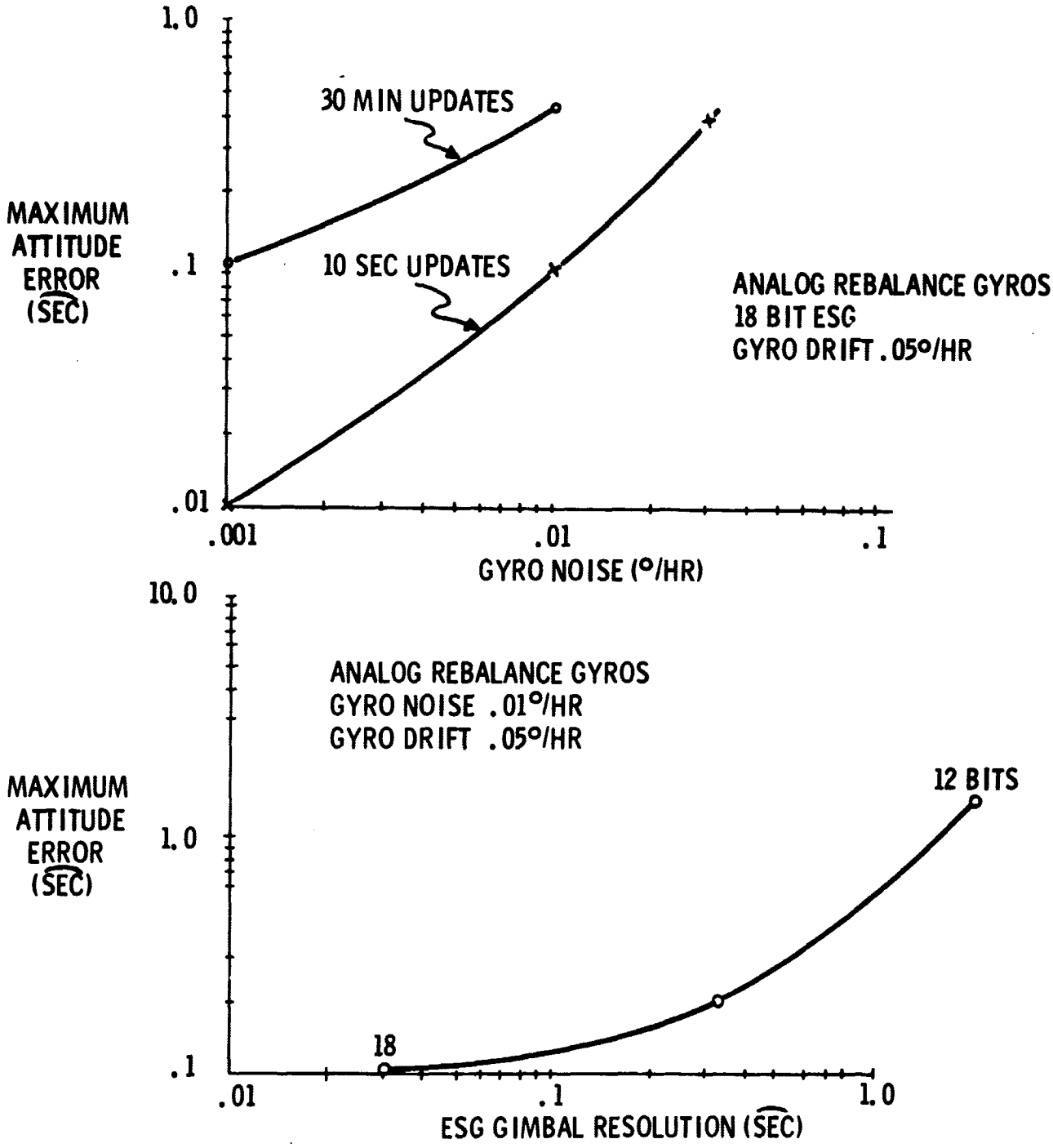

Figure 2-2. HPAR Summary Data

III. PRECISION TEST FACILITY CONCEPT

One approach to the problem of providing a highly accurate test reference with a wide dynamic range, is to utilize a test base composed of the most accurate inertial equipment available to measure all motions of the test base (including seismic disturbances). On the same test base would be mounted the equipment to be tested (Figure 1-1). The outputs of the reference inertial devices would be sent to a computer, the various outputs blended and filtered using extensive calibration data, and finally the unwanted disturbances would be subtracted from the output data of the device under test to provide "true attitude" reference. An extremely stable block between the inertial reference systen and the device under test, or an active alignment system is also required of course. In the case of an active alignment this error would also be fed to the computer for compensation.

Features of this approach are:

- Full advantage of the Laboratory Test Facility concept is utilized by having a flexible, general purpose, large capacity digital computer in the loop. The computer functions as a flexible recursive Kalman Filter to provide:
  a) Matching of the filter to the precision attitude reference system and the equipment under test.
  b) Real time parameter change by the operator for a complete analysis of the system under test.
  c) Extensive utilization of instrument calibration data.

  This results not only in a very flexible system but accuracy one or two orders of magnitude better than could be obtained with an analog

system or a small specially built digital computer located on the test platform.

- Any of the precision devices used for the test reference can be easily exchanged or updated as better devices become available through space program development.

More specifically the approach consists of three devices, each unique in its own function, operating as a system to provide a wide dynamic range precision attitude reference (figure 3-1).

These devices are:

(A) An inertial device to provide continuous three axes rate and attitude information over a wide dynamic range.

(B) A precision reference, generally of low dynamic range to provide update information to item (A) at selected time intervals (thus compensating for drift).

(C) A filter to blend the outputs of (A) and (B) and further remove noise and drift from the system. The filter function is provided by the digital computer which also allows operator interface with the reference system and test device and processes and compares the test device data with the attitude reference.

This concept approach has proved successful on the Honeywell SPARS program which is designed to provide precision attitude reference for a spacecraft.

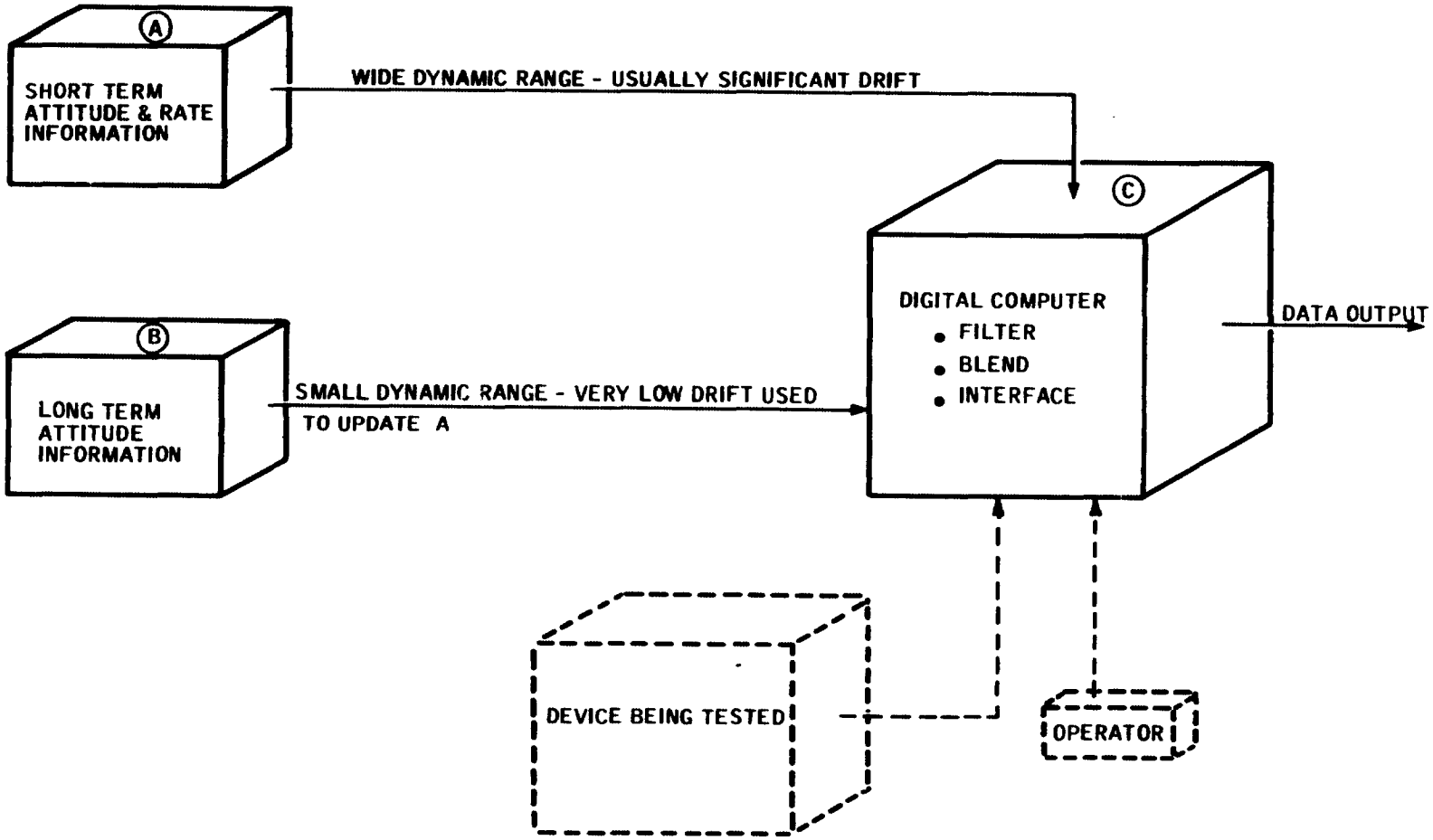

Figure 3-1. HPARS Approach

IV. DEVELOPMENT OF HPARS

A. Requirements

The basic requirements which led to the development of HPARS are shown in Figure 4-1. The requirements are of course not firm but rather are intended to serve as bounds on the study and as a guide toward yielding results which are applicable to a realistic test situation sufficient to cover several different types of development equipment.

The rate capability of HPARS was not investigated sufficiently to define the required gain changes and accuracy degradation due to large input rates. The performance figures given in the report are for rates of less than .1 rad/sec due to the increased computation time required at larger rate inputs.

B. Use of Existing Programs

Four existing Honeywell programs were used to meet the objectives and requirements of the HPARS study. Each program was unique in itself with regards to one or more of the HPARS requirements. Of particular importance was the fact that each of the basic math models selected (with the exception of the Laser Gyro) were proven against hardware test results. The task at hand was to modify the programs and blend them together into a single system and in such a way as to yield data toward the study objectives. (fig. 4-1A)

The SPARS program provided the basic filter technique desired. Modifications were required to achieve the desired accuracy and perform the blending of the gyro programs into an integrated system.

- BASIC APPROACH SHOULD BE SUFFICIENTLY BROAD AND FLEXIBLE THAT IT WOULD NOT BECOME OBSOLETE WITHIN THE NEXT 10 YEARS
- CAPABLE OF ANGULAR RATES UP TO 10 RAD/SEC
- ALL ATTITUDE CAPABILITY
- ATTITUDE ACCURACY APPROACHING .01 ARC SECONDS
- PRECISE ATTITUDE ACCURACY NOT REQUIRED DURING MANEUVERS BUT ATTITUDE INFORMATION MUST NOT BE LOST DURING MANEUVERS
- SYSTEM BANDWIDTH TO 25 Hz FOR SHORT PERIODS

Figure 4-1. Requirements for HPARS

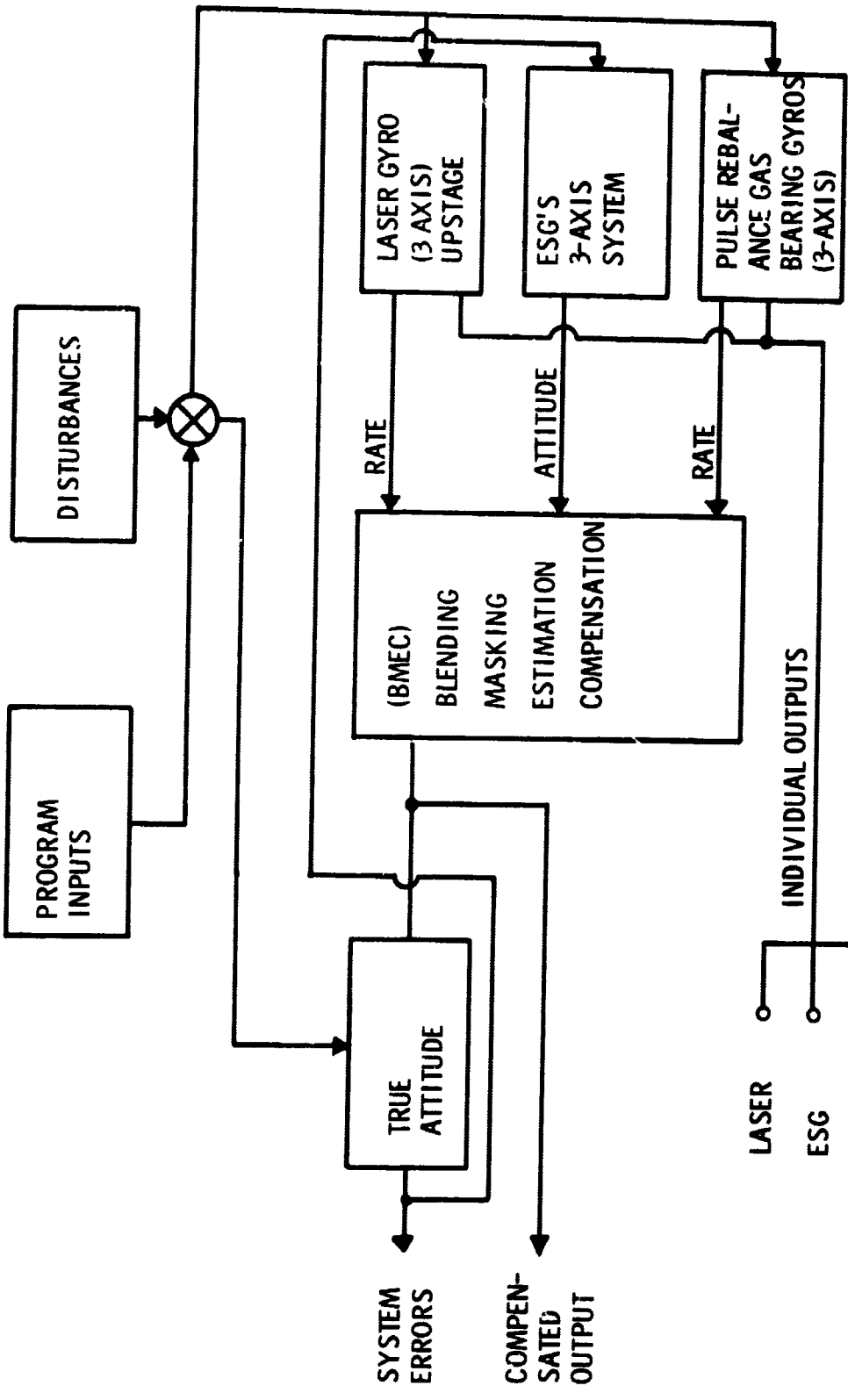

Figure 4-1(a). SDS 9300 HPARS Simulation

The platforms were selected due to their very low drift to provide attitude update information at selected intervals. Modifications here were to convert two, two-axes platform models into one tnree-axes platform.

A general LASER gyro program was modified to fit the Honeywell GG1300 laser thus providing high rate information and additional attitude information. Any benefit of the LASER (for other than high rate information) was also to be investigated.

The continuous attitude and rate (low rate) information for HPARS was supplied by a Honeywell precision STRAPPED DOWN GYRO using a pulse rebalance loop to provide pulse on demand torquing. The resultant rate output was integrated to provide attitude information.

All four computer simulations were set up for three axes. The hardware test was performed single axis.

C. Description of Gyro Packages

Precision Strapped Down Gyros

A pulse rebalance gyro is a gyro with a torquer on one end to reset the gyro to null when an angular rate input is applied. In the pulse rebalance gyro (PRG) the torquer is driven with a pulse train as opposed to the continuous signal of an analog rebalance gyro. In the PRG analyzed (Figure 4-2), a ternary pulse logic was used; i.e., the torquer could be excited with either positive, negative or zero pulses. When the output of the reset integrator (x_2) exceeds

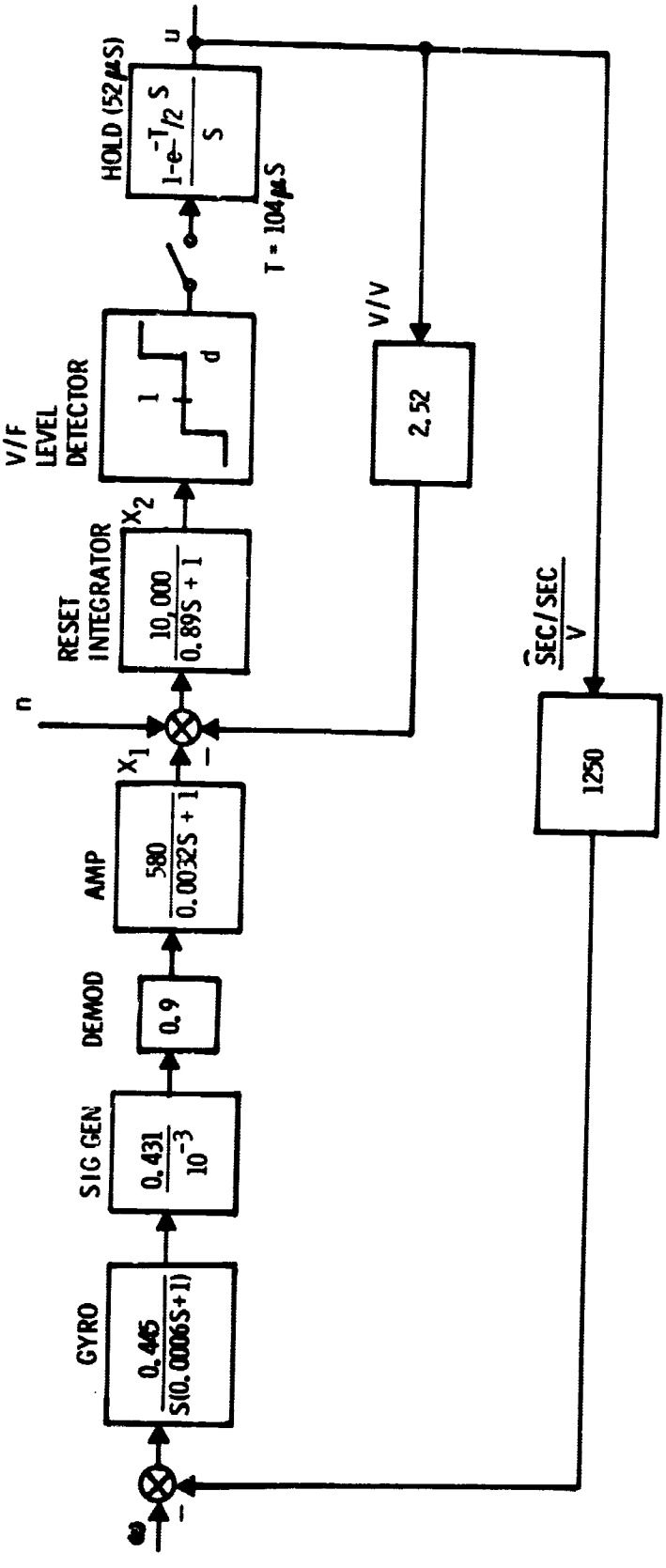

Figure 4-2. Non Linear Sample Data Model of PRG

the deadband (d), a pulse train (u(t)) is generated. The pulse train which has a maximum duty cycle of 50 percent (the hold is 1/2 the sample period), is fed back to zero the reset integrator and rebalance the gyro. Each output pulse is equivalent to an input of 0.056 sec. The output pulses are counted for 0.1 second to compute rate. Typical values are:

Output Scale Factor	0.056 sec/pulse
Output sample time	0.1 (to 0.02) sec
Input angular rate	0-540 sec/sec
Input frequency	0-500 cps
Maximum output pulse rate	9600 pulse/sec
Sample period T (frequency)	104 us (9600 cps)
Pulse Amplitude (u)	+1 0 -1
Deadband of level detector	±1 volt

This model (Figure 43) of the PRG is a nonlinear sample data system. Another unique feature is the hold period of only 1/2 the sample period.

The basic model and design values were selected and proven on other Honeywell programs. The output scale factor (pulse weight) was a variable for the HPARS program.

Gimballed ESG (Electrically Suspended Gyro) Platform

An existing three-axis ESG Platform System software simulation was utilized to provide low drift, long term stability to HPARS. Performance numbers used for the software simulations are not based on specific ESG performance, but are considered representative of what could be obtained from future development hardware. A gimballed system was selected to assess any significant problems

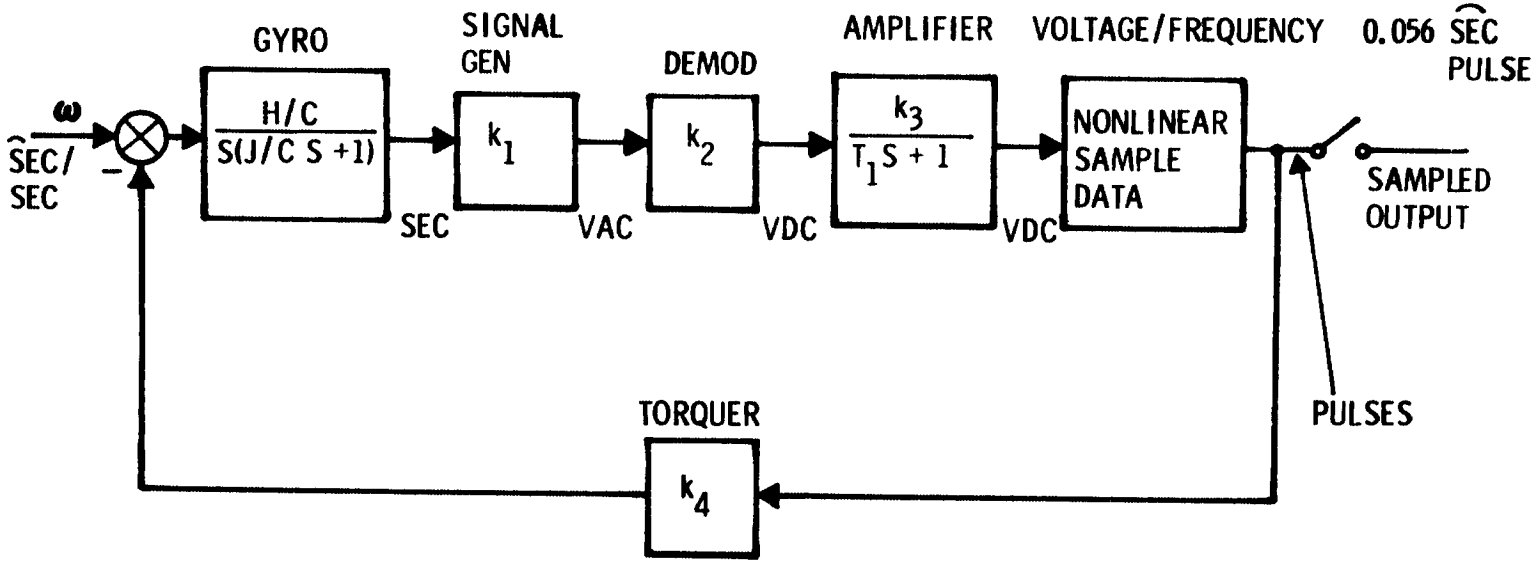

Figure 4-3. Pulse Rebalance Gyro for HPARS

(accuracy wise) associated with the gimbal approach, and also because gimballed systems to date have been able to give superior accuracy (due to readout techniques) than strapped-down ESG's.

The three axes system modeled consists of two, two axes platforms (Figure 4-4). Since a single ESG has only two degrees of freedom, two of them are needed to provide attitude reference for a three axis system. Two ESG's have four independent axes, of course, and some method of eliminating the "extra" degree of freedom must be provided. When each of the two ESG's has its own gimballing system the extra degree of freedom is usually eliminated in the computer which combines the gyro outputs (typically gimbal angle encoder readings) to produce the three reference axes.

Simulation of the compensated drift of two ESG's in inertial space is accomplished by conceptually considering four ESG spin vectors drifting in inertial space. Two of the four vectors represent the "true" gyro spin vectors, while the other two vectors represent the math model spin vectors. The two "true" spin vectors are used to simulate the gyro readout, the gimbal angle encoder outputs.

In concept, two gimbal assemblies each containing on ESG are mounted on a base. Readings taken from gimbal angle encoders allow the orientations of the two ESG spin vectors to be computed in a coordinate system fixed to the base. In a computer, the position of these two gyroscope spin vectors in an inertial frame is estimated by use of a mathematical model. Knowledge of the time and the latitude amd longitude of the table allows the computation of the orientations of these two "mathematical" spin vectors in an earth fixed coordinate frame. Assuming that the spin vectors given by the gimbal angle readouts and the spin vectors modeled in inertial space by the computer are the same, allows

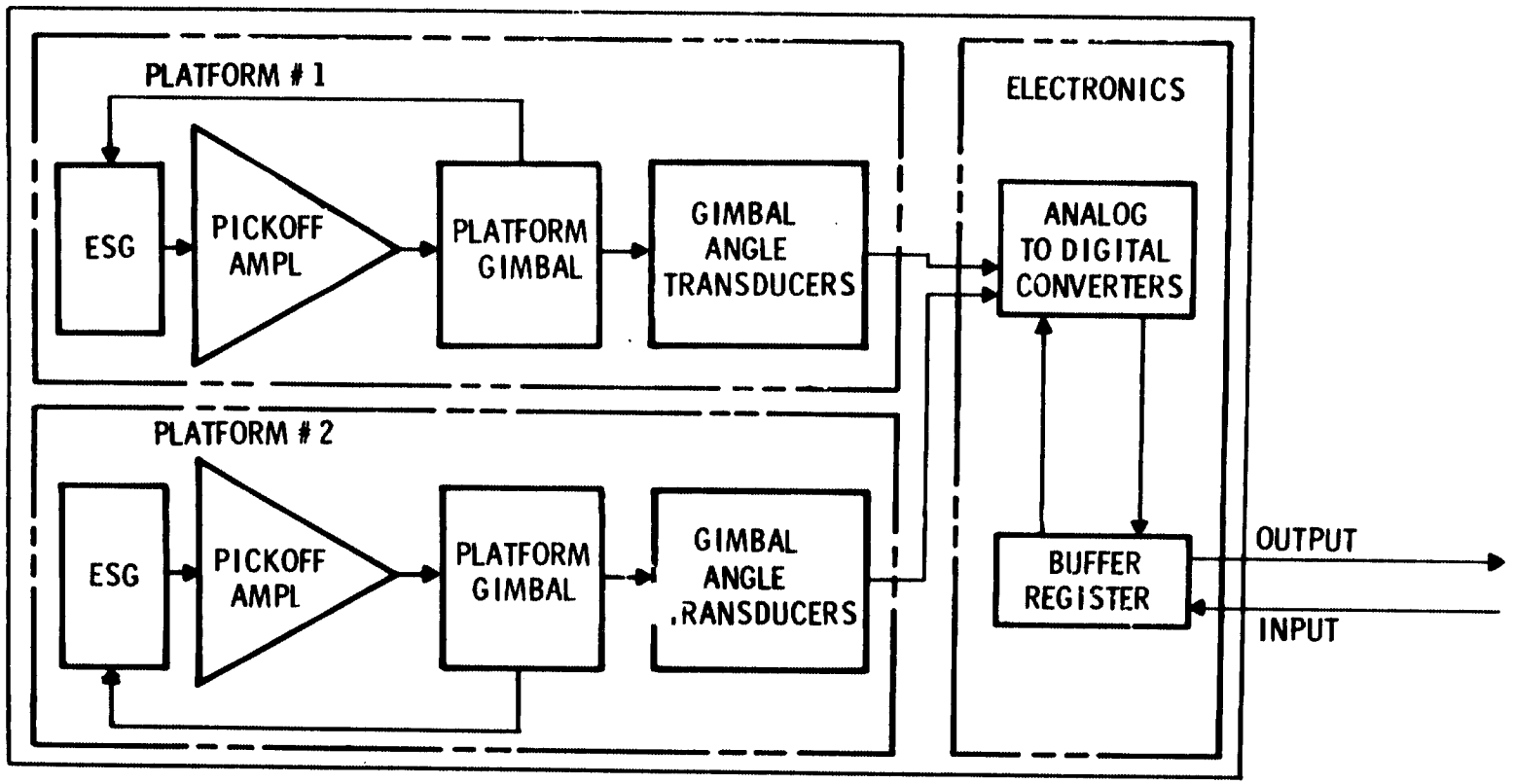

Figure 4-4. ESG Platform - Simplified Block Diagram

the computation of the relationship between the base coordinate frame and the earth fixed frame. This relationship is expressed both as a transformation matrix between the two frames and as a set of Euler angles relating the two frames. The process is "closed loop", however, since the transformation between base and earth coordinates is needed by the math model which estimates the spin vector orientations inertial space.

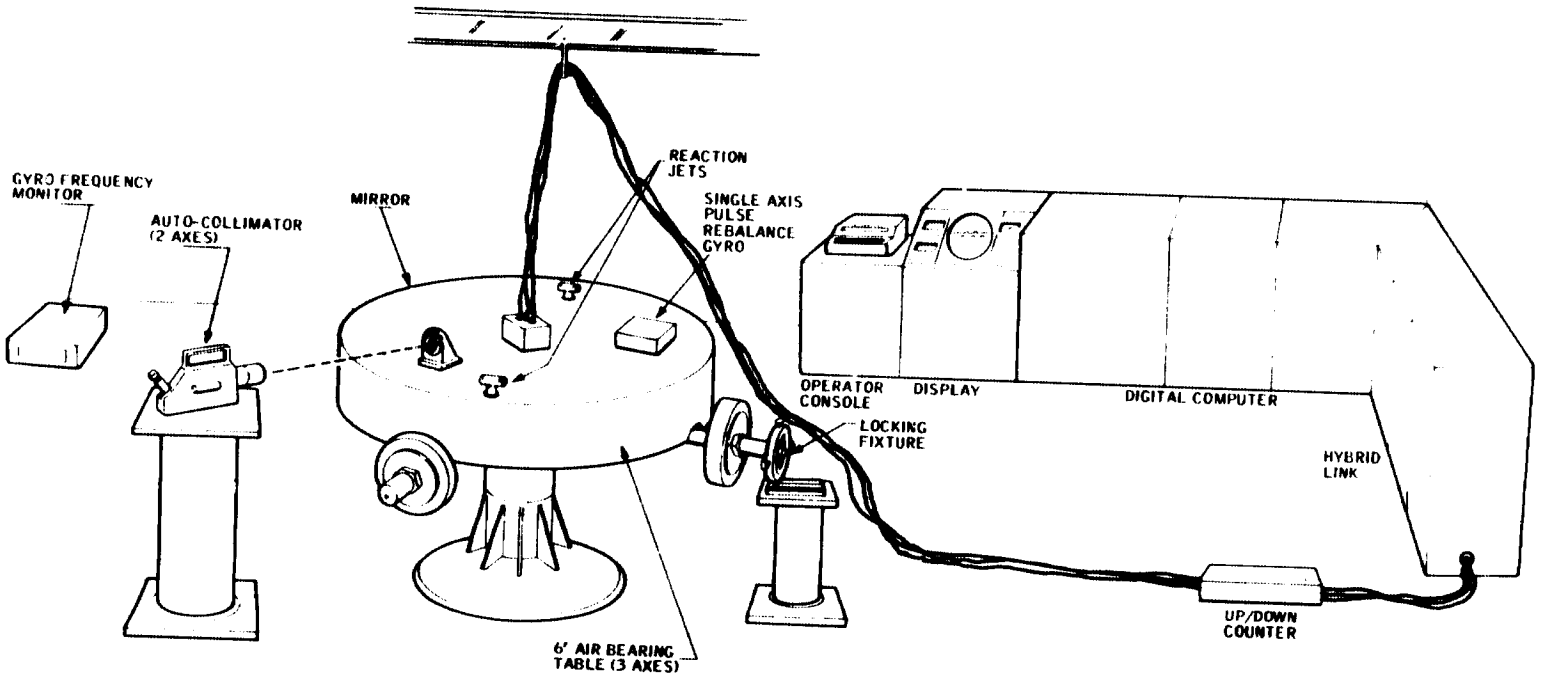

Figure 6-1(a). HPARS Single Axis Test

Laser Gyro

Three single axis triangular shaped (5.7" on a side) laser gyros were simulated for HPARS. The object was to provide the capability of rates greater than feasible for conventional gyros, and to determine if the laser gyro would be beneficial to the system at lower rates. The characteristics of the system simulates are listed in Figure 4-5. The errors included in the simulation were quantization errors due to the resolution of the gyro output, random drift, bias drift, and the dither subtraction error. Theoretically the dither subtraction error can be made zero. The drift characteristics of the laser gyro are very similar to a conventional gyro. At present a mechanical dither to reduce the error due to the laser gyro threshold (called lock-in rate) is used in preference to an electrical dither. Lock-in rates are typically 250-2500°/hr which is a significant threshold for our applications.

- SCHEDULED FOR DELIVERY TO ERC IN DECEMBER, 1968
- LOCK IN RATE — 500 - 1000°/HR
- DITHER RATE — 300,000°/HR
- DITHER FREQUENCY — 120 CPS
- WAVE LENGTH — 6328 A°
- RESOLUTION — 2^{-17} RAD (1-1/2 $\widehat{SEC}$/PULSE)/4
- SIZE — 5.7" ON A SIDE
- WEIGHT — 15 LBS PER AXIS WITH ELECTRONICS
- POWER — < 15 WATTS PER AXIS
  28 ± 4 VDC
- TYPE OF DITHER — MECHANICAL

PERFORMANCE

- RESOLUTION — 2^{-17} RAD (1-1/2 $\widehat{SEC}$/PULSE)/4
- ERROR SOURCES
  - SAMPLING ERROR - 2 COUNTS OR 3 $\widehat{SEC}$ OVER A SHORT PERIOD OF TIME DUE TO DITHER SUBTRACTION
  - RANDOM DRIFT - FOLLOWS A RANDOM WALK, VALVE <.1°/HR
  - BIAS DRIFT - <.1°/HR

Figure 4-5. GG1300 Characteristics

D. Description of HPARS Filter Concept

1.) General Concept

The High Precision Attitude Reference System developed during this study program uses the same conceptual approach used by the Honeywell SPARS Program (Space Precision Attitude Reference System). A brief description of this concept is given below.

A.) An estimate of true motion simulator rates about three orthogonal axes are obtained from either 3 laser gyros or 3 conventional rate integrating gyros operating in a pulse-rebalanced mode. This estimate is obtained by processing the gyro outputs using a SDS-9300 digital computer. A description of the estimation procedure is given in Appendix B.

B.) From the above rate estimate, a short term estimate of motion simulator attitude with respect to some orthogonal reference frame is obtained at a fast computation rate by numerically integrating 9 first order differential equations giving attitude reference direction cosines.

C.) An independent estimate (long term) of motion simulator attitude with respect to 3 orthogonal axes is periodically obtained at a slower rate than in (B) from electrically suspended (low drift) gyros mounted on the motion simulator.

D.) The equations of a discrete (recursive) Kalman Filter are solved using an SDS-9300 digital computer. The purpose of this filter is to make use of the long term attitude estimate in (C) above to

periodically update the rate estimate (A) and the short term attitude estimate (B). This updated (filtered) short term attitude estimate is then approximately the best estimate is then approximately the best estimate of true motion simulator attitude in the sense of minimum error variance.

2.) Discrete Kalman Filter

The theory of the discrete Kalman filter was presented by Kalman in reference 1. Applications of this theory are given in many references. Examples are references 2 and 3. A block diagram showing the structure of a typical discrete Kalman filter is given in Fig. 4-6. The equations which are solved for the Kalman filter are given in Appendix C.

As originally derived, the Kalman filter output yields a minimum variance estimate of the true state of the system only for linear systems where measurements are corrupted by white, gaussian noise. In the case of HPARS, the system or plant is nonlinear, hence Kalman filter theory does not apply directly. However for nonlinear systems, the theory can still be applied if the nonlinear process is linearized using perturbations about a reference solution (see reference 3, for example). This procedure has been carried out in the application to HPARS. For example, in the HPARS filter, the state vector is chosen to be:

$$X = \begin{pmatrix} \delta\phi \\ \delta\theta \\ \delta\psi \\ \delta p_b \\ \delta q_b \\ \delta r_b \end{pmatrix} \qquad (1)$$

TYPICAL DISCRETE KALMAN FILTER BLOCK DIAGRAM

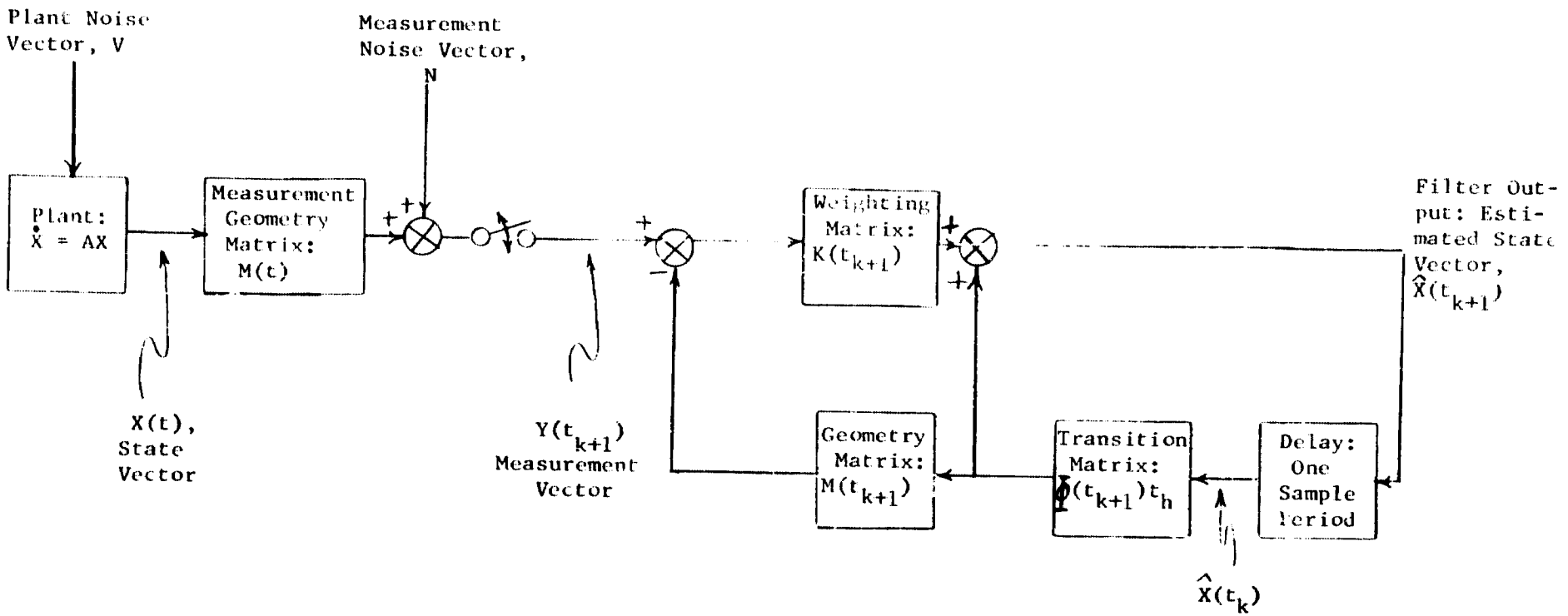

FIGURE 4-6

Where the first three components of X are incremental Euler angles and the last three components are incremental rate bias correction terms.

The measurement vector is defined to be:

$$Y = \begin{matrix} \delta\phi_{meas} \\ \delta\theta_{meas} \\ \delta\psi_{meas} \end{matrix}$$

Note that three independent Euler angles have been used as measures of attitude. In the initial stage of the HPARS study, 4 gimbal angles were used as the state variables defining attitude and also as the measured variables. This was done because the Electrically Suspended Gyro configuration consisted of two 2 degree of freedom gimballed ESG's. The fact that 4 gimbal angles (4 attitude state variables) do not uniquely define attitude with respect to inertial space led to very undesirable performance of the filter (failure to converge to steady state operation even with no disturbances). For this reason, the choice of Euler angles was made. See Figure 4-7 for a sketch of a desired output from this filter application. This can be compared with actual outputs shown plotted in Section V.

3.) Limitations

The chief limitation of this application of Kalman recursive filter theory to a nonlinear system was not due to the effects of linearization about a nominal solution. The chief limiting factor was due to the fact that the plant noise and measurement noise were not white, gaussian noise. The attitude measurements from the simulated Electrically Suspended Gyros are

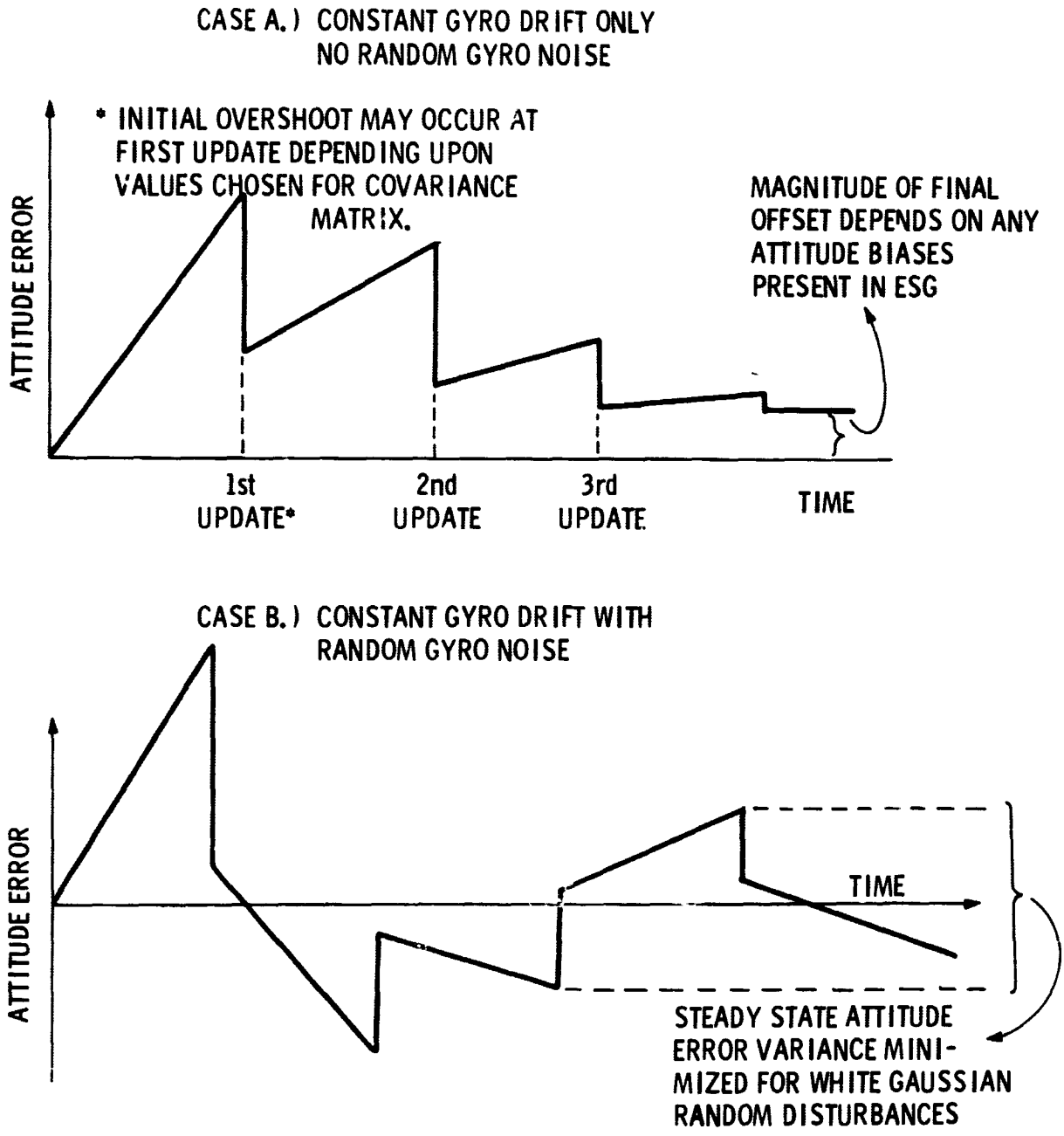

Figure 4-7. Expected HPARS Filter Performance

obtained by a nonlinear transformation operating upon the gimbal angle readouts, which have significant quantization noise. In addition, imperfect knowledge of ESG spin vector drift yields errors which are highly correlated with a correlation time on the order of hours. The Kalman filter approach is significantly degraded by this type of error. In addition, pulse rebalanced gyros are nonlinear processes having errors which deviate markedly from white noise.

The HPARS simulation is a valuable tool to be used to determine the degradation of the filter performance as the measurement errors deviate more and more from white noise.

E. Description of HPARS Simulation

1) General

A broad picture summary of the HPARS simulation is shown in Figure 4-8. The simulation is all digital and was performed on the SDS-9300 computer. The three gyro package simulations were adapted from existing simulations. The filter or BMEC is based on the SPARS Kalman filter approach (discussed in Section D) and the experience and data fallout from that program was most useful. In a real facility the three gyro packages would of course be hardware, whereas the BMEC would be a digital general purpose on-line computer.

The total simulation used up more than the entire 24000 words of memory available with the SDS-9300 computer. Because of this, the initialization portion of the program had to be input as a separate program and its output written on magnetic tape. The contents of this magnetic tape were then used as an input to the main HPARS program. A summary flow chart of the complete HPARS program is shown in Figure 4-9.The program was written in FORTRAN IV as a series of subroutines which were called by the main controlling program in sequence computation cycle (Δ observation time). For example, each simulated sensor (laser gyros, ESG's, etc.) was a separate subroutine with its own solution time increment. Typical Δ observation times used were 1 to 2 seconds, while the shortest solution time increment was approximately 1 millisecond for the pulse rebalance gyro subroutine. The total simulation ran about 3 to 4 times slower than real time. The following significant parameters could be modified on the on-line typewriter in between runs:

Filter Covariance Matrix Initial Values (P)

Filter Measurement Error Matrix Values (Q)

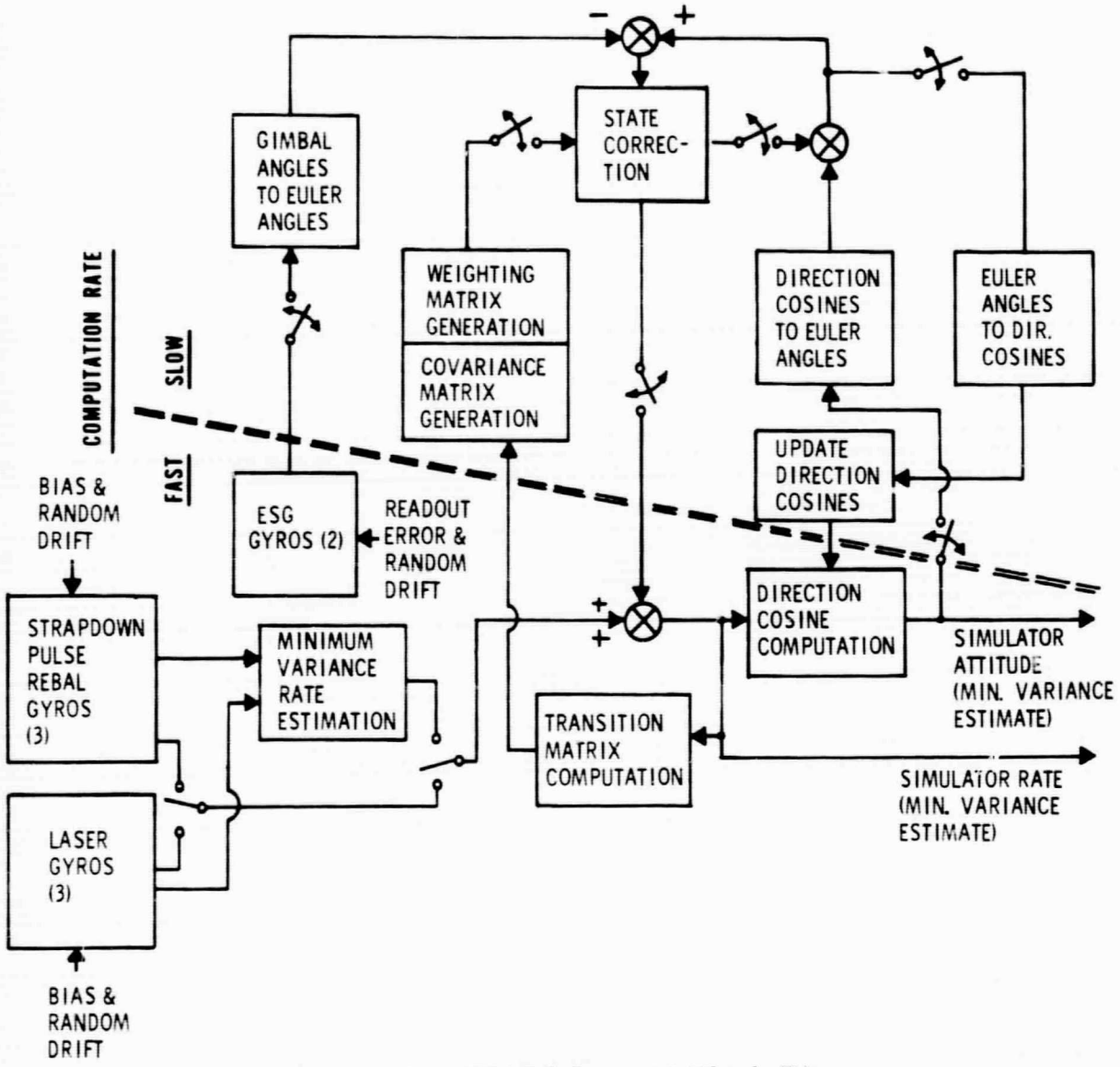

Figure 4-8. HPARS Concept Block Diagram

Filter Stability Matrix Values (N)

Pulse Rebalance Gyro Drift & Noise Variance and pulse weight

Laser Gyro Drift & Noise Variance

ESG Attitude Measurement Errors & Quantization

Solution Time Increments, etc.

Descriptions of the sensor subroutines are given in the Reference 1. A description of the BMEC (filter) subroutine is given in Section D. Other subroutines are briefly discussed below:

2) Short Term Attitude Reference Computation

Fourth order Runge-Kutta numerical integration of direction cosine first order differential equations. Automatically orthogonalized during each iteration.

$$\dot{\ell}_i = r\, m_i - q\, n_i \qquad (1)$$

$$\dot{m}_i = P\, n_i - r\, \ell_i \qquad (2)$$

$$\dot{n}_i = q\, \ell_i - P\, m_i \qquad (3)$$

$i = 1, 3$

The direction cosine matrix [A] is then given by the following:

$$[A] = \begin{bmatrix} \ell_1 & m_1 & n_1 \\ \ell_2 & m_2 & n_2 \\ \ell_3 & m_3 & n_3 \end{bmatrix} \qquad (4)$$

Orthogonalization of the direction cosine matrix was accomplished by the following:

$$[A_o] = \frac{1}{2}\,[A] + \frac{1}{2}\,[A^{-1}]^T \qquad (5)$$

$[A_o]$ orthogonalized dir. cos. matrix

3) True Attitude Computation

True motion simulator attitude was obtained in closed form as a function of time by solving the following equations:

$$[A(t)] = [B_1(t)]\,[B_2(t)]\,[A_{IC}] \qquad (6)$$

where:

$$[B_1(t)] = \begin{bmatrix} 1-\left(\frac{q^2+r^2}{\omega^2}\right)(1-c\omega t) & \frac{r}{\omega}s\omega t + \frac{pq}{\omega^2}(1-c\omega t) & -\frac{q}{\omega}s\omega t + \frac{pr}{\omega^2}(1-c\omega t) \\ -\frac{r}{\omega}s\omega t + \frac{pq}{\omega^2}(1-c\omega t) & 1-\frac{(p^2+r^2)}{\omega^2}(1-c\omega t) & \frac{p}{\omega}s\omega t + \frac{qr}{\omega^2}(1-c\omega t) \\ \frac{q}{\omega}s\omega t + \frac{pr}{\omega^2}(1-c\omega t) & -\frac{p}{\omega}s\omega t + \frac{qr}{\omega^2}(1-c\omega t) & 1-\frac{p^2+q^2}{\omega^2}(1-c\omega t) \end{bmatrix}$$

$[B_2(t)]$ = same as $B_1(t)$ except replace p, q, r with $\dot{p}$, $\dot{q}$, $\dot{r}$; Replace ω with $\dot{\omega}$; Replace t with $\frac{t^2}{2}$

In the above equations: C = Cosine

S = Sine

$$\omega^2 = p^2 + q^2 + r^2$$
$$\dot{\omega}^2 = \dot{p}^2 + \dot{q}^2 + \dot{r}^2$$

It can be shown that the closed form attitude solution is given by equation (6) for constant rate and constant acceleration inputs provided that the following restriction is met:

$$\frac{p}{\dot{p}} = \frac{q}{\dot{q}} = \frac{r}{\dot{r}} \qquad (9)$$

This restriction was met in all of commanded rate profiles used in the HPARS simulation.

4) Attitude Error Computation

For the HPARS study the compensated attitude output is compared to the computed (from program inputs) true attitude by taking the dot products. Filter parameters or the basic filter design were iterated until the system errors were at a minimum. In addition, hardware changes were made to determine the effect on the total system accuracy. The desired result being to define the hardware and filter requirements and limitations, and the feasibility of a .01 arc sec attitude reference system.

5) Commanded Rate Inputs

Commanded rate inputs were inserted to simulate the platform moving to a new attitude orientation. Of necessity, due to the computation time restirctions as a function of simulated gyro saturation rates, the commanded rates used were less than 0.03 degrees/second. This restriction could be relaxed in the future by changing to a less accurate simulation of the pulse rebalance gyros. The commanded rate profile used is given below.

FIGURE COMMANDED RATE PROFILE - HPARS

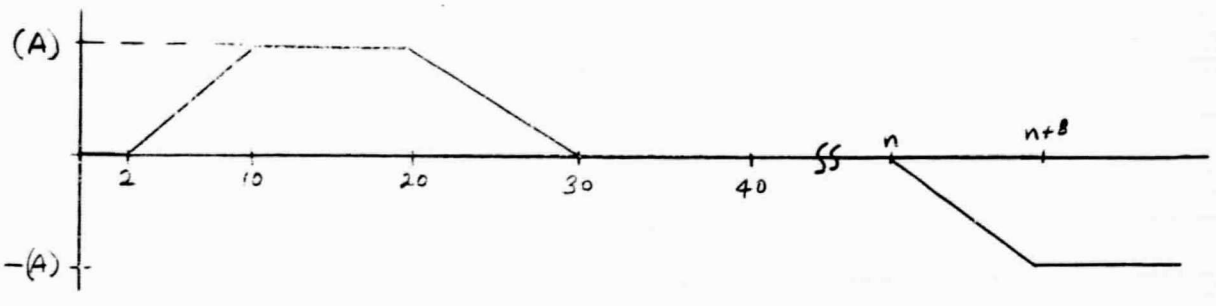

(A) = 0.024 deg/sec in roll, pitch

(A) = 0.03 deg/sec in yaw

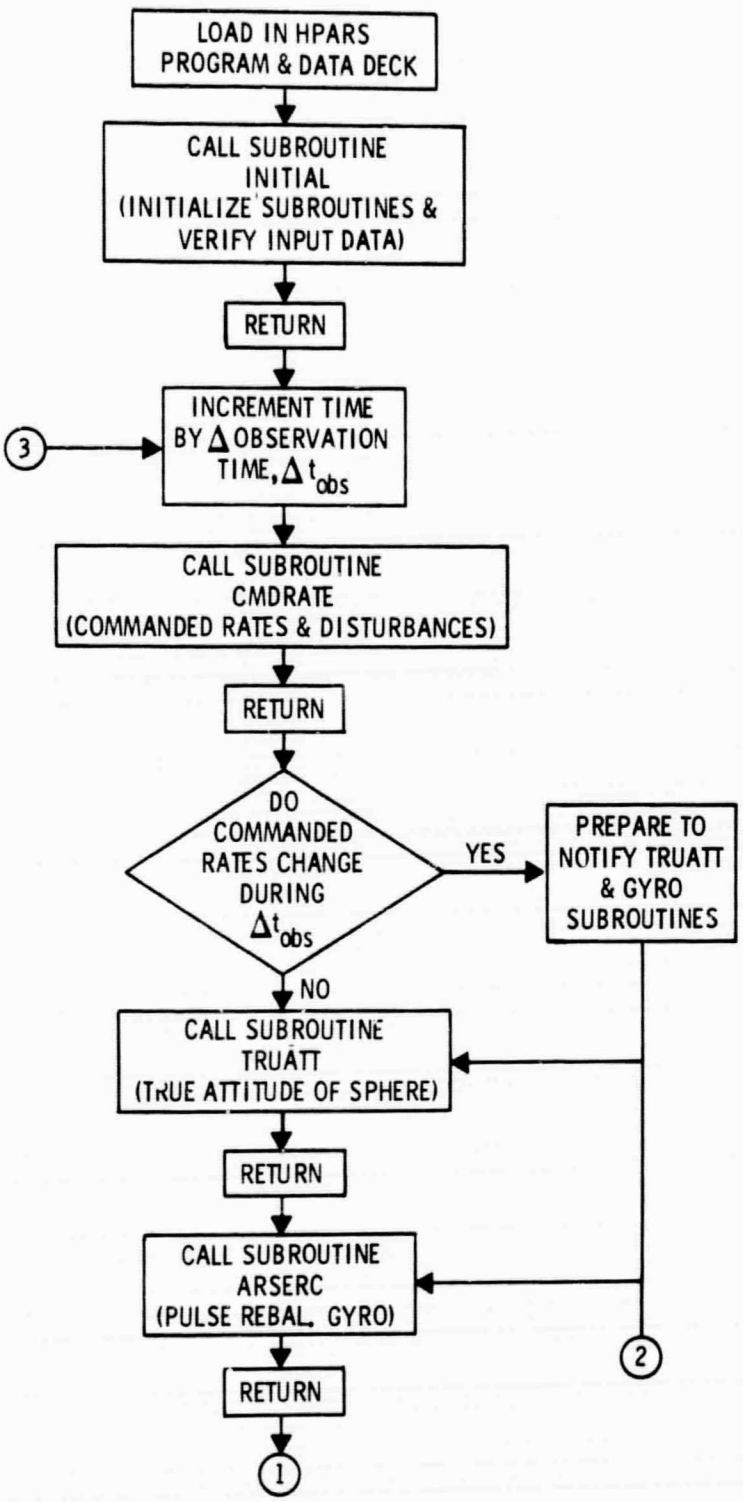

Figure 4-9(a). HPARS Digital Simulation Program Flow Chart

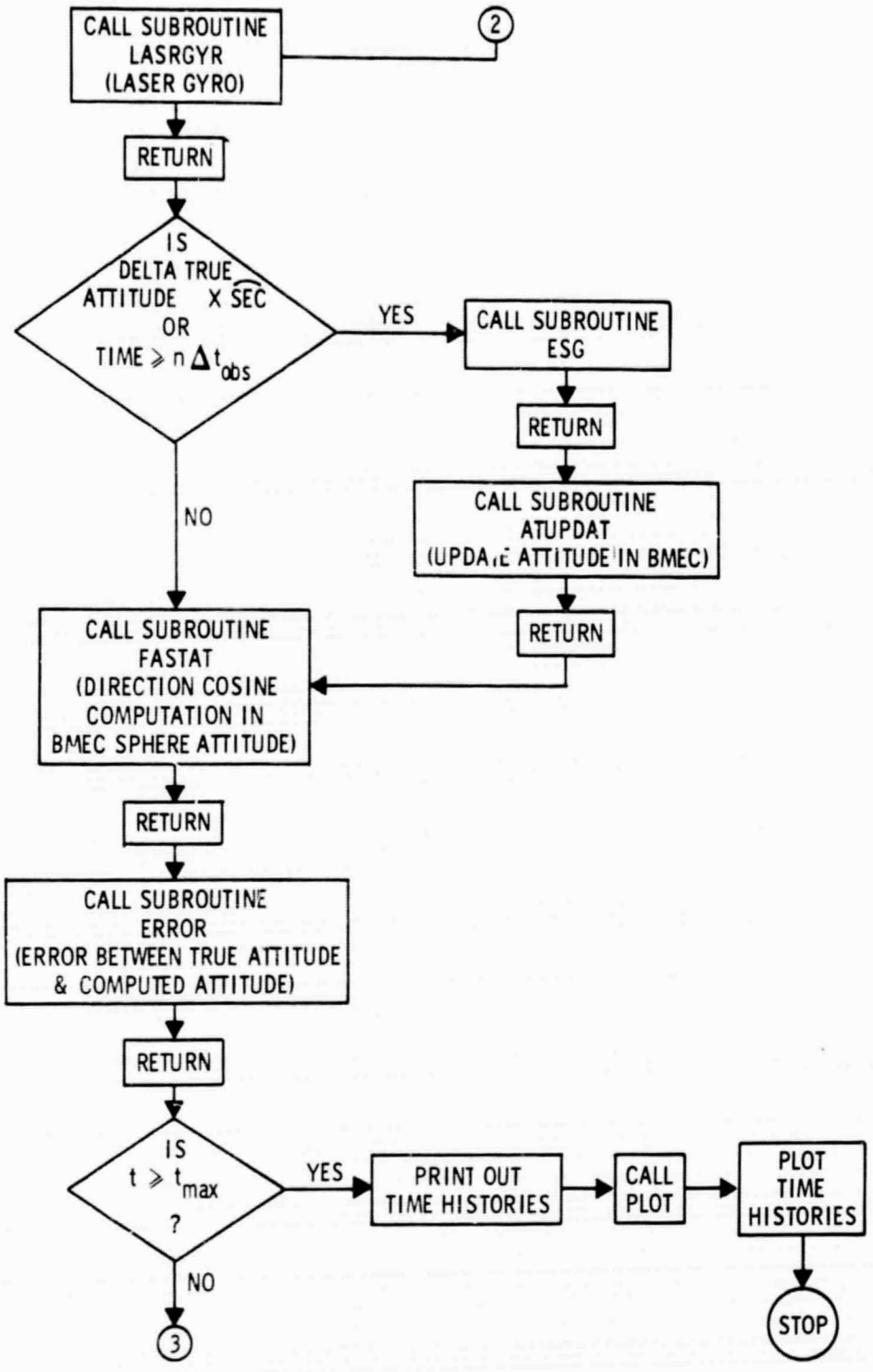

Figure 4-9(b). HPARS Digital Simulation Program Flow Chart

V. SIMULATION RESULTS

The results of the software simulation along with much of the plotted data is discussed in this section. With few exceptions the data plots are for maximum attitude error vs. time. The maximum attitude error is the largest body error (or platform error) of Θ, $\emptyset$, or ψ existing at the sample time. Thus the plots are representative of the worst 1σ errors that occur in any of the three axes. It would have been desirable to have rms values but this could have enlarged the program beyond the computer capacity.

All of the runs shown here are for approximately two minute duration which is sufficient to get good data in light of the short response time of the system and with the system updates occuring every 10 sec. The run times were approximately 1/4 real time thus two minute data time runs were desirable. Errors due to ESG drift over a two minute period were insignificant. Two twenty four funs were also performed and as expected the errors are significant with respect to our system requirements for short term accuracy. This data is available but being classified it is not included in this report.

A. The Perfect System

Figure 5-1 shows the filter operating under ideal conditions--and giving ideal results. The parameter inputs are:

Gyro Drift	.05°/hr
Gyro Noise	0
Analog Rebalance Gyros	(Thus no deadbands, quantization errors, or non-linearities)
Perfect ESG	(Thus no deadbands, quantization errors, or non-linearities)

The system behaves as expected under these conditions; reducing the gyro drift at each successive update (every 10 sec) until t=100 sec the system error (gyro drift) has been reduced to zero.

HPARS
Simulation Run #13-12
Gyro Drift 0.05 °/hr
Gyro Noise 0
Analog Rebalance Gyros
No Commanded Rates
Perfect ESG
Observation Time 2 sec
Update Time 10 sec

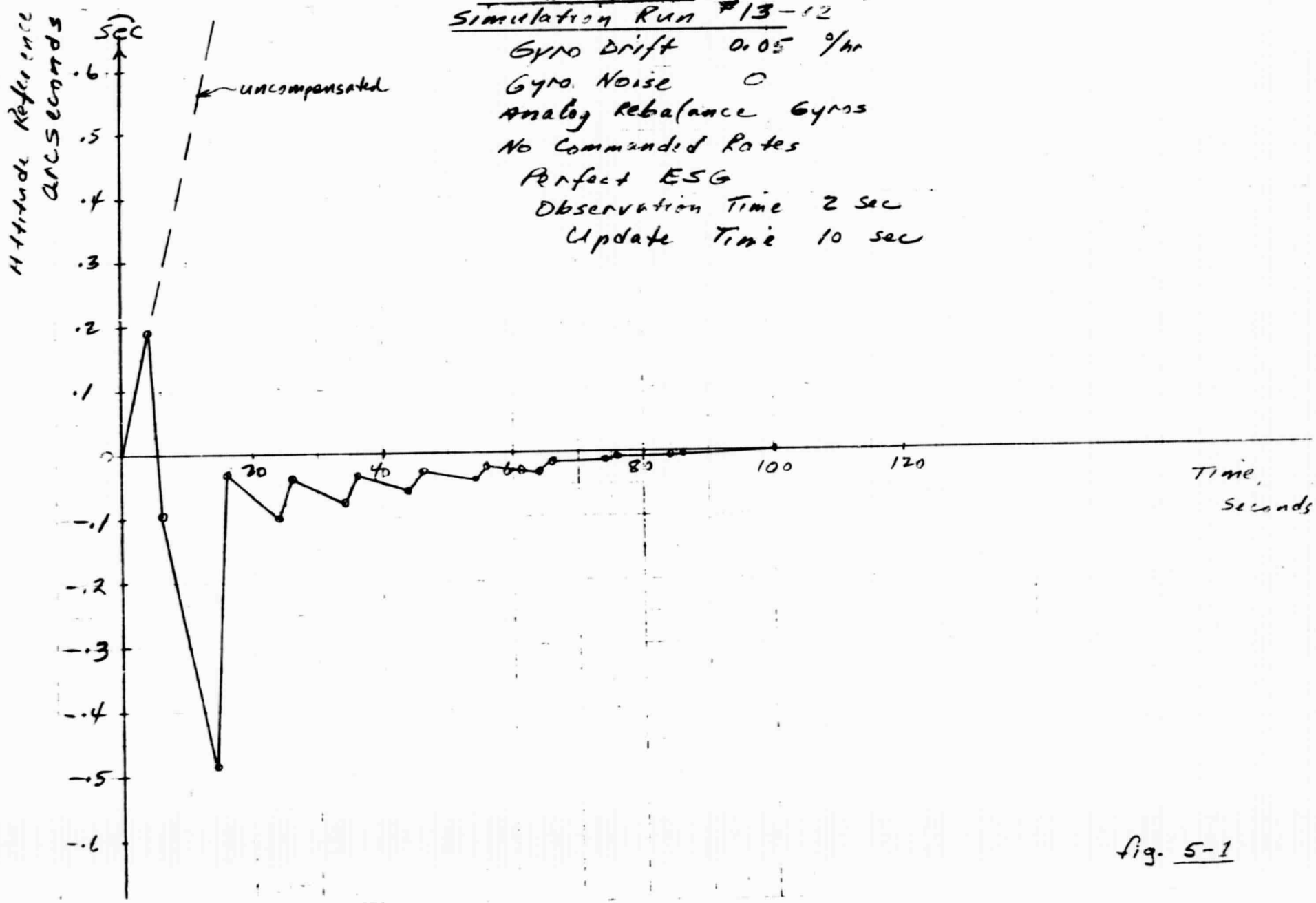

fig. 5-1

B. Effect of Gyro Noise

Perhaps the most significant single factor in limiting the system accuracy is the noise component present in the single degree of freedom gyros. The Kalman filter compensates quite well for gyro drift of the reaction torque type. In fact as shown in Figure 5-1 it has perfectly compensated for it in 100 sec. However, with gyro noise of the form described in Section V is added the filter reduces the noise less perfectly. Figures 5-2 and 5-3 are somewhat representative of the filter effect on random noise of .01°/hr. Comparing Figure 5-2 which has the filter out of the system with Figure 5-3 the noise after 100 sec (after the .05°/hr drift is removed) has been reduced 70-80%. Other factors are involved when running without any filter such as the building of truncation errors in the computer but the figures allow a rough comparison.

Figures 5-3, 5-4, and 5-5 show the effect of a continued buildup of the gyro noise level (from .001°/hr to .028°/hr and figure 5-6 compares the approximate rms values of figures 5-3 through 5-5 with a zero noise system.

Due to already using all the memory capacity of the 9300 computer it was not possible with the present program to obtain accurate rms error plots. It may be that further optimization of the filter could be made, thus reducing the system error due to gyro noise, by reiterating the filter design based on rms error values in lieu of maximum error values.

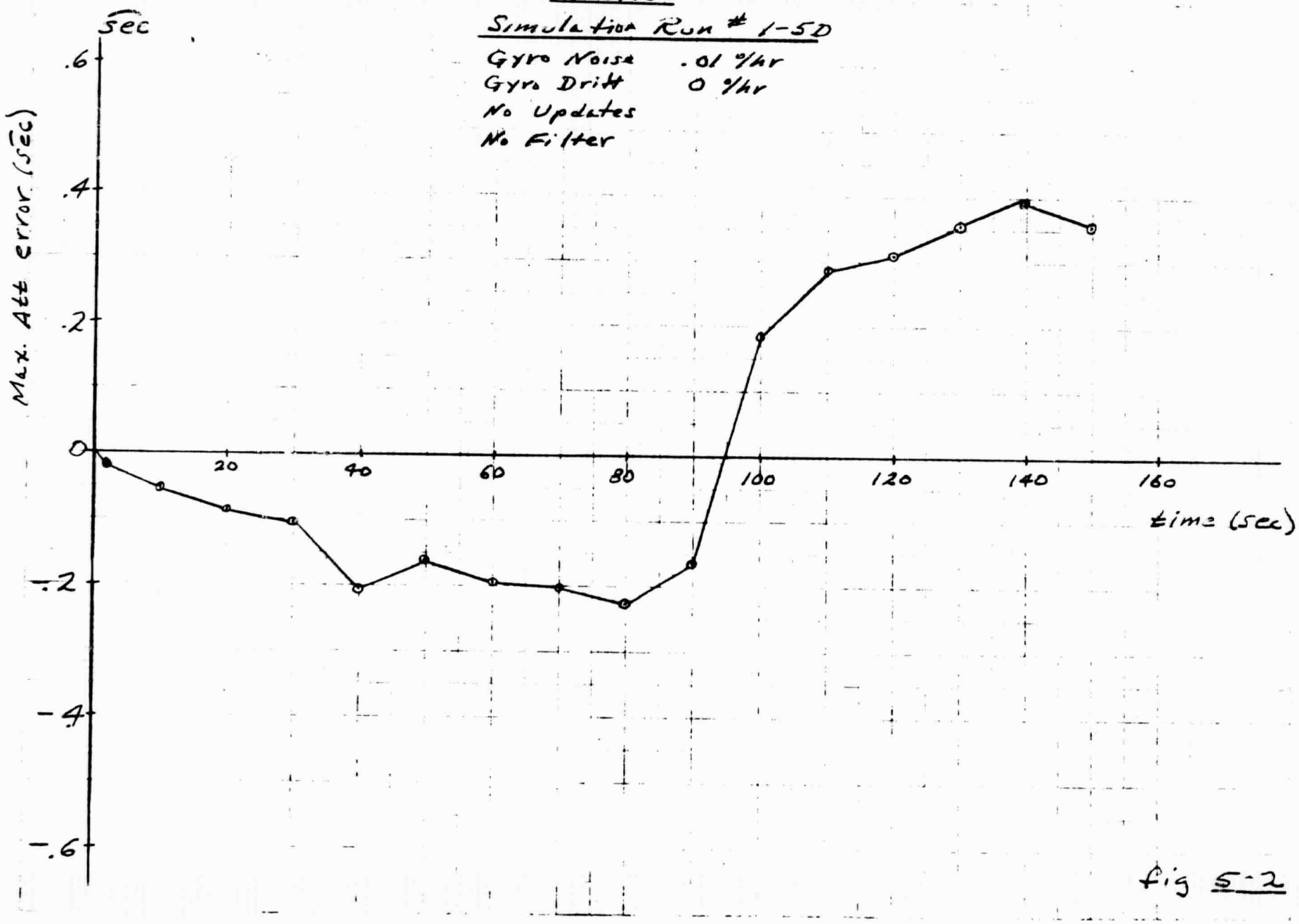
HPARS
Simulation Run # 1-5D
Gyro Noise .01 °/hr
Gyro Drift 0 °/hr
No Updates
No Filter
Max. Att error (sec)
sec
.6
.4
.2
0
-.2
-.4
-.6
20
40
60
80
100
120
140
160
time (sec)

fig 5-2

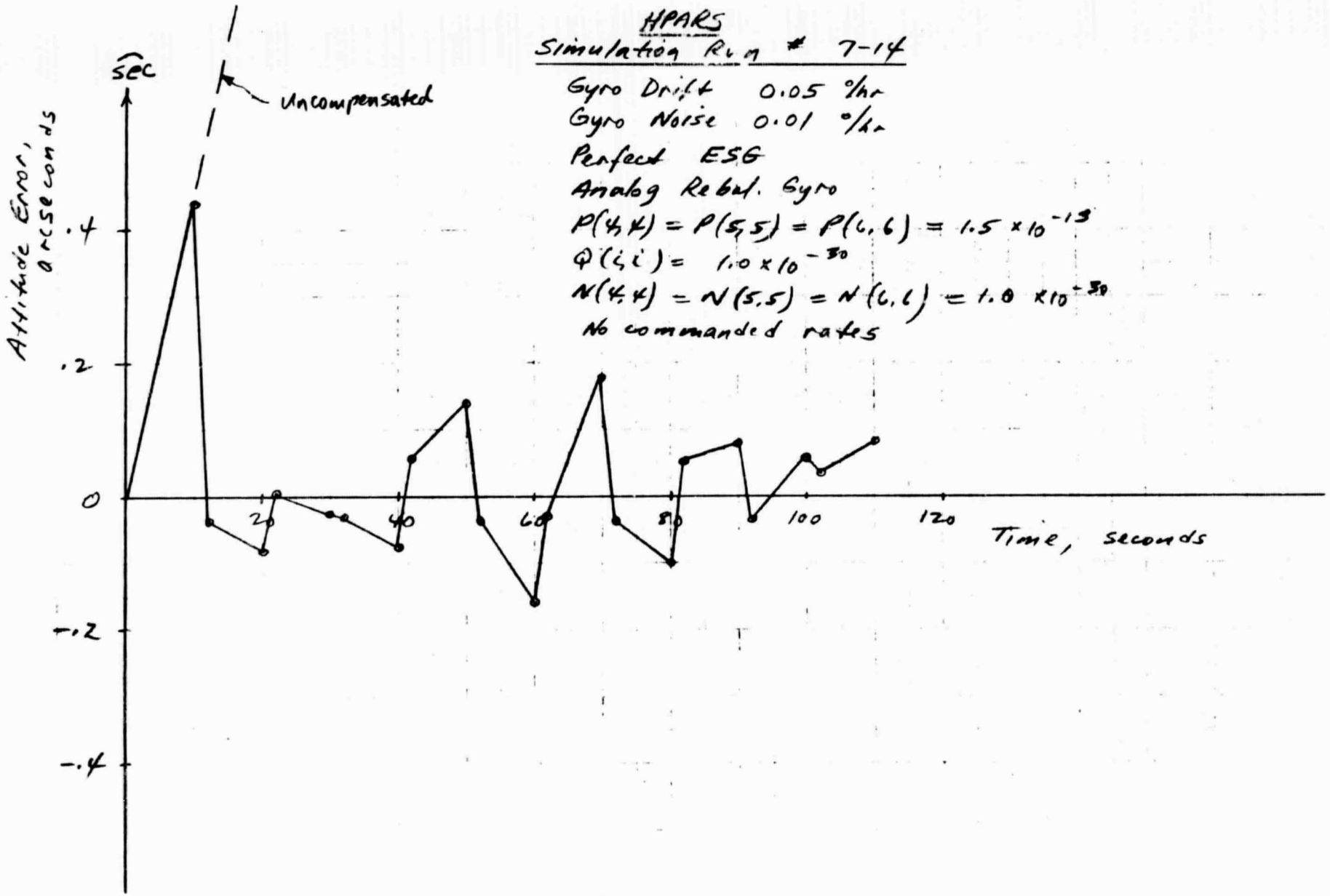
HPARS
Simulation Run # 7-14
Gyro Drift 0.05 °/hr
Gyro Noise 0.01 °/hr
Perfect ESG
Analog Rebal. Gyro
P(4,4) = P(5,5) = P(6,6) = 1.5 x 10^-13
Q(i,i) = 1.0 x 10^-30
N(4,4) = N(5,5) = N(6,6) = 1.0 x 10^-30
No commanded rates
sec
Uncompensated
Attitude Error, arcseconds
.4
.2
0
-.2
-.4
20
40
60
80
100
120
Time, seconds

fig 5-3

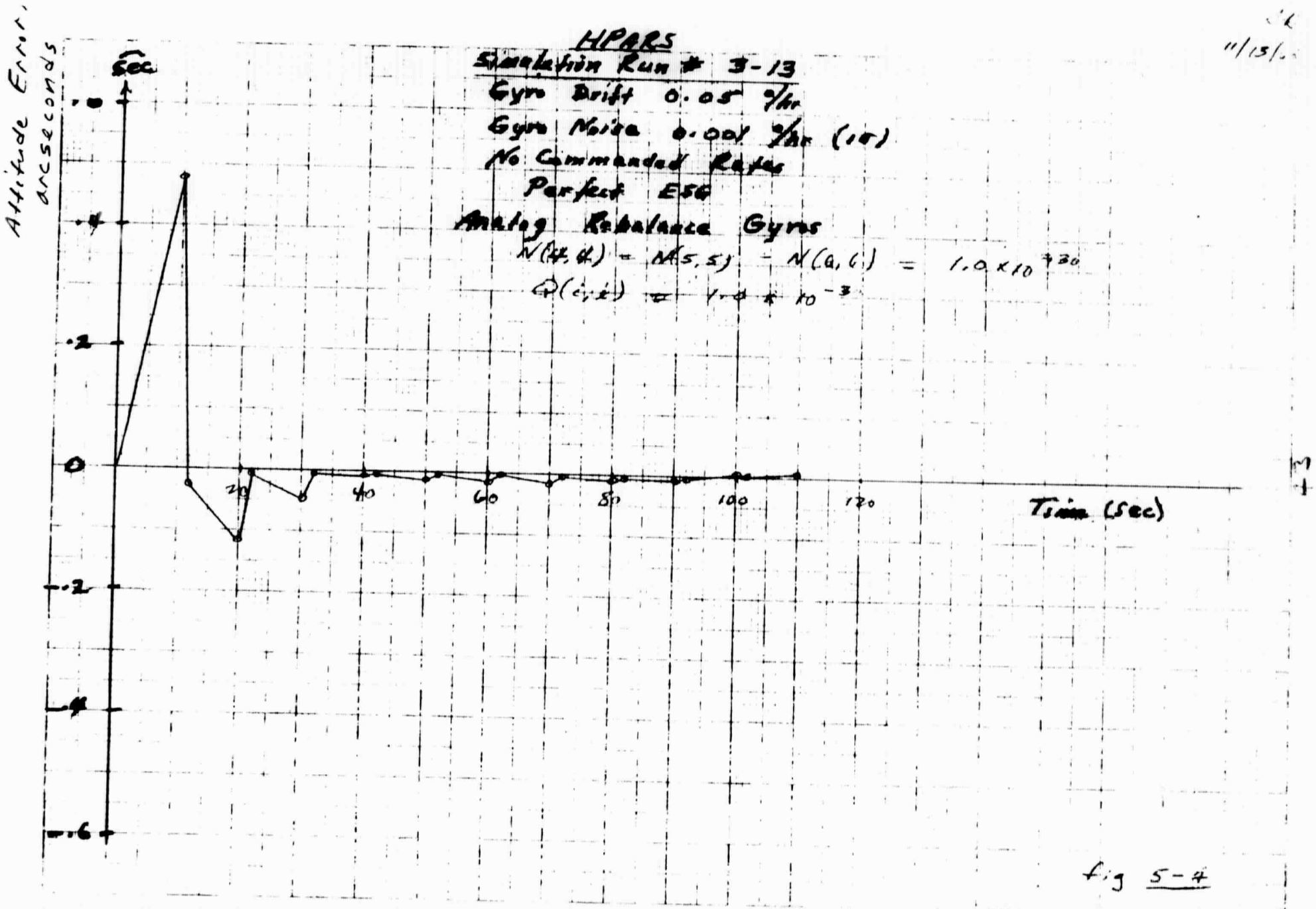
HPARS
Simulation Run # 3-13
Gyro Drift 0.05 °/hr
Gyro Noise 0.001 °/hr (1σ)
No Commanded Rates
Perfect ESG
Analog Rebalance Gyros
N(4,4) = N(5,5) = N(6,6) = 1.0 x 10^+30
Q(i,i) = 1.0 * 10^-3
Attitude Error, arcseconds
Sec
.8
.4
.2
0
-.2
-.4
-.6
20
40
60
80
100
120
Time (Sec)

fig 5-4

HPARS

Simulation Run # 11-12

Gyro Drift 0.05 °/hr

Gyro Noise 0.028 °/hr (1σ)

No Commanded Rates

Perfect ESG

Analog Rebalance Gyros

$N(4,4) = N(5,5) = N(6,6) = 1.0 \times 10^{-20}$

$Q(i,i) = 9.0 \times 10^{-18}$

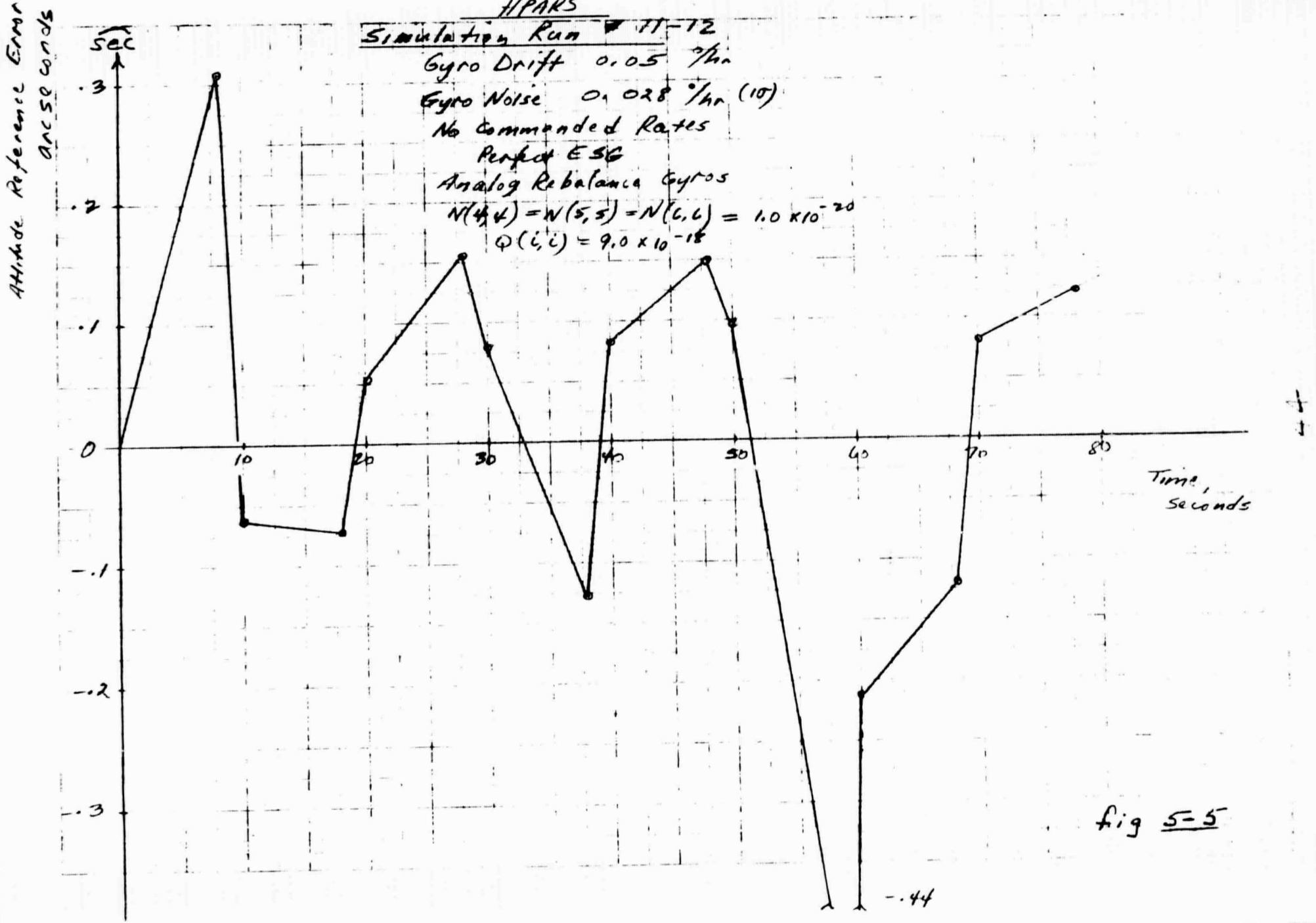

fig 5-5

HPARS—EFFECT OF GYRO NOISE

GYRO DRIFT - .05 °/hr
PERFECT ESG
ANALOG REBALANCE GYROS

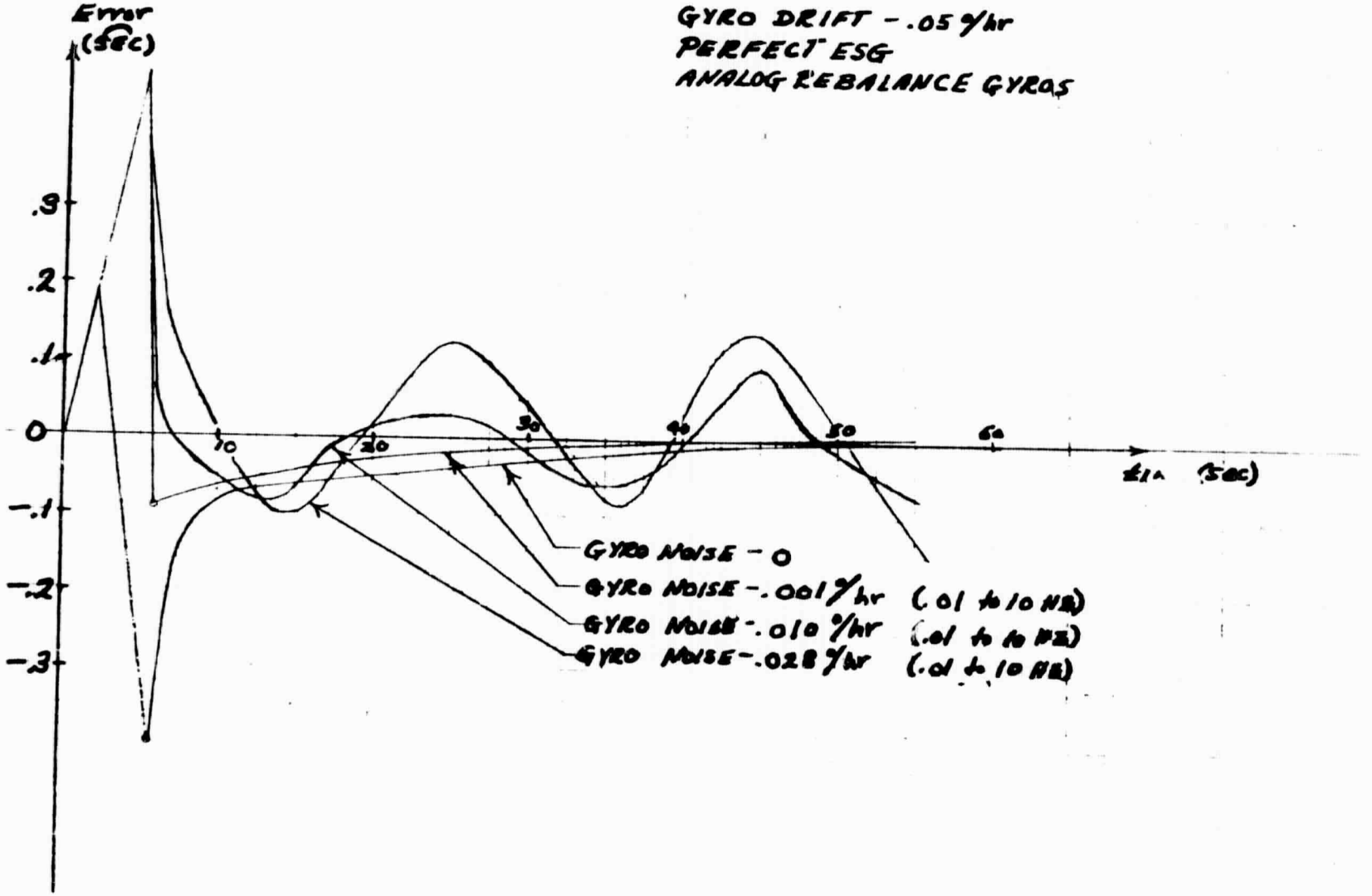

fig 5-6

C. Analog Vs. Pulse Rebalance

In precision systems there has been toward pulse rebalance gyros to obtain the advantages of operations near null and digital data processing. Analog rebalance loops can also be used to keep the gyro near null so that other factors such as scaling, reliability, component drift, size and power, and producibility must be included in any trade-offs between the two approaches for a specific system.

Due primarily to availability of the model a pulse rebalance loop was selected for the HIARS study, but being a software simulation it was also examined as an analog loop simply by decreasing the pulse weight to zero. Thus we can compare an "ideal" analog rebalance gyro with a pulse rebalance unit.

Figures 5.7 and 5.8 show the system operating with low gyro noise levels (.001°/hr) and a perfect ESG. The only difference between the two runs was in the gyro loop closure.

Figure 5.7 with an analog rebalance loop shows the error bounded after 100 sec to less than .01 sec. Figure 5.8 with a pulse rebalance loop and a pulse weight of .056 sec/pulse can only bound the system to about .025 sec. The error difference is of course due to the finite deadband and quantization error present in the pulse rebalance loop. Further study in this area is recommended to provide data on the minimum required pulse weight as a function of gyro noise and system accuracy. The object being to not limit the system accuracy due to pulse weight and at the same time not require an analog loop.

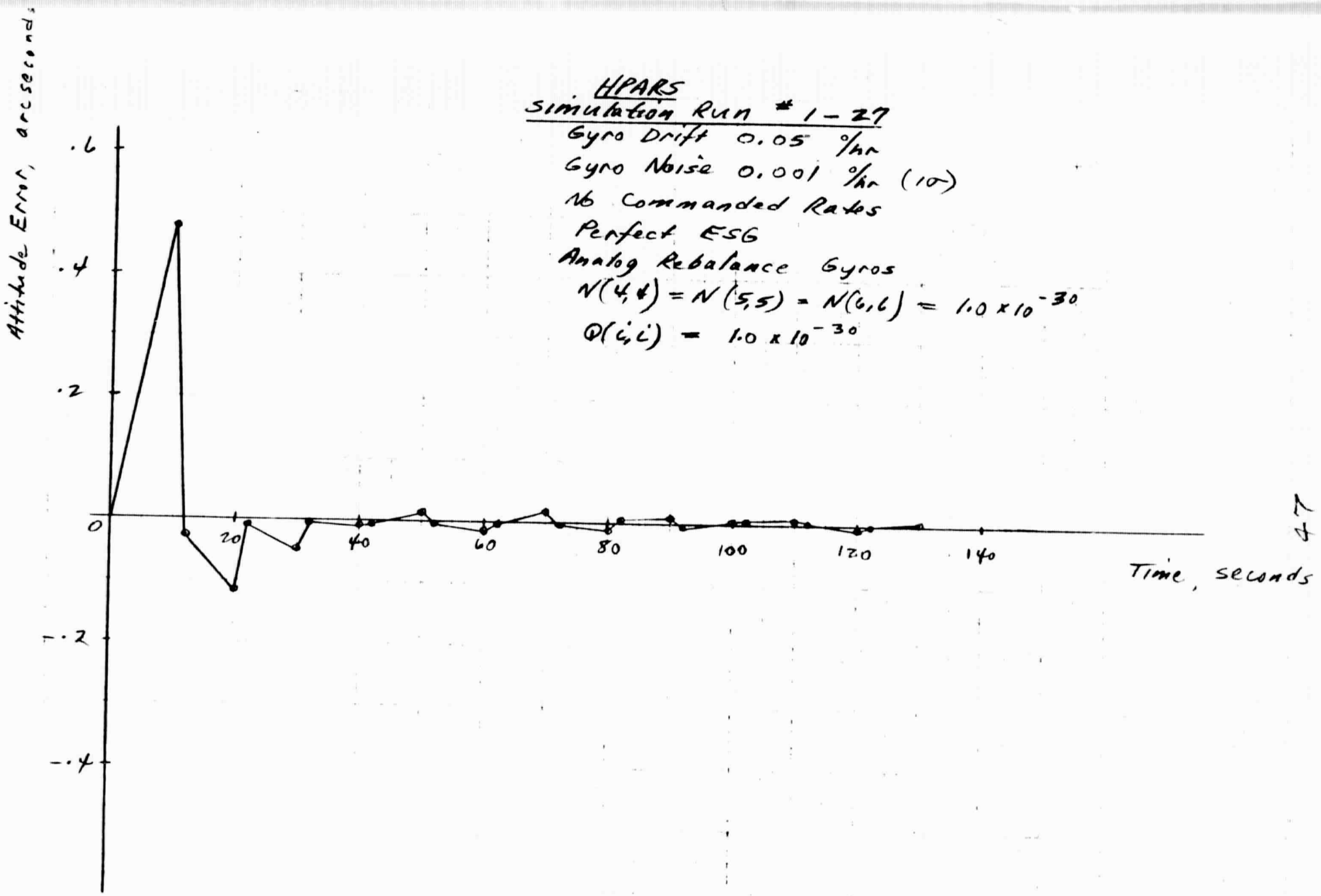
HPARS
Simulation Run # 1-27
Gyro Drift 0.05 °/hr
Gyro Noise 0.001 °/hr (1σ)
16 Commanded Rates
Perfect ESG
Analog Rebalance Gyros
N(4,4) = N(5,5) = N(6,6) = 1.0 x 10^-30
Q(i,i) = 1.0 x 10^-30
Attitude Error, arcseconds
.6
.4
.2
0
-.2
-.4
20
40
60
80
100
120
140
Time, seconds

fig 5-7

HPAK-3

Simulation Run # 2-25

Gyro Noise 0.001°/hr (1σ)

Gyro Drift 0.05°/hr

Perfect ESG

Pulse Rebalance Gyros (.056 sec/pulse)

$N(4,4) = N(5,5) = N(6,6) = 1.0 \times 10^{-30}$

$Q(i,i) = 1.0 \times 10^{-30}$

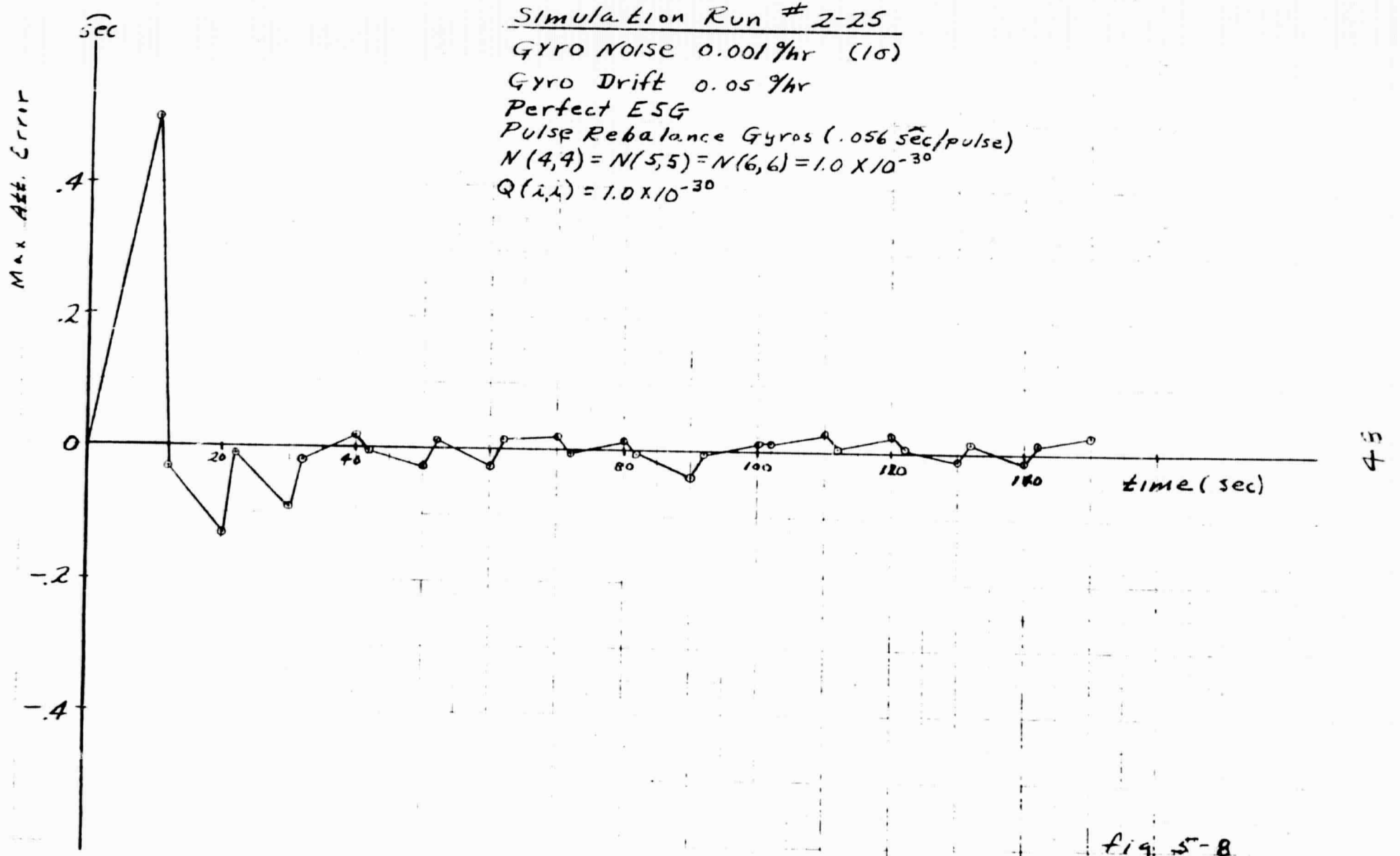

fig 5-8

D. ESG Gimbal Resolution

The resolution of the ESG gimbals was varied from 12 BITS (1.75 sec) to a perfect or analog system. As would be expected, the system performance improves accordingly, but the effect of gyro noise must be taken into account before selecting correct gimbal readout device for the system.

Figures 5-9, 5-10 and 5-11 show the effect of increasing gimbal deadband and quantization errors on the system. However, when compared to a perfect ESG in Figure 5-12 there is very little difference in performance between the perfect, 18 BIT (.03 sec), and 15 BIT (.33 sec) ESG's. The reason being that the gyro noise of .01°/hr becomes the limiting factor.

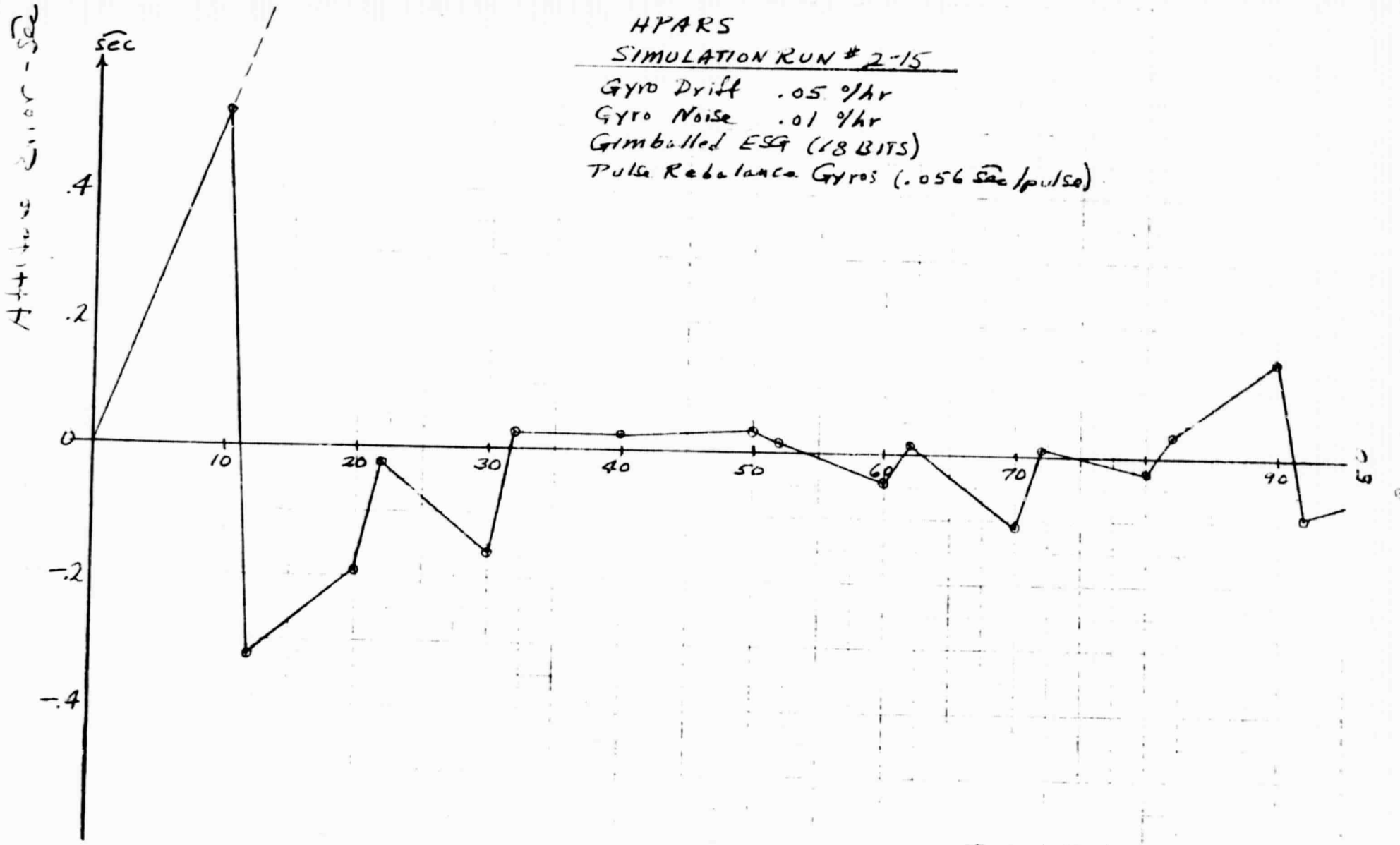
HPARS
SIMULATION RUN # 2-15
Gyro Drift .05 °/hr
Gyro Noise .01 °/hr
Gimballed ESG (18 BITS)
Pulse Rebalance Gyros (.056 sec/pulse)
sec
.4
.2
0
-.2
-.4
10
20
30
40
50
60
70
80
90

fig 5-9

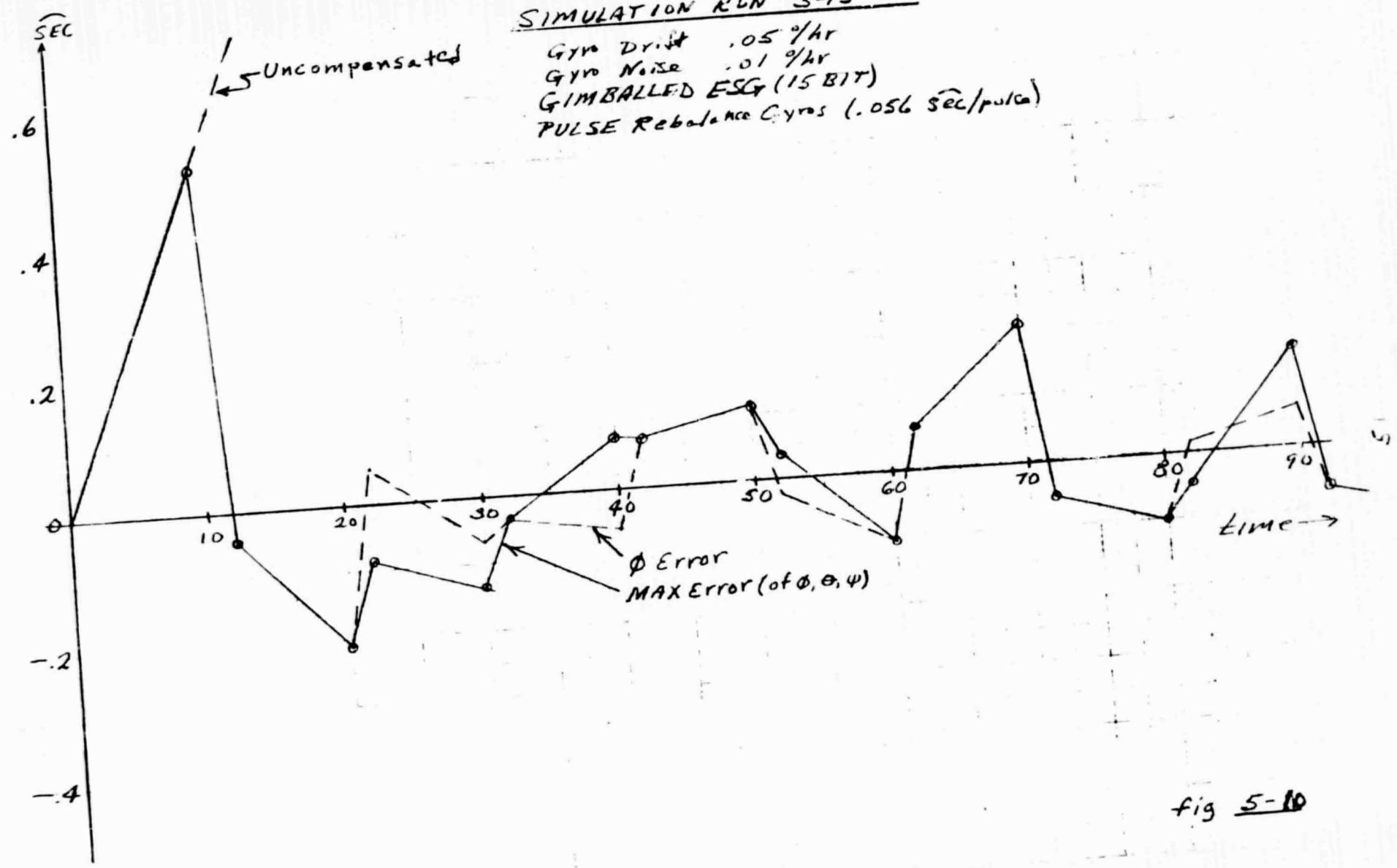
HPARS
SIMULATION RUN #3-15
Gyro Drift .05 °/hr
Gyro Noise .01 °/hr
GIMBALLED ESG (15 BIT)
PULSE Rebalance Gyros (.056 sec/pulse)
SEC
Uncompensated
.6
.4
.2
0
-.2
-.4
10
20
30
40
50
60
70
80
90
Time →
Ø Error
MAX Error (of Ø, Θ, Ψ)

fig 5-10

JM
11/13/68

HPARS
Simulation Run # 11-13

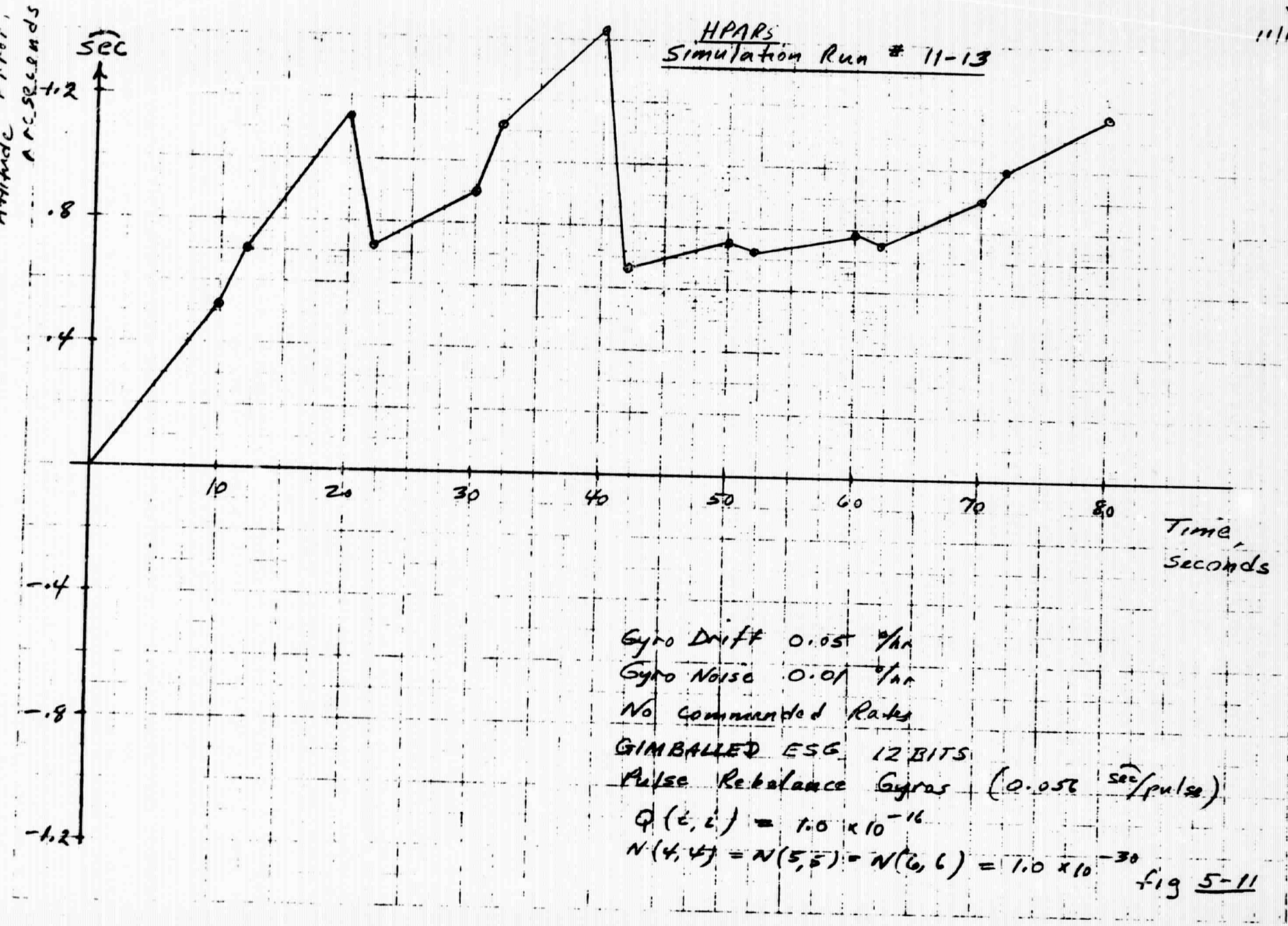

Gyro Drift 0.05° /hr
Gyro Noise 0.01 °/hr
No commanded Rates
GIMBALLED ESG 12 BITS
Pulse Rebalance Gyros (0.05" sec/pulse)
$Q(i,i) = 1.0 \times 10^{-16}$
$N(4,4) = N(5,5) = N(6,6) = 1.0 \times 10^{-30}$

fig 5-11

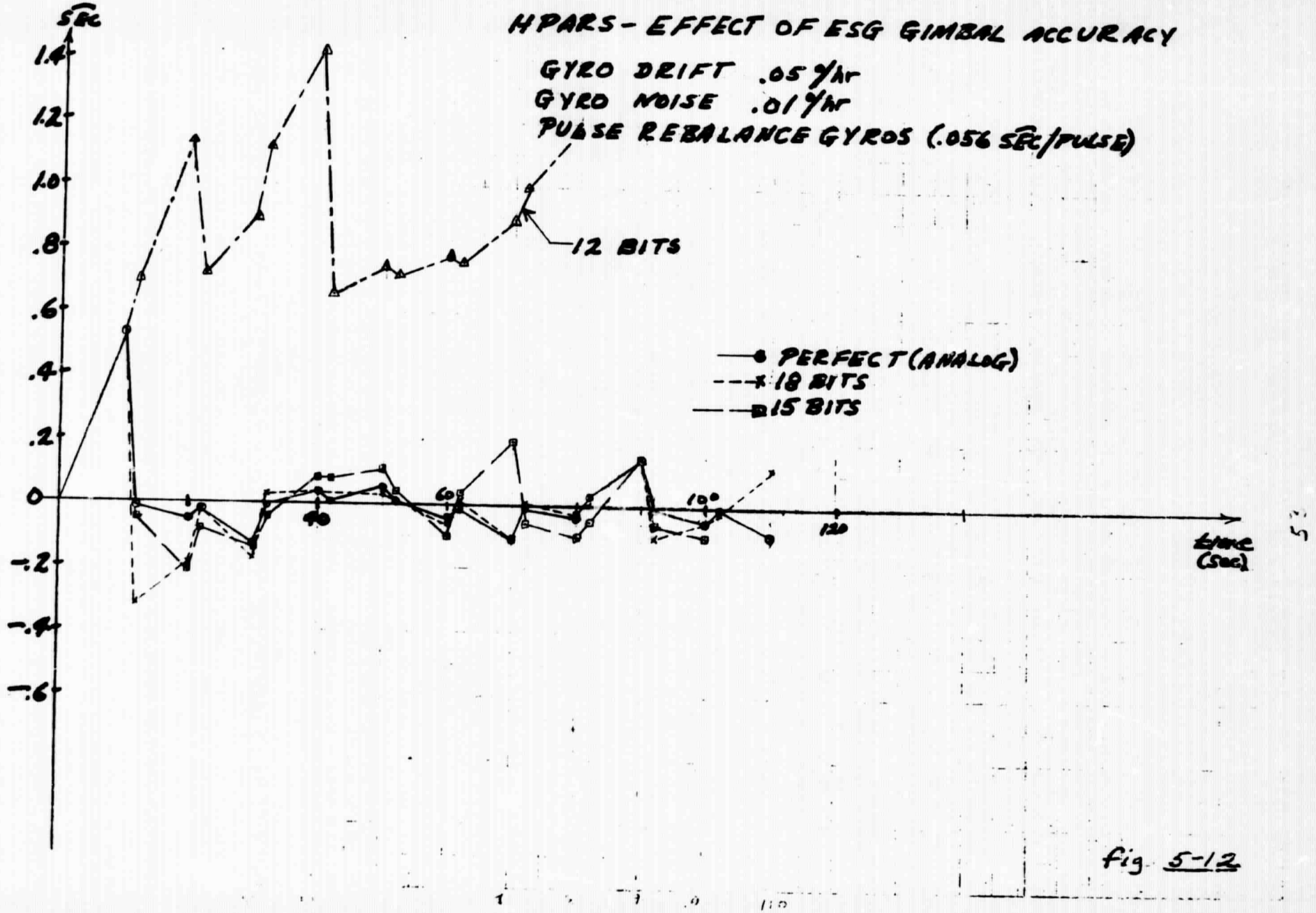
HPARS - EFFECT OF ESG GIMBAL ACCURACY
GYRO DRIFT .05°/hr
GYRO NOISE .01°/hr
PULSE REBALANCE GYROS (.056 SEC/PULSE)
12 BITS
PERFECT (ANALOG)
18 BITS
15 BITS
SEC
1.4
1.2
1.0
.8
.6
.4
.2
0
-.2
-.4
-.6
40
60
100
120
time (sec)

fig 5-12

E. The Effect of Q and N

The major filter design variables for fine tuning control were the Q and N matrices. They are relatively dependent upon the hardware and its error sources and thus would require some adjustment if different hardware were substituted for any of the HPARS components.

Figures 5-13 through 5-17 show the effect of different values of Q and N (primarily N). Finally the value of N was decreased to 1×10^{-30} which is the near optimum value used during the majority of the subsequent runs.

Figures 5-18 through 5-20 show the effect of a mismated between the ESG error and the value of Q (the estimate of ESG error). In Figure 5-18 the value of Q is relatively large but a perfect ESG is simulated. The result is an attitude bias. Figure 5-19 is similar but the gyro noise is reduced thus showing more clearly the bias present.

Figures 5-20, 5-21, and 5-22 again show the effect of Q/ESG mismated. In Figure 5-20 Q is small (1×10^{-30}) but a 12 BIT ESG is simulated, thus producing a bias in the attitude error. In Figure 5-21 the ESG is improved to 15 BIT thus reducing the bias error, and in Figure 5-22 the correct combination of Q and ESG resolution is used and no bias error is present. In these last three runs note the effect of using a coarse (.224 sec/pulse) pulse weight for the strapped down gyros.

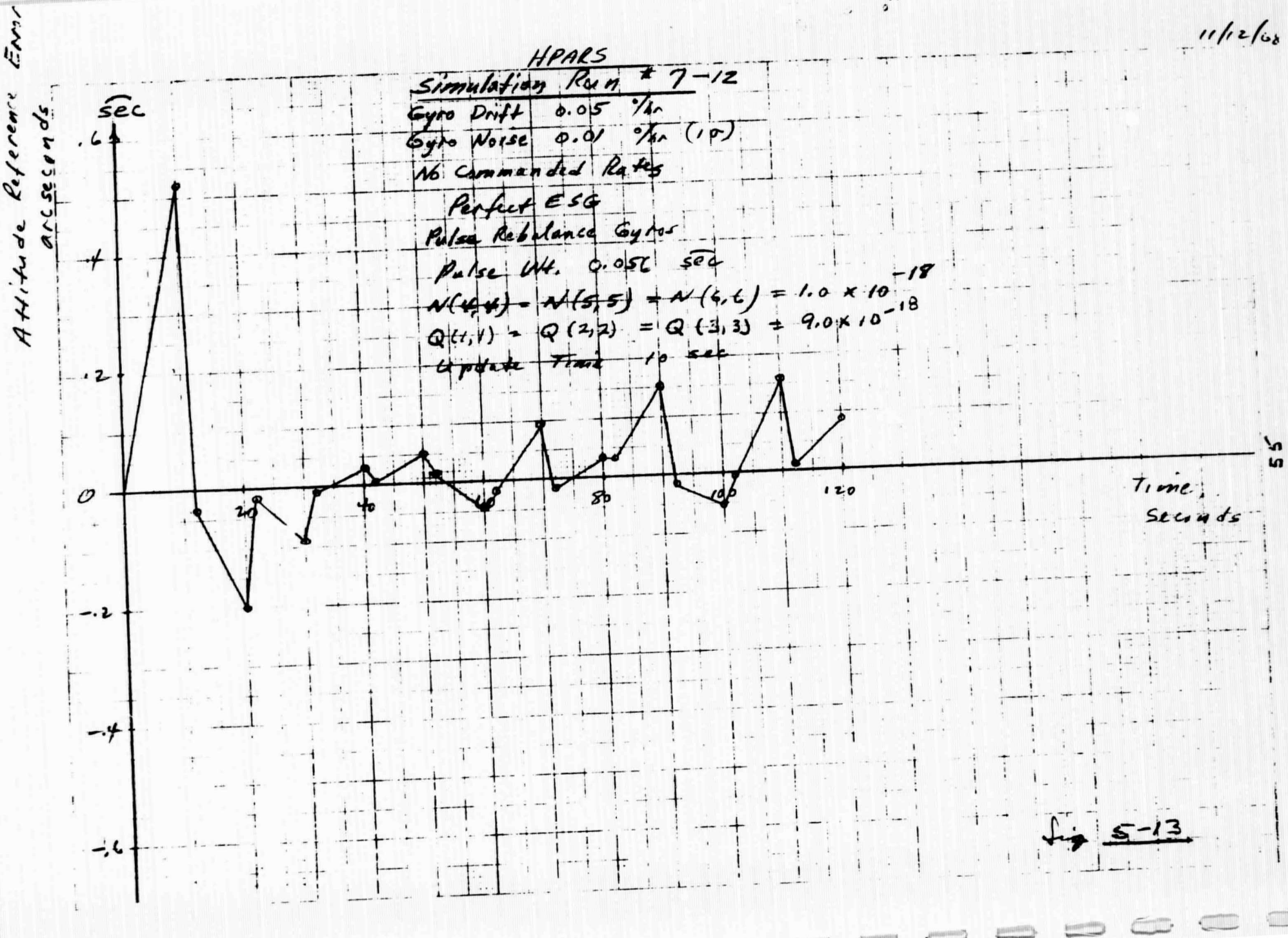
HPARS
Simulation Run # 7-12
Gyro Drift 0.05 °/hr
Gyro Noise 0.01 °/hr (1σ)
No Commanded Rates
Perfect ESG
Pulse Rebalance Gyros
Pulse Wt. 0.05 sec
N(4,4) = N(5,5) = N(6,6) = 1.0 × 10^-18
Q(1,1) = Q(2,2) = Q(3,3) = 9.0 × 10^-18
Update Time 1.0 sec
Attitude Reference Error arcseconds
sec
.6
.4
.2
0
-.2
-.4
-.6
20
40
60
80
100
120
Time, Seconds

Fig 5-13

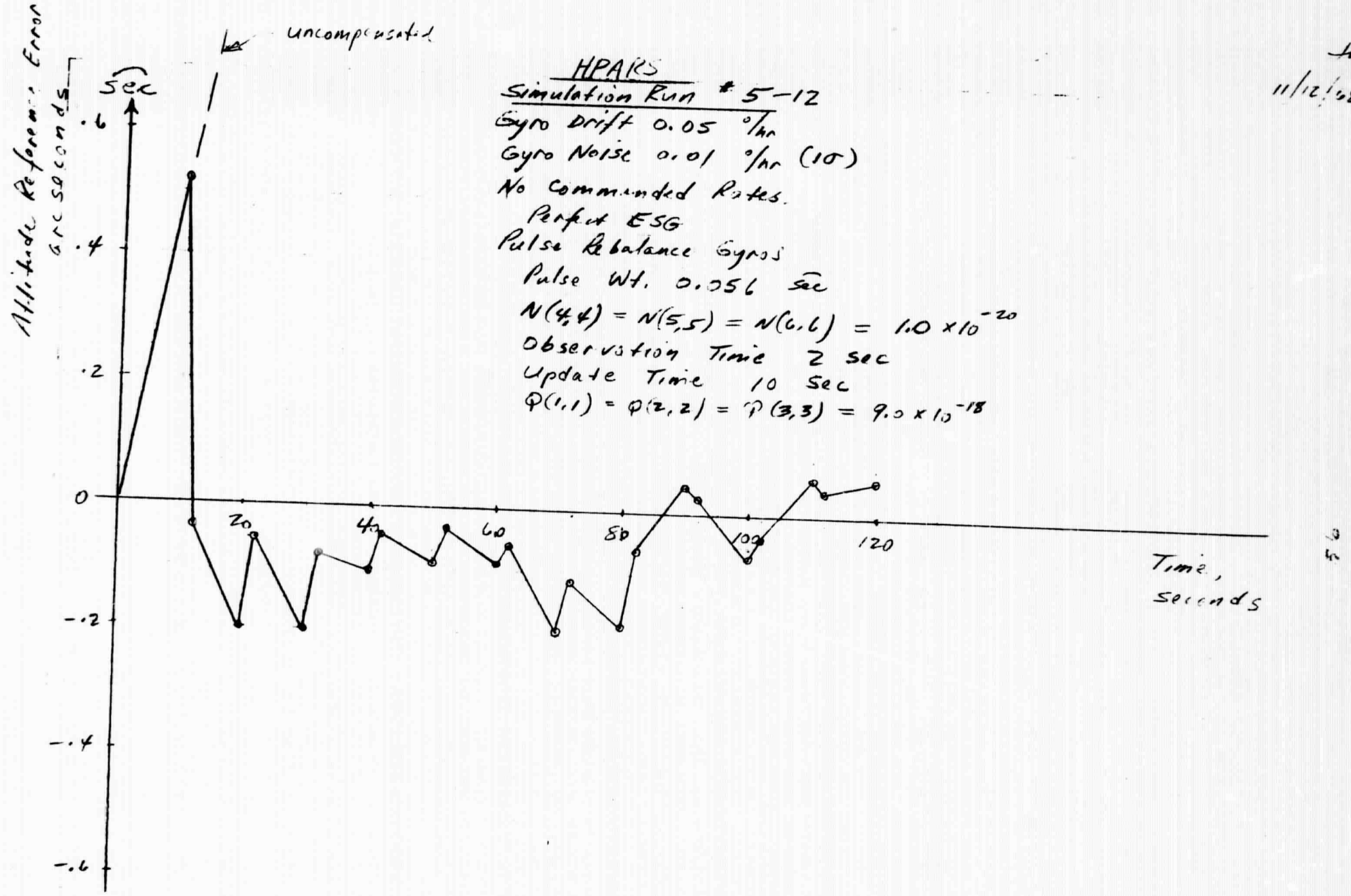

HPARS
Simulation Run # 5-12

Gyro Drift 0.05 °/hr
Gyro Noise 0.01 °/hr (1σ)
No Commanded Rates.
Perfect ESG
Pulse Rebalance Gyros
Pulse Wt. 0.056 sec
$N(4,4) = N(5,5) = N(6,6) = 1.0 \times 10^{-20}$
Observation Time 2 sec
Update Time 10 sec
$Q(1,1) = Q(2,2) = Q(3,3) = 9.0 \times 10^{-18}$

11/12/68

fig 5-14

HPARS
Simulation Run # 6-12
Gyro Drift 0.05 °/hr
Gyro Noise 0.01 °/hr (1σ)
No commanded rates
Perfect ESG
Pulse Rebalance Gyros (0.056 sec/pulse)
$N(4,4) = N(5,5) = N(6,6) = 1.0 \times 10^{-20}$
$Q(1,1) = Q(2,2) = Q(3,3) = 2.0 \times 10^{-25}$

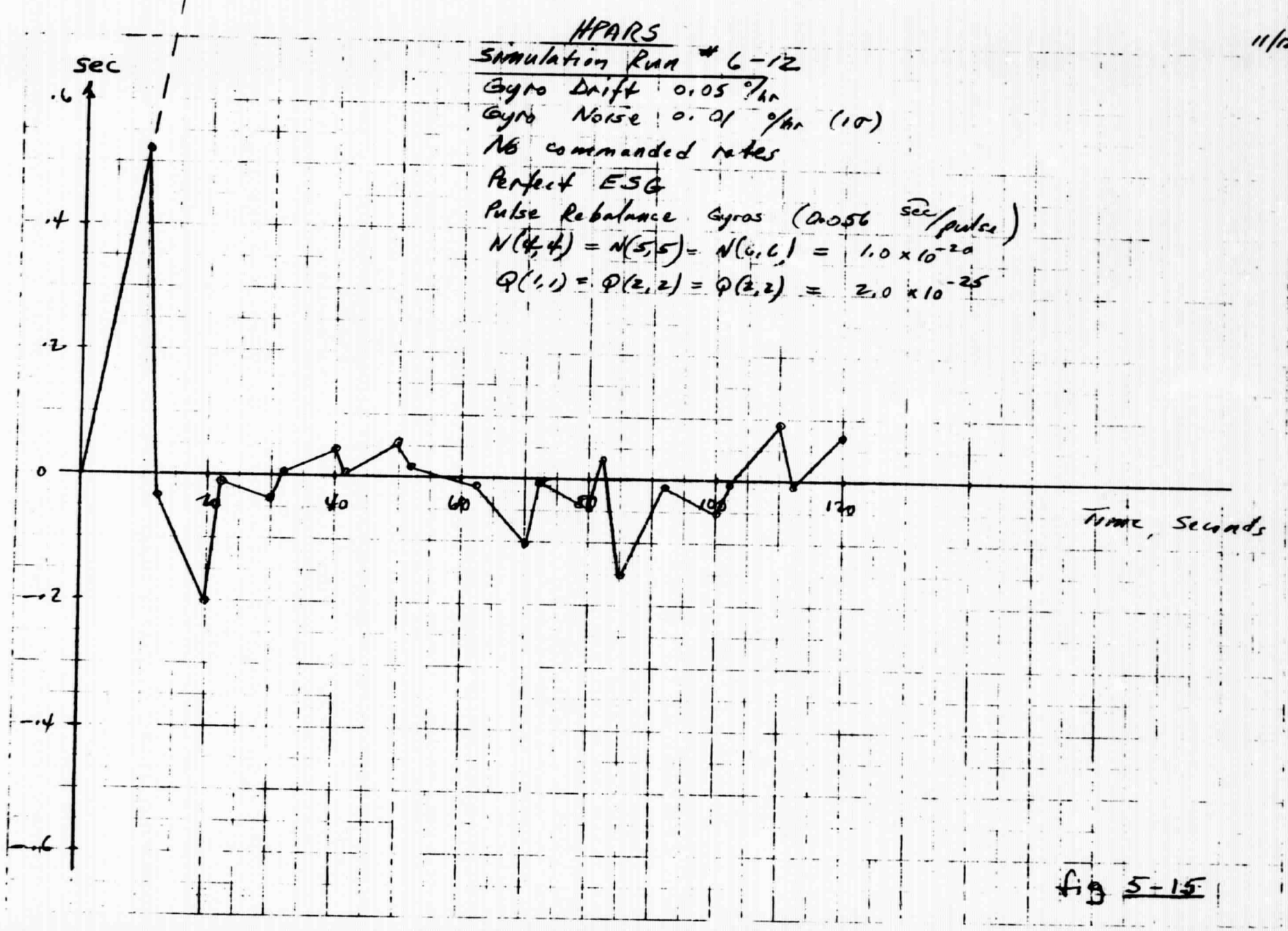

fig 5-15

HPARS

Simulation Run # 6-13

Gyro Drift 0.05 °/hr

Gyro Noise 0.01 °/hr (1σ)

No Commanded Rates

Pulse Rebalance Gyros (0.056 sec/pulse)

$N(4,4) = N(5,5) = N(6,6) = 1.0 \times 10^{-3}$

$Q(i,i) = 1.0 \times 10^{-30}$

$N(1,1) = N(2,2) = N(3,3) = 1.0 \times 10^{-18}$

Perfect ESA

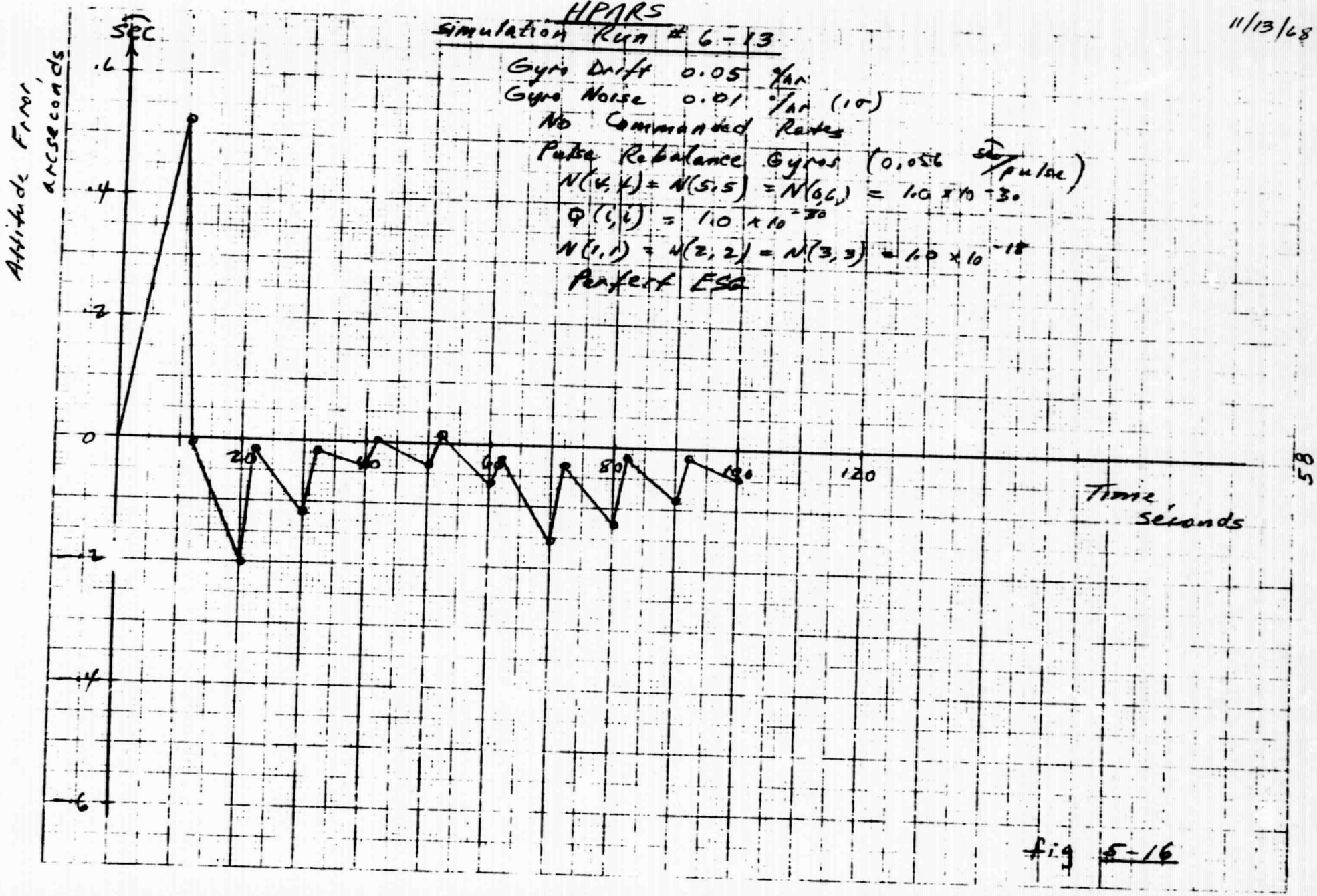

fig 5-16

HPARS

Simulation Run # 5-13

Gyro Drift 0.05 °/hr

Gyro Noise 0.01 °/hr (1σ)

No Commanded Rates

Pulse Rebalance Gyros (0.056 sec/pulse)

$N(4,4) = N(5,5) = N(6,6) = 1.0 \times 10^{-30}$

$Q(i,i) = 1.0 \times 10^{-30}$

Perfect ESG

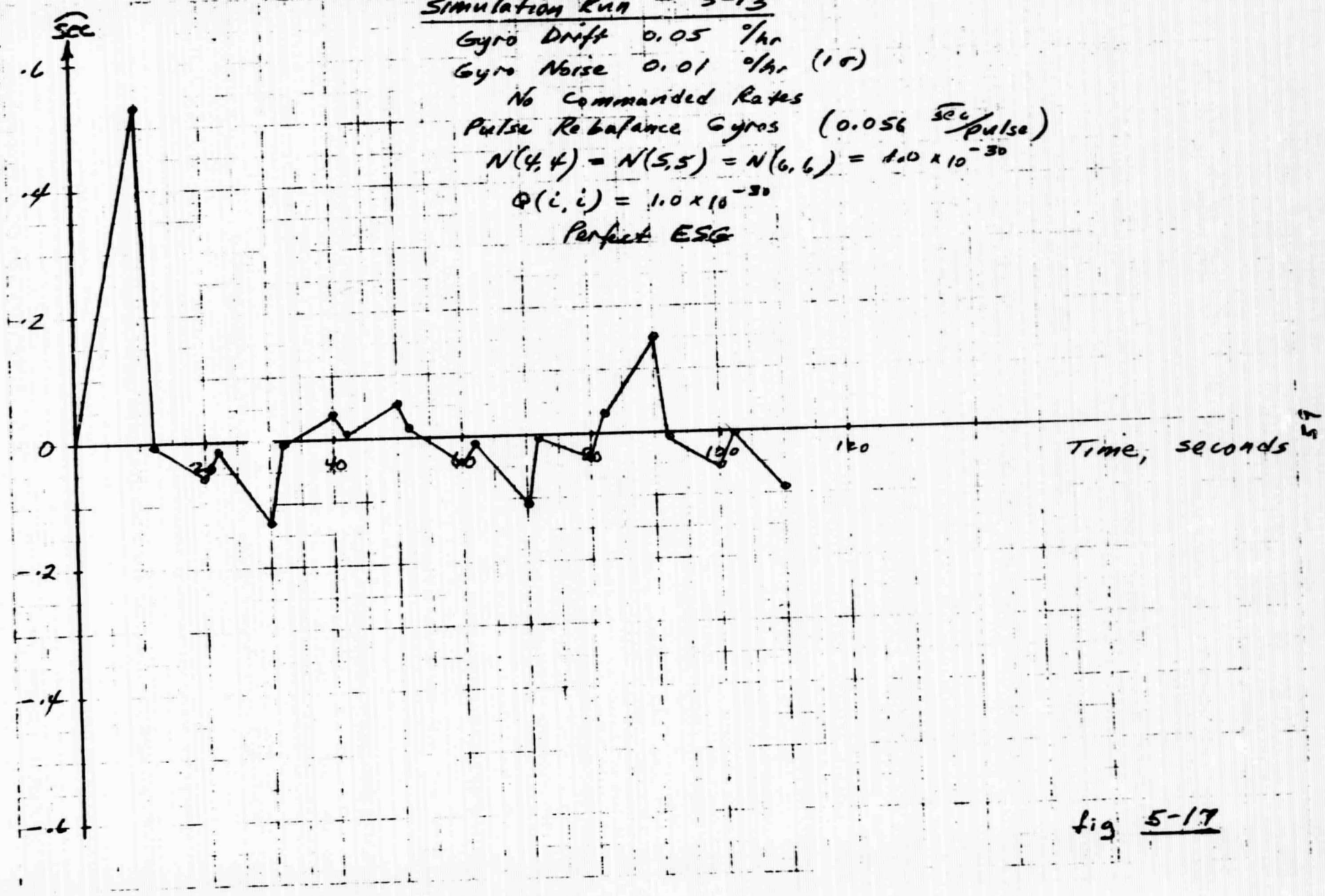

fig 5-17

SH 11/13/68

HPARS
Simulation Run # 1-13

Gyro Drift 0.05 °/hr
Gyro Noise 0.01 °/hr (1σ)
No commanded Rates
Perfect ESG
Analog Rebalance Gyros
$N(\phi,\phi) = N(\theta,\theta) = N(\psi,\psi) = 1.0 \times 10^{-30}$
$Q(i,i) = 9.0 \times 10^{-18}$

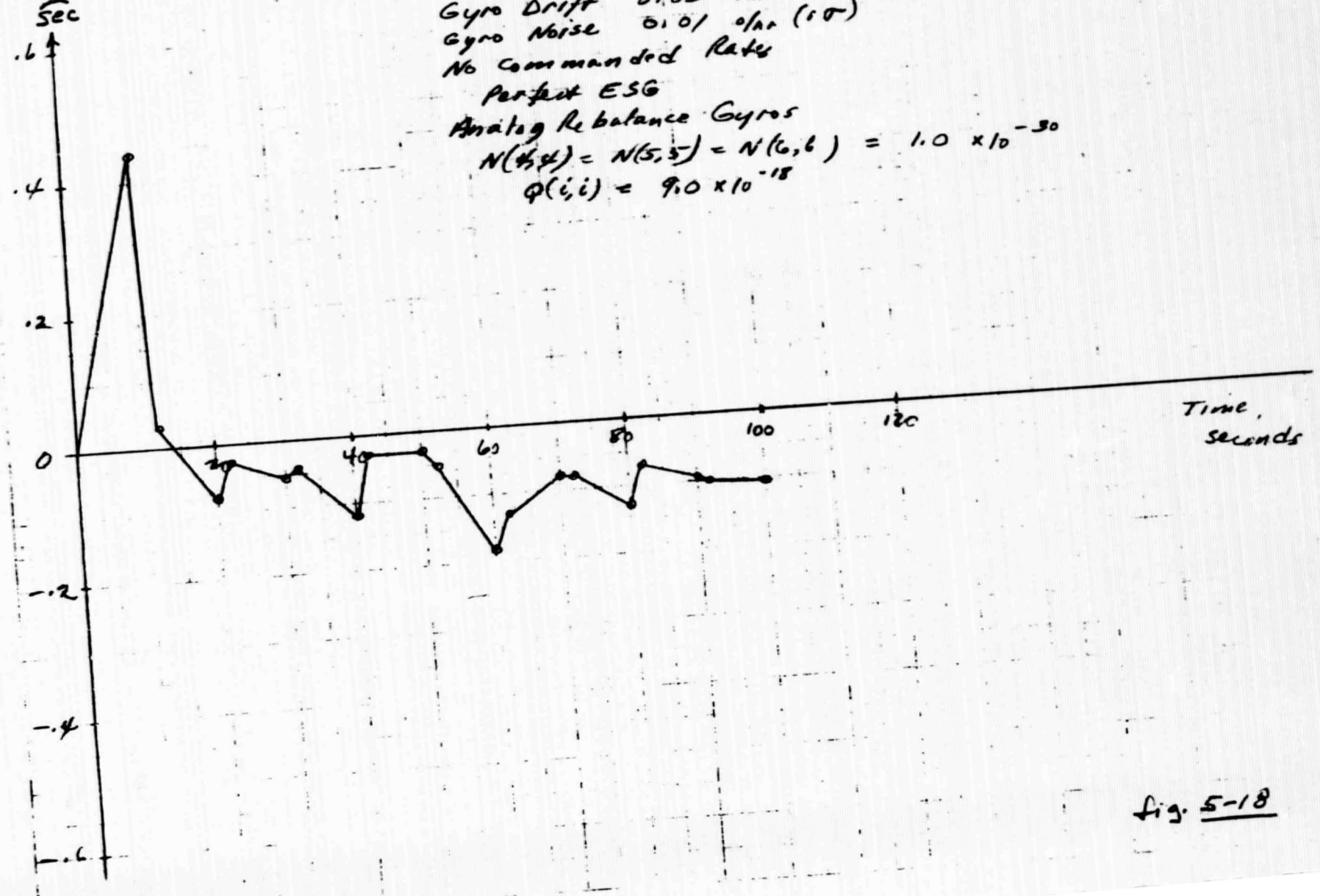

fig. 5-18

AH

11/13/68

HPARS

Simulation Run #2-13

Gyro Drift 0.05 °/hr
Gyro Noise 0.001 °/hr (1σ)
No Commanded Rates
Perfect ESG
Analog Rebalance Gyros
$N(4,4) = N(5,5) = N(6,6) = 1.0 \times 10^{-30}$
$Q(i,i) = 9.0 \times 10^{-18}$

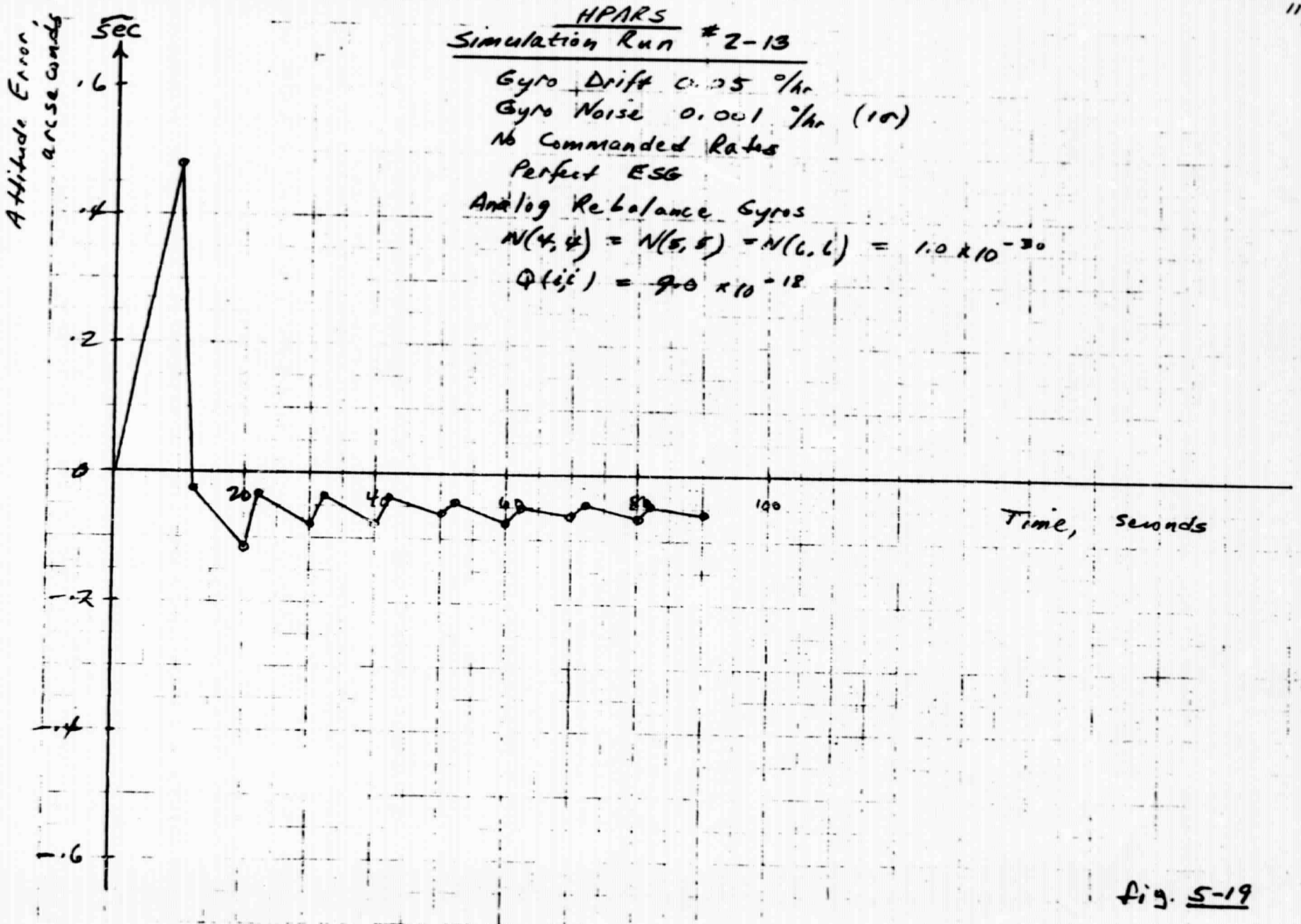

fig. 5-19

HPARS
Simulation Run # 8-14

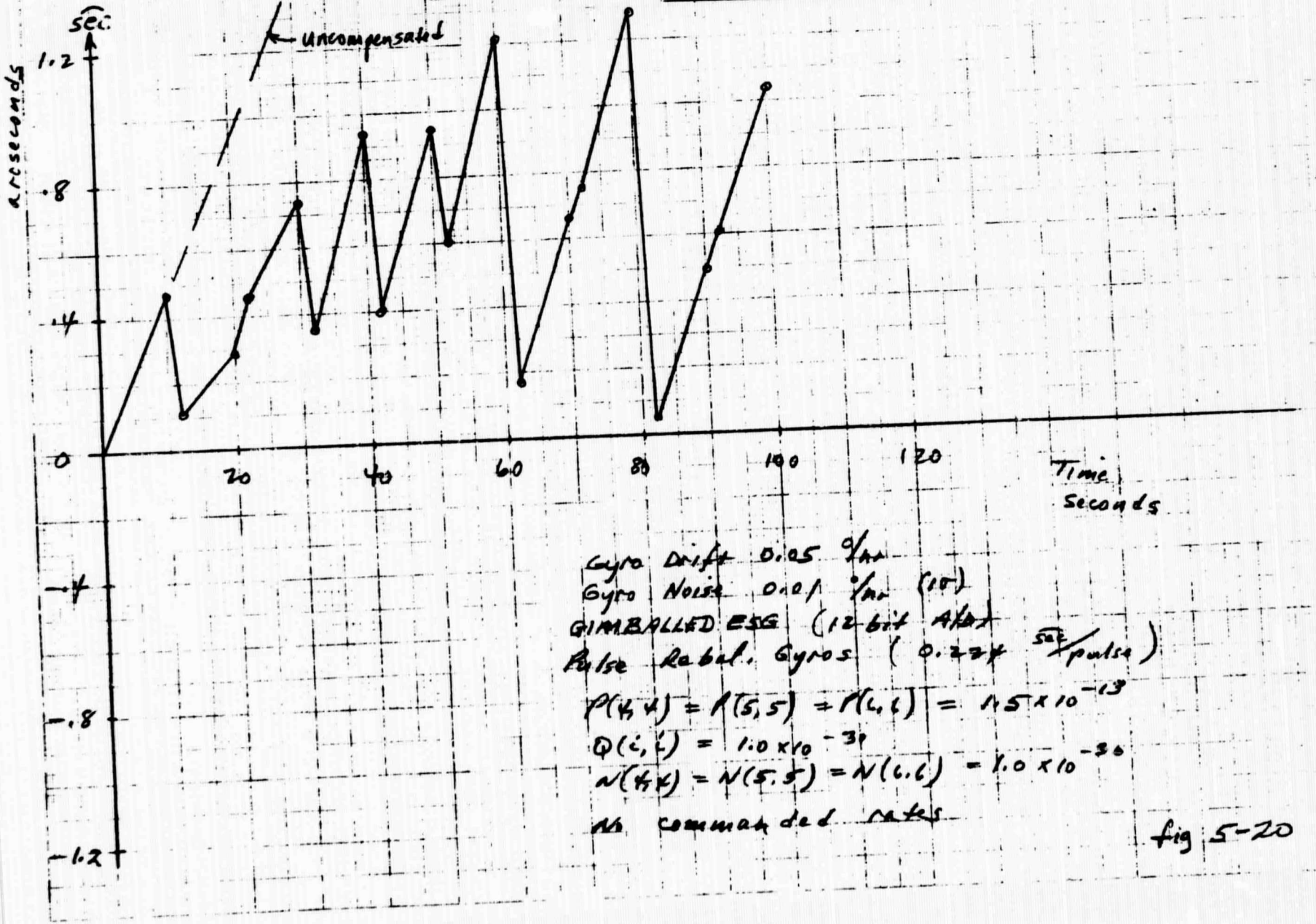

Gyro Drift 0.05 °/hr
Gyro Noise 0.01 °/hr (1σ)
GIMBALLED ESG (12 bit A/D)
Pulse Rebal. Gyros (0.22" sec/pulse)

$P(4,4) = P(5,5) = P(6,6) = 1.5 \times 10^{-13}$
$Q(i,i) = 1.0 \times 10^{-30}$
$N(4,4) = N(5,5) = N(6,6) = 1.0 \times 10^{-30}$
No commanded rates

fig 5-20

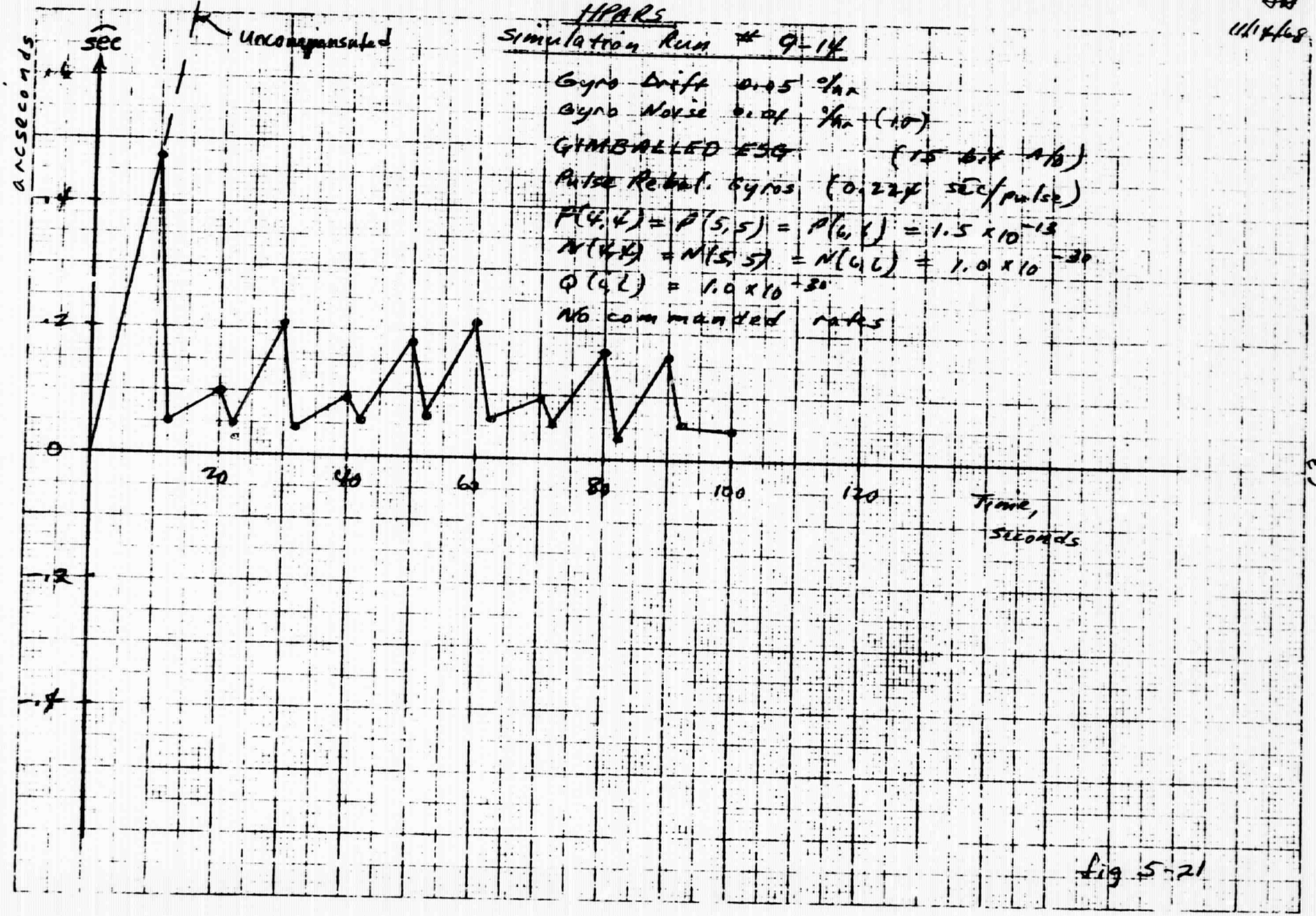
HPARS
Simulation Run # 9-14
Gyro Drift 0.05 °/hr
Gyro Noise 0.01 °/hr (1σ)
GIMBALLED ESG (15 bit A/D)
Pulse Rebal. Gyros (0.22" sec/pulse)
P(4,4) = P(5,5) = P(6,6) = 1.5 x 10^-13
N(4,4) = N(5,5) = N(6,6) = 1.0 x 10^-20
Q(6,6) = 1.0 x 10^-30
No commanded rates
Uncompensated
sec
arcseconds
+.4
+.2
0
-.2
-.4
20
40
60
80
100
120
Time, seconds
fig 5-21

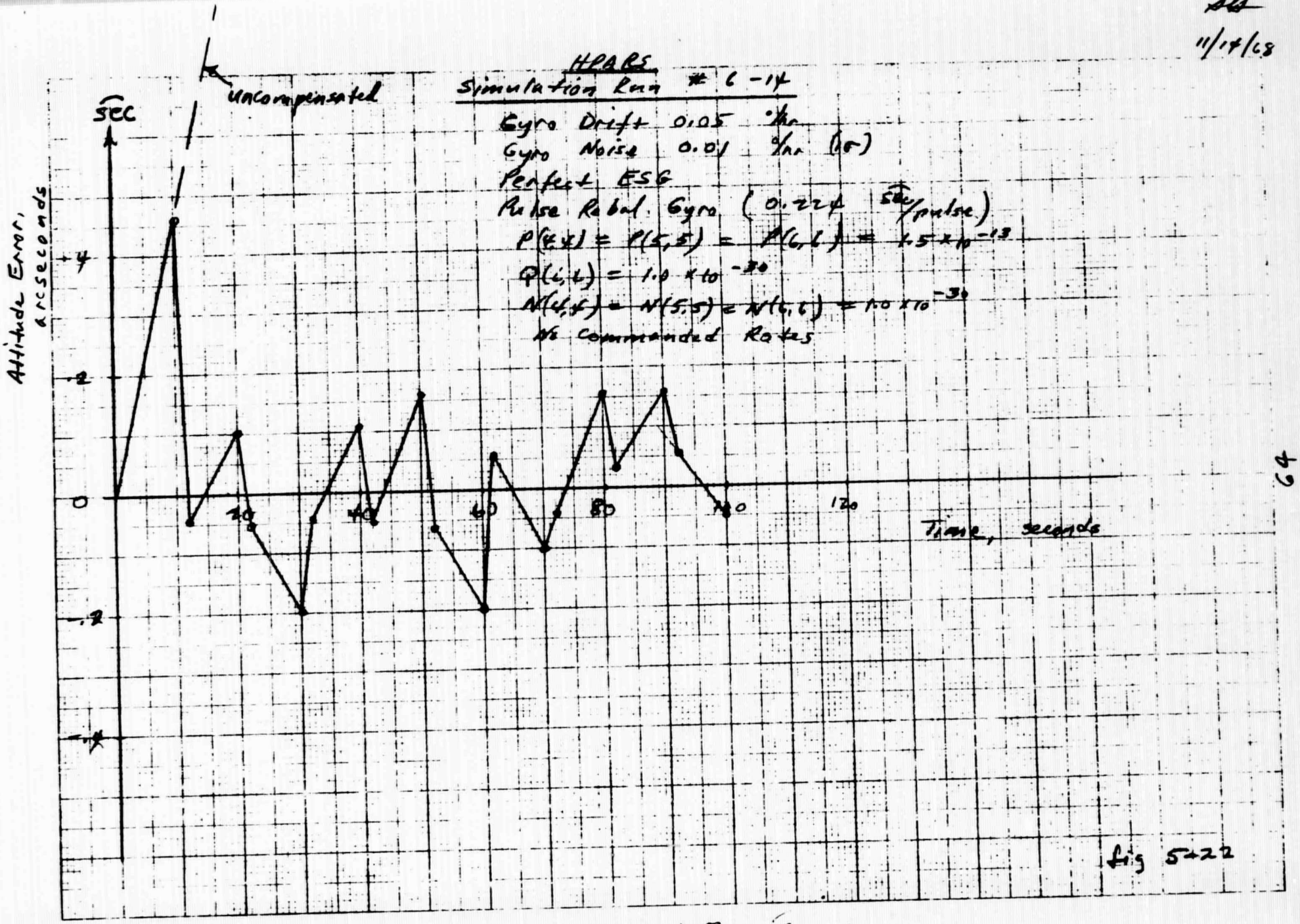
HRARS
Simulation Run # 6-14
Gyro Drift 0.05 °/hr
Gyro Noise 0.01 °/hr (1σ)
Perfect ESG
Pulse Rebal. Gyro (0.22" sec/pulse)
P(4,4) = P(5,5) = P(6,6) = 1.5 x 10^-13
Q(i,i) = 1.0 x 10^-30
N(4,4) = N(5,5) = N(6,6) = 1.0 x 10^-30
No Commanded Rates
Uncompensated
sec
Attitude Error, arcseconds
+4
+2
0
-2
-4
20
40
60
80
100
120
Time, seconds
fig 5-22
τ = .102 sec

F. Commanded Rates

Figures 5-23 and 5-24 show system operating in response to the command rate profile described in section IV. The errors shown during the first 40 sec (when the commands are present) are errors with respect to the command, not system null. Two items are of interest:

a) The system accuracy during the maneuver is poor

b) Upon completion of the manuever the system accuracy returns to normal.

Attitude information is not lost during the maneuver but it may be advantageous to bound this error to some practical value. Additional study to improve the system dynamic accuracy is recommended.

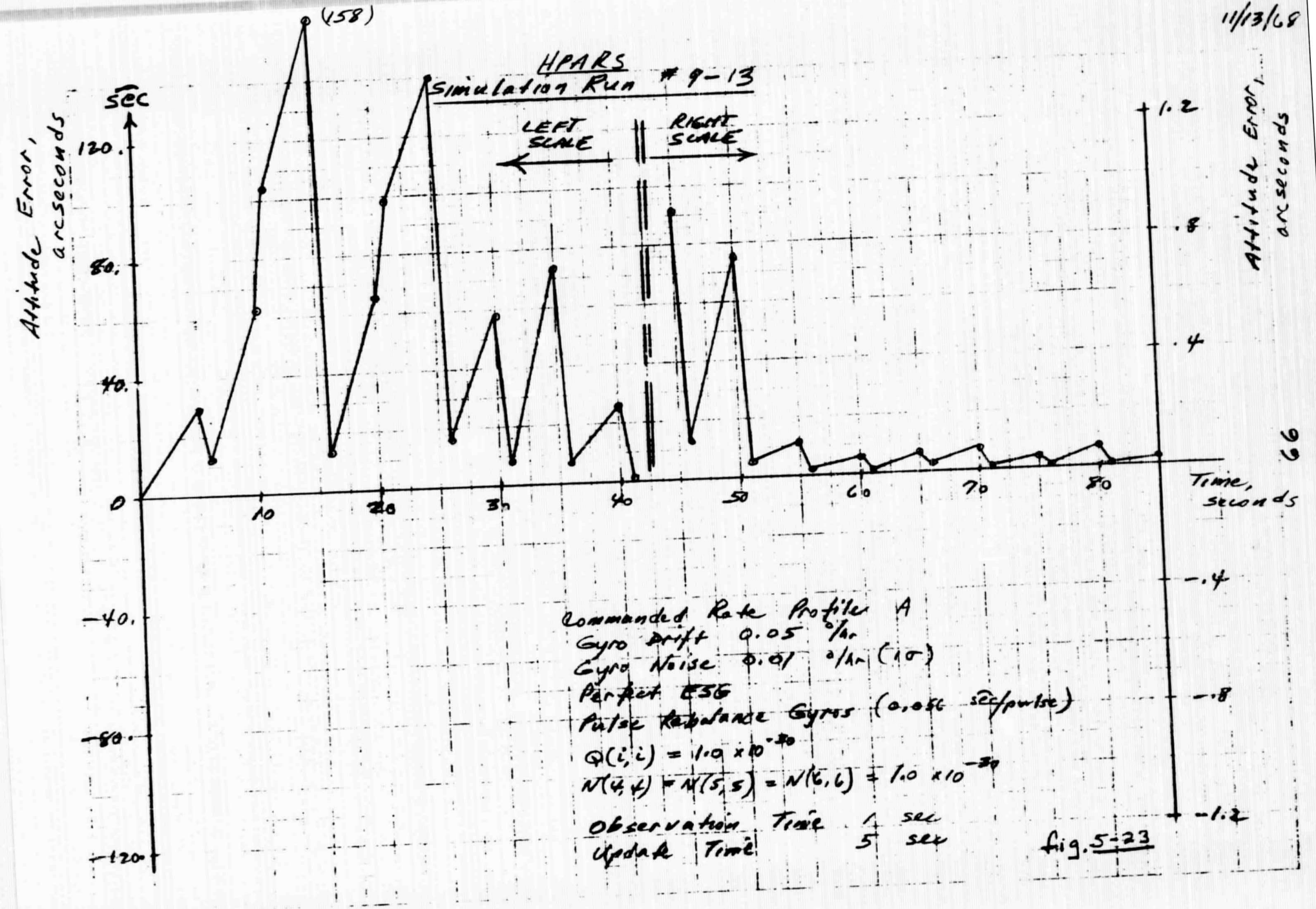
HPARS
Simulation Run # 9-13
(158)
LEFT SCALE
RIGHT SCALE
Attitude Error, arcseconds
sec
120.
80.
40.
0
-40.
-80.
-120
10
20
30
40
50
60
70
80
Time, seconds
1.2
.8
.4
-.4
-.8
-1.2
Attitude Error, arcseconds
Commanded Rate Profile A
Gyro Drift 0.05 °/hr
Gyro Noise 0.01 °/hr (1σ)
Perfect ESG
Pulse Rebalance Gyros (0.05 sec/pulse)
Q(i,i) = 1.0 x 10^-30
N(4,4) = N(5,5) = N(6,6) = 1.0 x 10^-30
Observation Time 1 sec
Update Time 5 sec

fig. 5-23

AM
11/04/68

HPARS
Simulation Run # 5-14

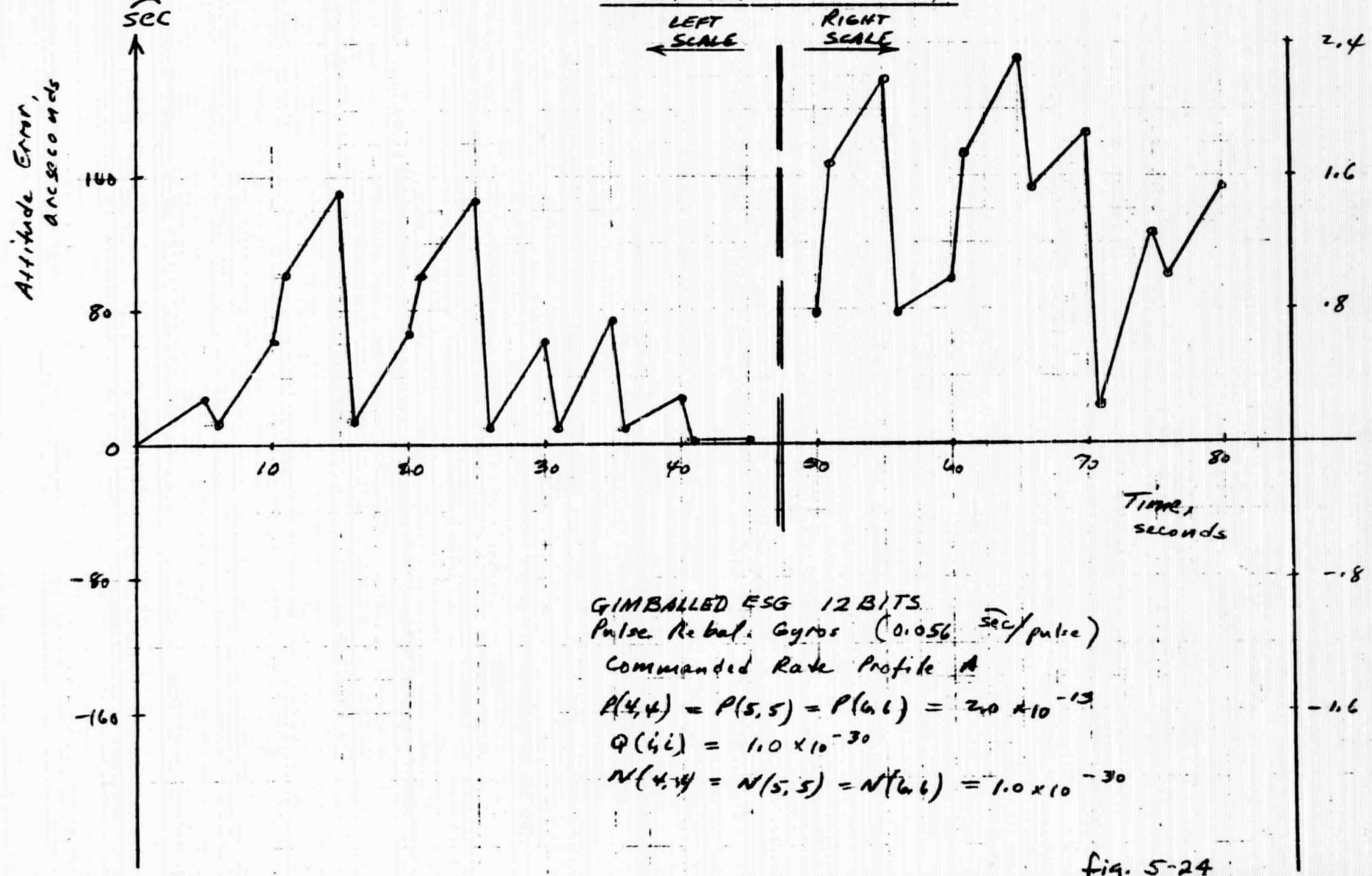

GIMBALLED ESG 12 BITS
Pulse Rebal. Gyros (0.056 sec/pulse)
Commanded Rate Profile A

$P(4,4) = P(5,5) = P(6,6) = 2.0 \times 10^{-13}$

$Q(i,i) = 1.0 \times 10^{-30}$

$N(4,4) = N(5,5) = N(6,6) = 1.0 \times 10^{-30}$

fig. 5-24

G. Laser Gyro Runs

Few runs were performed with the laser gyro due primarily to the HPARS simulation being set up for low rate inputs thus not requiring the benefits of the laser. It was anticipated that the simulation would be modified to allow larger rate inputs but sufficient time was not available in the program to complete this portion.

One run is included here (Figure 5-25) which has commanded rates until 40 sec. The dynamic error is large due to the filter characteristics, not the gyro itself. The laser for this run did not have drift or noise simulated, only the quantization error. The performance is similar to a perfect (no noise) PRG gyro with the exception of the error being bounded no better than the resolution of the laser gyro ($\pm.38$ $\widehat{\text{sec}}$). This of course is the obvious disadvantage of the laser and point out why it should be used to supplement a conventional gyro at rates beyond the conventional gyro's capability.

JH
11/15/68

HPARS
Simulation Run # 6-15

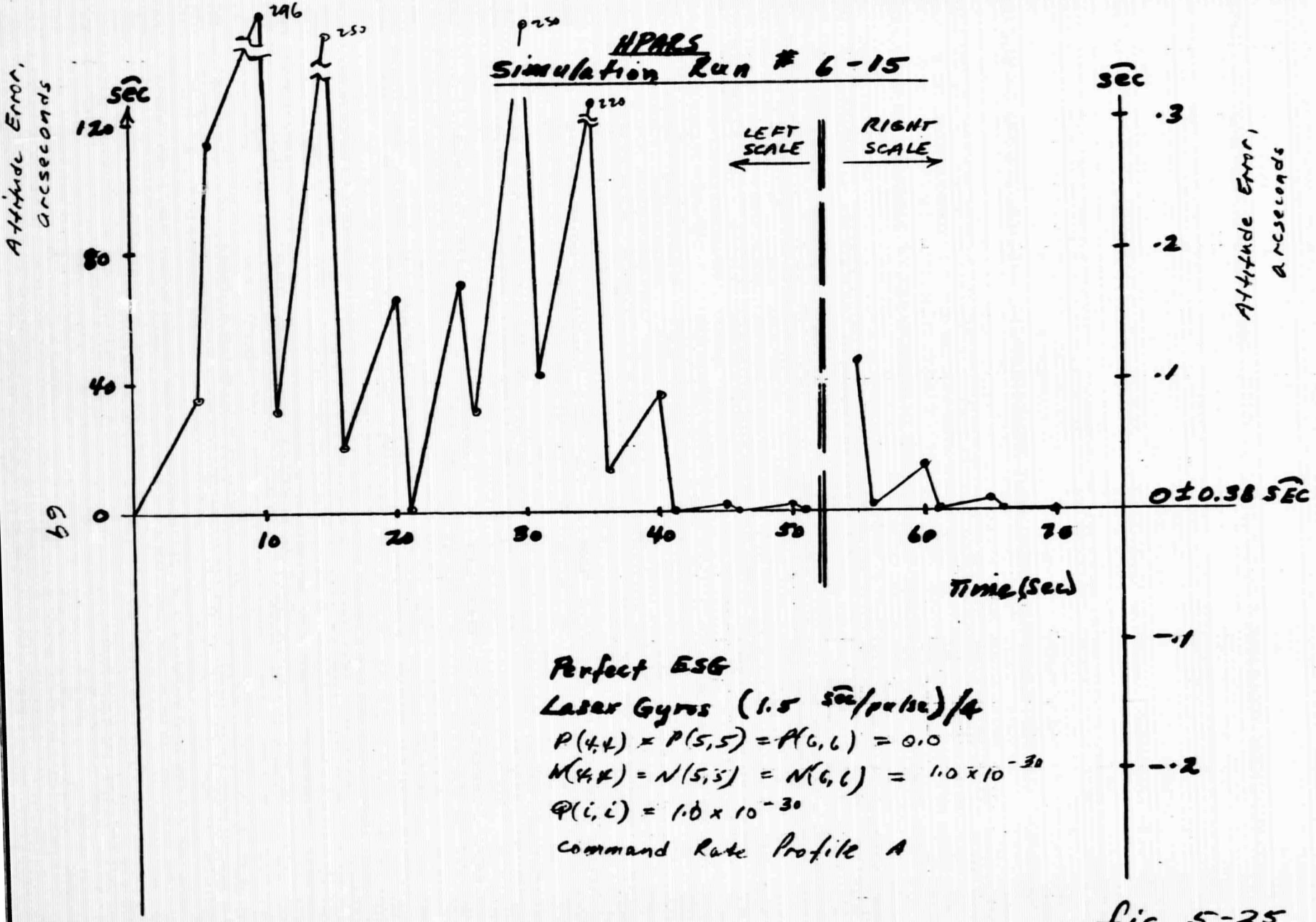

Perfect ESG

Laser Gyros (1.5 sec/pulse)/4

$P(4,4) = P(5,5) = P(6,6) = 0.0$

$N(4,4) = N(5,5) = N(6,6) = 1.0 \times 10^{-30}$

$Q(i,i) = 1.0 \times 10^{-30}$

Command Rate Profile A

fig 5-25

VI. HARDWARE TESTS

A single-axis gyro and pulse rebalance electronics were available to allow a test using the newly designed BMEC filter, thus adding confidence to the design and concept. An autocollimotor provided the attitude update information in lieu of the ESG, and the input rates were kept below the saturation level of the gyro/electronics (.15°/Sec.), thus negating the need for the laser gyro.

The test setup is shown in Figure 6 1. The tests were performed about the azimuth axis of a six-foot diameter, air-bearing table. The table was balanced bottom heavy to maintain stability about the lateral axes.

Tests were performed using either of two methods:

a) The table was floated and maintained in a locked position by the positioning ring. A null reading was taken through the autocollimotor and the gyro output pulses switched to enter the up/down counter and computer. The positioning ring was carefully slid back to free the table and reaction jets on the table were manually pulsed until a rate between approximately .02 and .12 deg./sec. was established about the table azimuth axis. After moving through approximately 15 degrees, the table rate was reversed (using the reaction jets) and the table returned to a position near the null position. At this point the positioning ring was used to bring the table (and gyro) back to the original null position as determined by the autocollimotor. At this point an "update" signal was programmed and the sequence repeated starting the table in the opposite direction. A sequence of 5-10 runs and "updates" was performed per test.

This page intentionally left blank

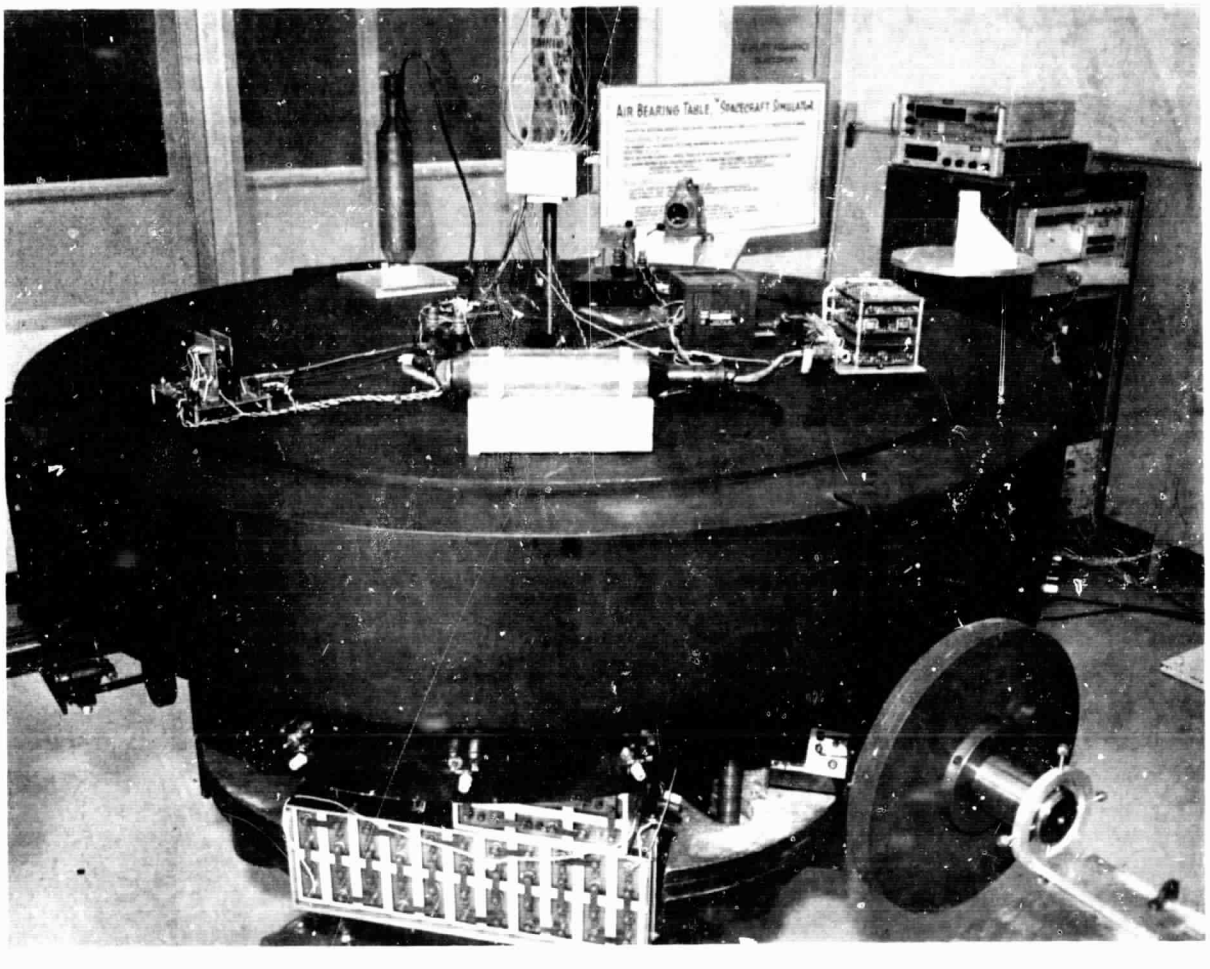

Figure 6-1(b). HPARS Single Axis Test

The earth rate component was subtracted via the computer from the gyro data.

b) A much simpler but less realistic test was performed by leaving the table in a locked position and letting only earth-rate precess the gyro. An "update" was given at one-minute intervals. This has the advantage of eliminating the autocollimotor and mirror errors.

The autocollimotor used was:

accuracy - 1 sec

mirror - .5 sec

The gyro was a Honeywell GG287 engineering model with the following characteristics:

Torquer-highly linear, moving coil, P.M.

Wheel Momentum - 2×10^5 cgs

Torque Capability - 10°/sec.

Torque Linearity - ± .05%

Rate Threshold - 10^{-7} rad/sec.

Reaction torque - approximately .2°/hr. max.

g-sensitive drift - approximately .3°/hr. max.

gyro noise - approximately .3°/hr. max.(.01-10Hz)

Gyro Electronics

The pulse rebalanced gyro loop (Figure 6-2) utilizes "pulse on demand" torquing. As the name implies, this system delivers current pulses to the gyro torquer at a rate which is just sufficient to establish gimbal equilibrium with rate input. A rate input will produce a gimbal displacement and, hence, a gyro signal generator output. This output is a suppressed carrier signal which is demodulated and amplified to yield a d-c voltage whose polarity indicates the direction of rotation and whose magnitude is proportional to the rate input. A voltage-to-frequency conversion is added which provides pulses whose rate is proportional to the input voltage.

These pulses provide gating, in the switching bridge, for the torquing current derived from the constant current supply. Thus, the gyro torquer receives the proper amount of current (amphere seconds/second) to balance the gimbal against the rate input.

Amp-Demand-Amp

An error signal from the gyro signal generator (modulated 19.2 kc) is amplified and demodulated. The output of the demodulator is a d-c voltage whose amplitude is proportional to the gyro displacement angle and whose polarity indicates the direction of displacement. This d-c voltage is further amplified to develop the proper gain scale factor for loop operation.

Voltage-to-Frequency Converter

The equivalent attitude error signal from the amp-demod-amp is sensed by the voltage-to-frequency converter. The converter is a pulse-reset-integrator which generates pulses on the positive or negative lines corresponding to the polarity of the input attitude error and at a frequency proportional to its magnitude.

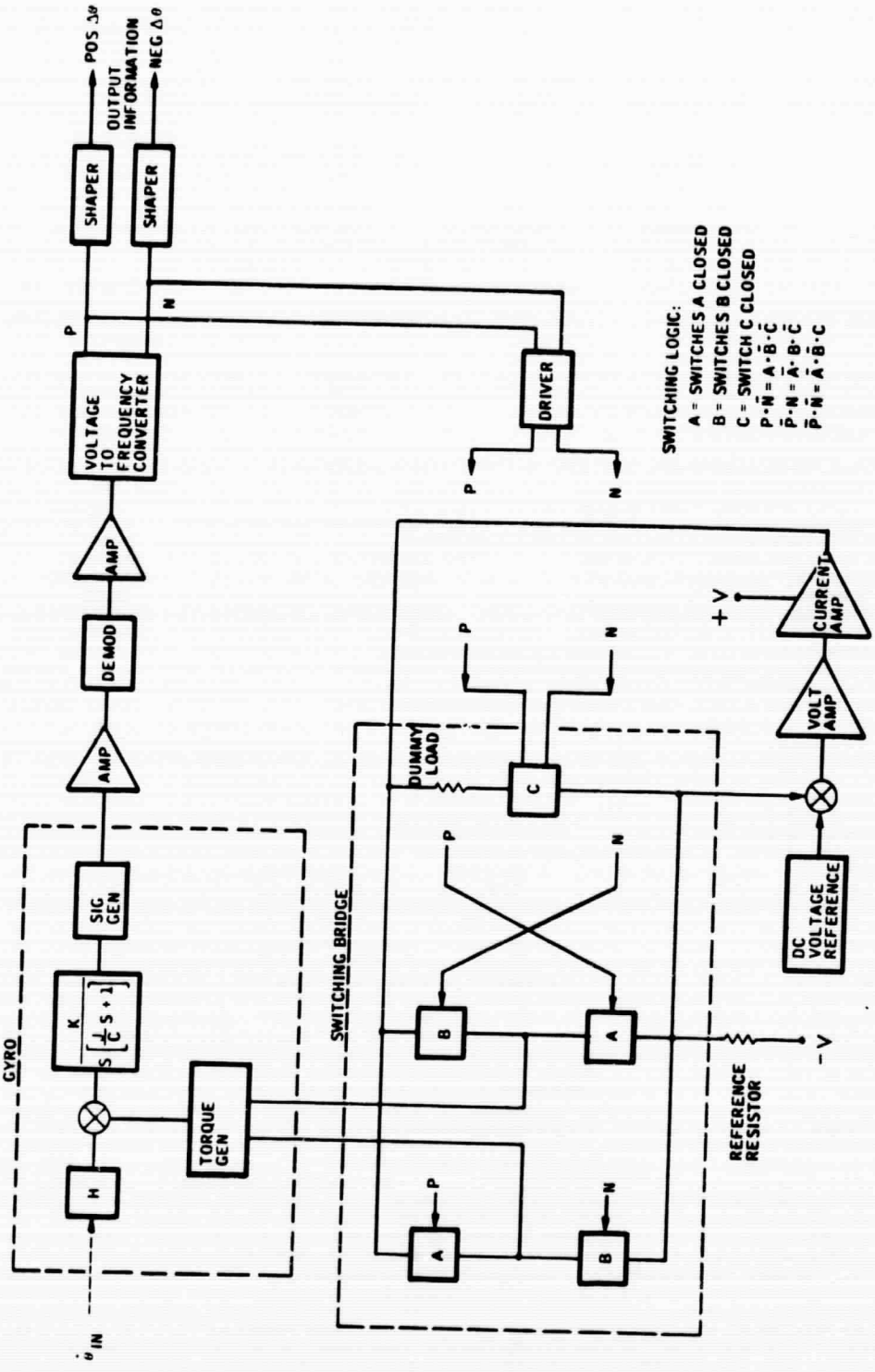

Figure 6-2. Functional Block Diagram of Gyro Sensor Loop Closure Electronics for HPARS Test (Single Axis)

Switching Bridge

The switching bridge receives the command pulses from the voltage-to-frequency converter and gates the torquing pulses through the gyro torquer in the proper direction. When no torquing pulse is needed, the precision current is gated through the dummy load. This technique is employed to keep a constant load on a pulse amplifier. To ensure accuracy, the energy content of the torquer current pulses is carefully controlled. By the use of clocked drive pulse and a constant current supply, the energy input into the bridge can be closely controlled. To maintain accuracy, the switches must neither add nor subtract from the energy injected into the bridge.

Oscillator and Countdown and Clock Pulse Generators

A crystal oscillator provides the basic time base for the system. Frequency stability is achieved by maintaining the oscillator circuit at a near constant temperature by mounting it on the gyro block. The oscillator runs at 19.2 kc. The clock pulses are derived from the crystal by digital (countdown) techniques to obtain maximum accuracy.

Seismic Disturbances

Seismic sensors were mounted on the air bearing table to determine the frequency and magnitude of disturbances on the table. Figures 6-3 and 6-4 show the results for the table not floated (Figure 6-3) and floated (Figure 6-4). Surprisingly no significant difference in frequency or magnitude can be detected between the floated and non-floated modes in either the azimuth or lateral axes.

The dominate frequencies are 5 cps and .8 Hz about the azimuth axis and .8, 5, and 29 Hz about the lateral axis.

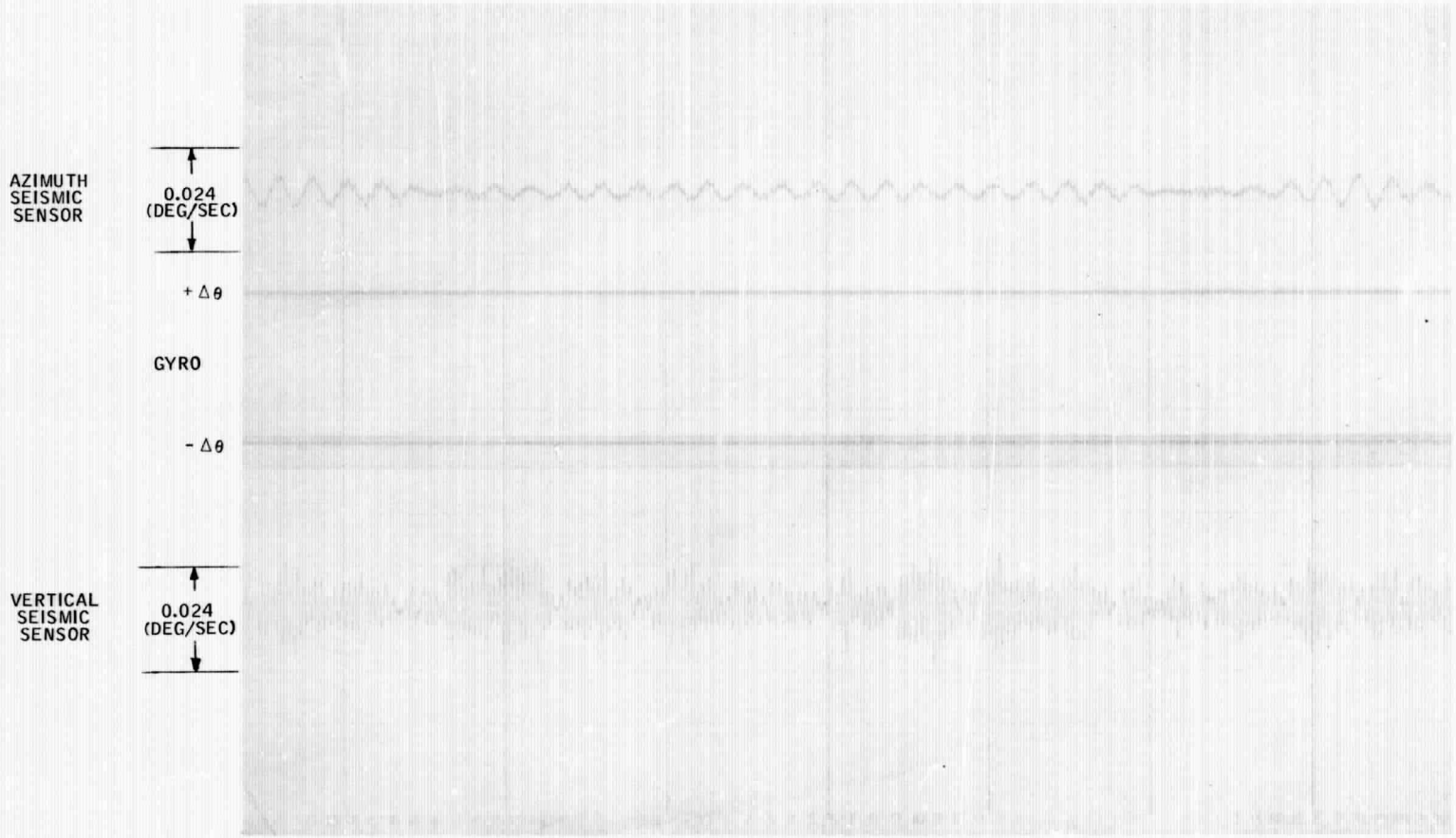

Figure 6-3. Seismic Disturbances - Table Not Floated

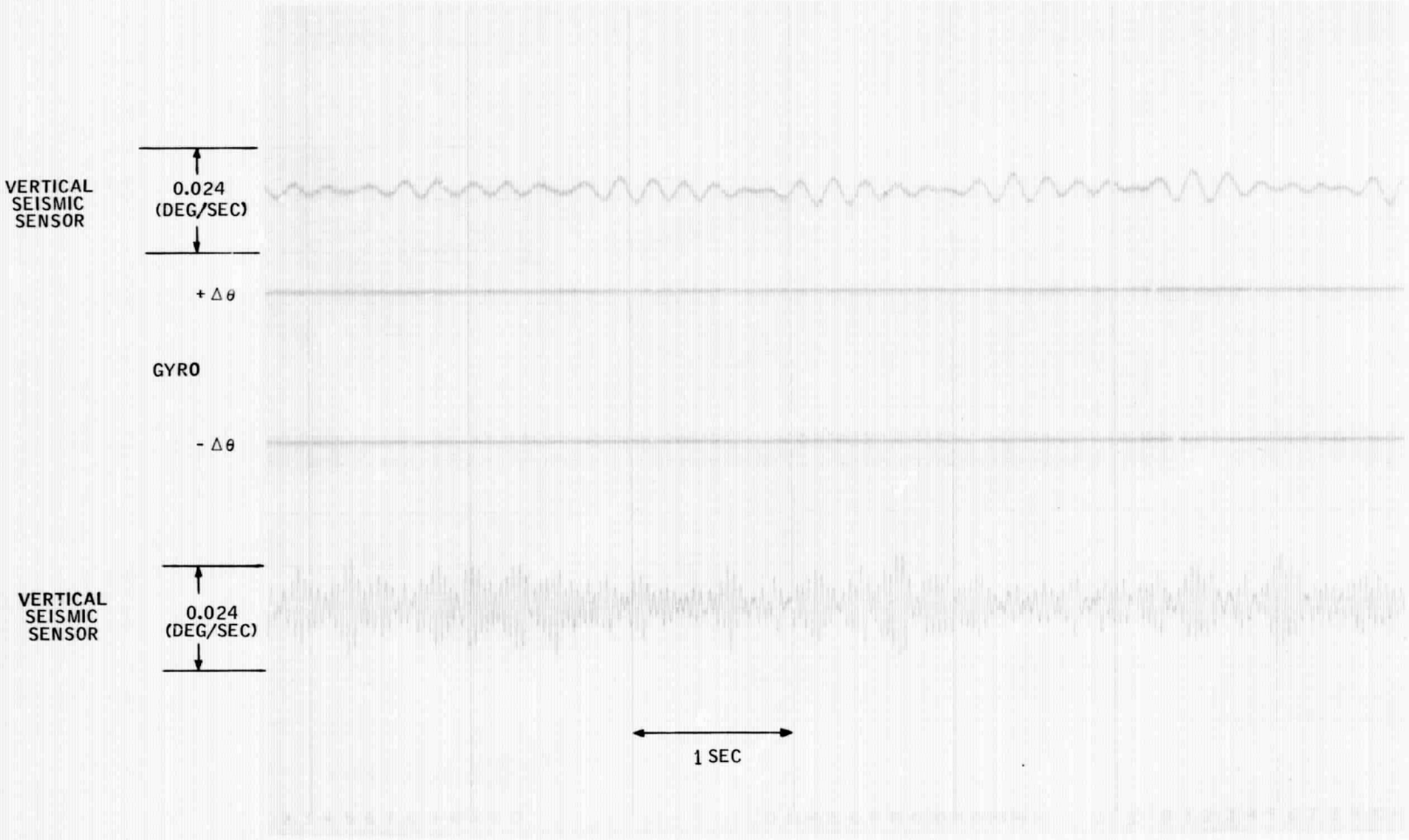

Figure 6-4. Seismic Disturbances - Table Floated

Results

Figures 6-5, 6-6, and 6-7 show representative results from the hardware tests. Figure 6-5 was performed under test sequence a) moving the table off null and returning again. The error was bounded to 23 arc sec which was not satisfactory. The values of Q and N were modified and the tests rerun with sequence b). Figure 6-6 shows the results. The updates were made frequently and the system errors were bounded to approximately 1 arc sec. The filter was slightly modified and the test b) rerun with the updates at longer intervals (60 sec) as shown in Figure 6-7. The system was bounded to 1.5 arc sec which is considered good for the drift and noise present in the gyro.

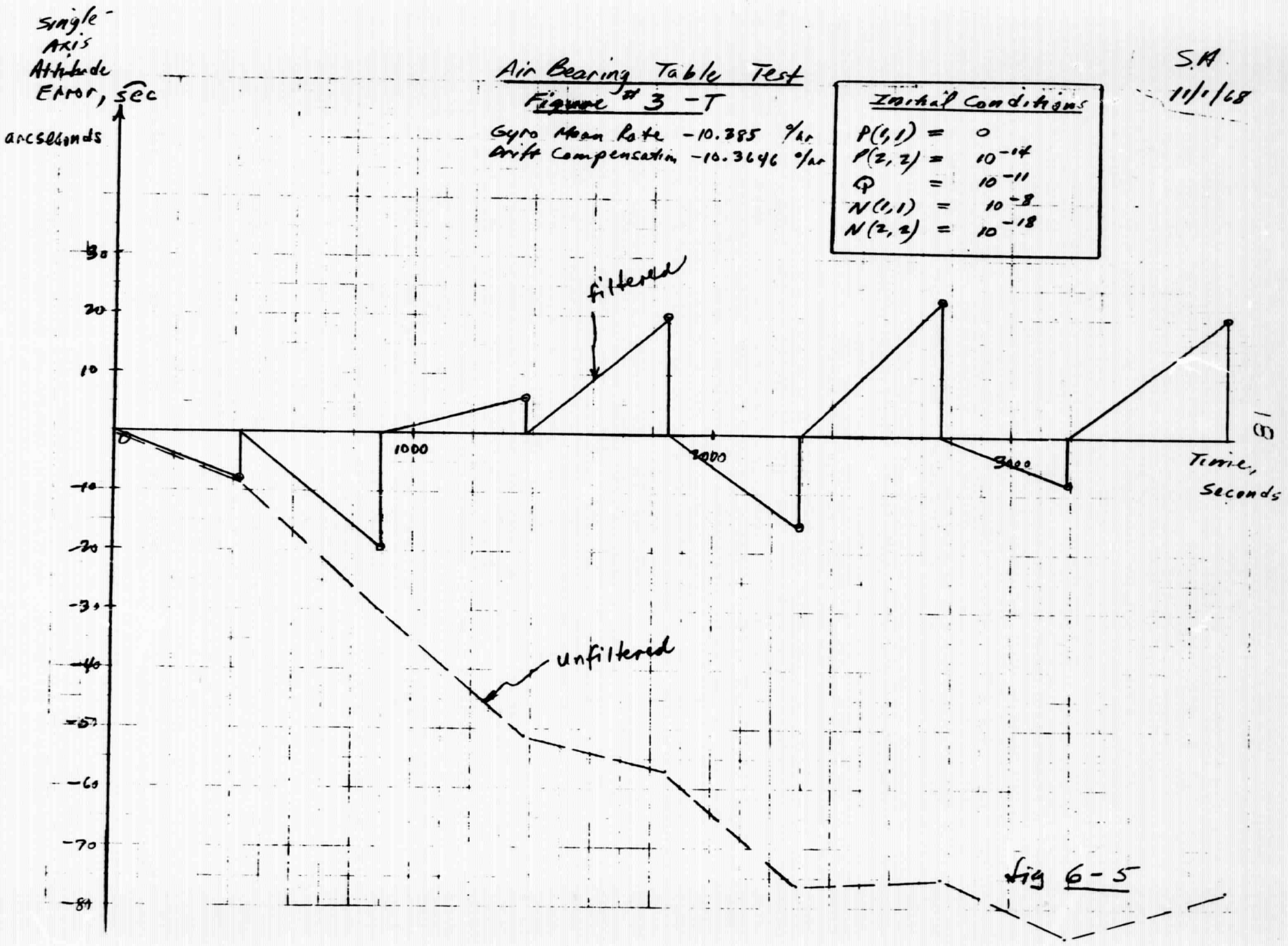
Single-Axis Attitude Error, sec
arcseconds
Air Bearing Table Test
Figure # 3 -T
Gyro Mean Rate -10.385 °/hr
Drift Compensation -10.3646 °/hr
Initial Conditions
P(1,1) = 0
P(2,2) = 10^-14
Φ = 10^-11
N(1,1) = 10^-8
N(2,2) = 10^-18
S.A. 11/1/68
30
20
10
-10
-20
-30
-40
-50
-60
-70
-80
1000
2000
3000
filtered
unfiltered
Time, Seconds
fig 6-5

HPARS

Air Bearing Table Test - Single Axis

Table Locked

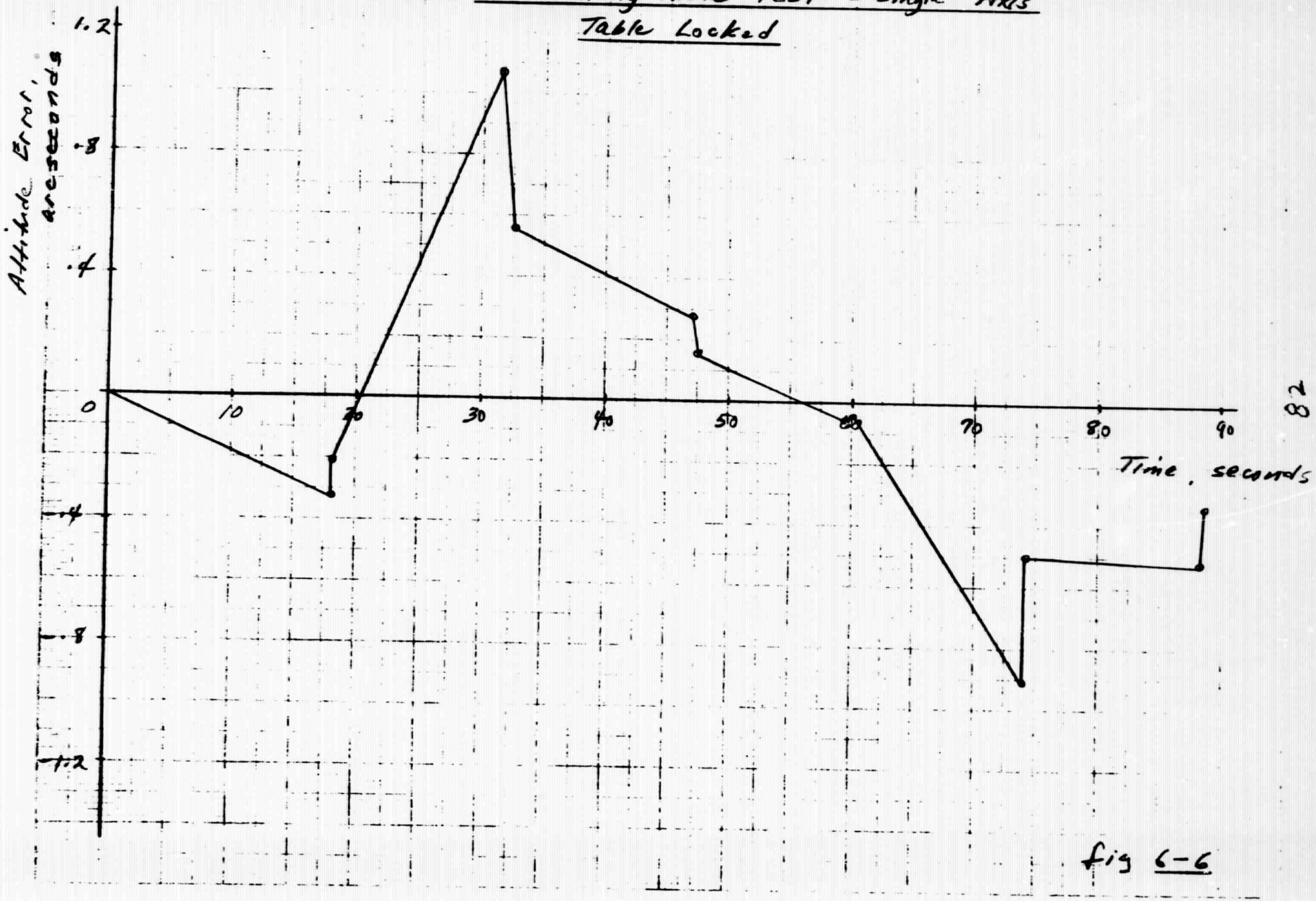

fig 6-6

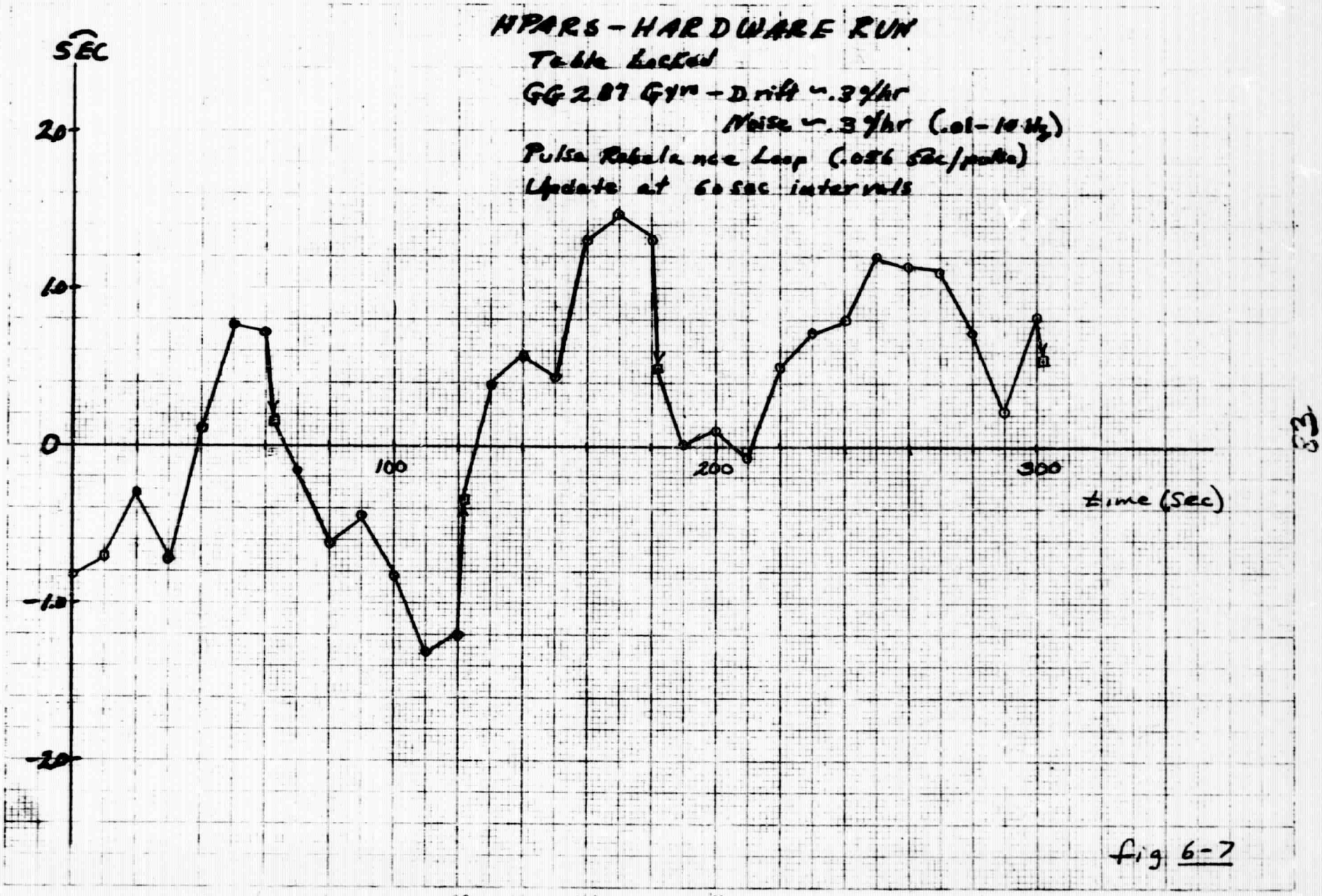
HPARS - HARDWARE RUN
Table Locked
GG 287 Gyro - Drift ~.3°/hr
Noise ~.3°/hr (.01-10 Hz)
Pulse Rebalance Loop (.0256 Sec/pulse)
Update at 60 sec intervals
SEC
20
10
0
-10
-20
100
200
300
time (Sec)

fig 6-7

VII. Recommended Future Work

Figure 7-1 briefly summarizes the recommended follow on work to the HPARS study. The study has proved very useful in getting some real feel and numbers for what can be done. The real work was in setting it up and from this point on the system will be very efficient with regards to performing hardware and parameter tradeoffs toward obtaining high precision attitude reference system concepts and design.

- LONGER RUNS SUCH AS 1 HOUR SHOULD BE MADE TO OBTAIN BETTER DATA ON UPDATE TIME INTERVAL VS. ACCURACY AND MORE DATA ON HARDWARE PARAMETER TRADEOFFS.
- FURTHER OPTIMIZATION OF THE FILTER SHOULD BE INVESTIGATED USING RMS RESULTS IN LIEU OF MAXIMUM ERROR CRITERIA.
- INVESTIGATE A DIFFERENT FILTER STRUCTURE TO REDUCE DYNAMIC ERRORS WHILE THE PLATFORM IS IN MOTION.
- A SMALL GIMBALLESS ESG/STRAPPED DOWN GYRO SYSTEM SHOULD BE SIMULATED TO DETERMINE THE FEASIBILITY OF THIS APPROACH. PERFORM A TRADEOFF OF SYSTEM ACCURACY VS. UPDATE TIME VS. ESG ACCURACY AND DETERMINE THE BEST FORM FOR THE MEASUREMENT ERRORS (E.G., GAUSSIAN, UNIFORMLY DISTRIBUTED, AND CORRELATED ERRORS).
- PERFORM RUNS USING A SMALLER PULSE WEIGHT TO DETERMINE THE POINT WHERE THE PERFORMANCE IS LIMITED BY FACTORS OTHER THAN PULSE WEIGHT.
- THE LASER SIMULATION SHOULD BE RE-RUN USING AN IMPERFECT LASER BASED ON LATEST LASER HARDWARE TEST DATA.

Figure 7-1. Recommended Future Work

APPENDIX A

ESG FOR HPARS

An ESG is a two degree of freedom attitude gyroscope. The attitude sensed by an ESG is usually expressed by the direction cosine coordinates of a unit vector along the gyro spin axis in an inertial reference frame. The orientation of an ESG spin vector with respect to an inertial reference frame is nearly constant, that is, ESG's have low drift in inertial space. What drift they do have is closely described by a mathematical model for gyro drift. The mathematical model contains several imperical constants which are determined by testing the gyro under controlled conditions. The model is then used operationally, often in real time, to partially compensate for the "raw" drift of the gyroscope. The difference between the actual, or raw, gyro drift and that drift generated by the math model is termed the "compensated" drift of the gyro. The operational accuracy of an ESG is a function of its compensated drift.

Since a single ESG has only two degrees of freedom, two of them are needed to provide attitude reference for a three axis system. Two ESG's have four independent axes, of course, and some method of eliminating the "extra" degree of freedom must be provided. When each of the two ESG's has its own gimballing system the extra degree of freedom is usually eliminated in the computer which combines the gyro outputs (typically gimbal angle encoder readings) to produce the three reference axes.

Simulation of the compensated drift of two ESG's in inertial space is accomplished by conceptually considering four ESG spin vectors drifting in inertial

space. Two of the four vectors represent the "true" gyro spin vectors, while the other two vectors represent the math model spin vectors. The two "true" spin vectors are used to simulate the gyro readout, the gimbal angle encoder outputs.

Errors enter the process at two points. One, the math model estimates of gyro spin vector orientations in inertial space differ from the true orientations, and, two, errors are made in computing the spin vector orientations in table coordinates from gimbal angle outputs.

Simulating the above process is straight forward. Two "true" ESG spin vectors are simulated in inertial space, just as the two estimates are simulated, except that instead of using the computed transformation from table coordinates to earth fixed coordinates as input to the process a "true" simulated transformation is used. The true spin vectors are transformed to earth fixed coordinates just as the estimates are, but then the true spin vectors are further transformed to table coordinates, again using the true transformation matrix. Once in table coordinates, the spin vectors are used to simulate gimbal angle outputs, complete with readout errors, and the gimbal outputs are then used to regenerate the spin vectors in table coordinates, but now with the effect of readout errors added. Drift errors show up as the difference between the simulated true spin vectors in inertial space and the estimated spin vectors.

The process diagram given previously is altered only in that the gimbal angle

outputs block is replaced by the more complex diagram below.

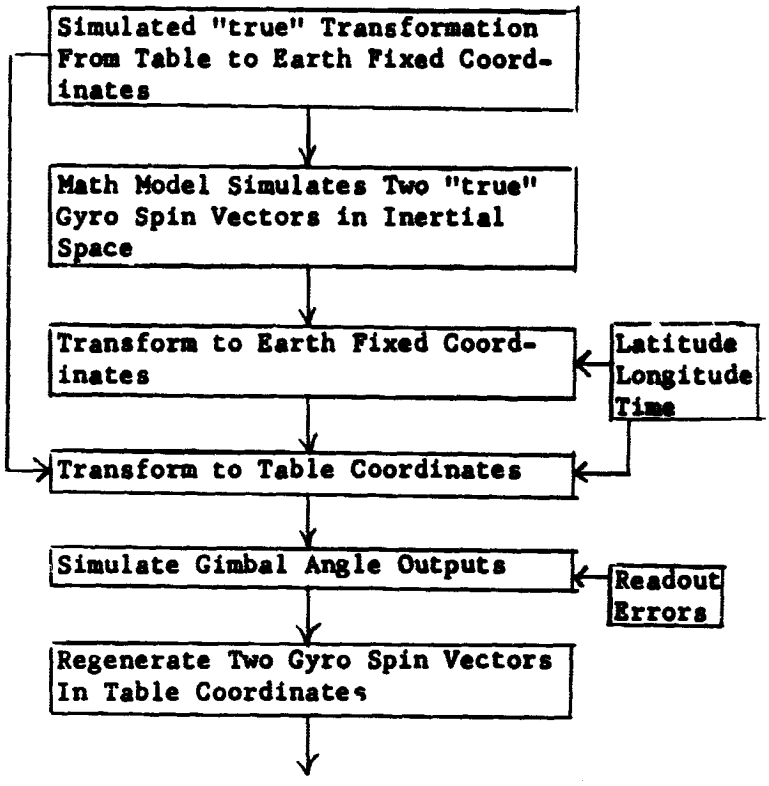

As was discussed previously, four ESG spin vectors must be considered in inertial space to simulate the operation of a two gyro system. Each of the four spin vectors has three components, making twelve "state variables". While there is no interaction between spin vectors in inertial space, all four spin vectors must be updated at the same time, and so all twelve components are regarded as one state vector when solving the differential equations of motion. The same math model, the one given earlier, is used for each of the four spin vectors. Also, all four gyros are assumed to have the same principle moment of inertia value and the same rotor spin speed profile.

Drift

Assume that $\hat{S}$ is a unit vector along the spin axis of an ESG. Let $\hat{F}_x$, $\hat{F}_y$, and $\hat{F}_z$ be an orthonormal triad of vectors conceptually attached to the ESG case. The gimballing arrangement acts to keep $\hat{F}_z$ coincident with $\hat{S}$, and, if $\hat{T}$ is a unit vector (called the train vector) along the outer gimbal or train axis of the gimbal structure, it always happens that

$$\hat{F}_y = \frac{\hat{T} \times \hat{S}}{|\hat{T} \times \hat{S}|}$$

with

$$\hat{F}_x = \hat{F}_y \times \hat{F}_z = \hat{F}_y \times \hat{S}$$

of course. Additionally, let $\hat{G}$ represent a unit vector in the direction of the earth's gravity field, positive downward.

In terms of the above vectors, and in terms of the empirical torque coefficients (μ, ν, γ_{10}, γ_{13}, γ_{20}, γ_{23}) and the gyrotor principle moment about its spin axis, I, and rotor spin speed ω, nominally 500 rps, the drift model may be written as:

$$\begin{aligned} \vec{dS}/dt = 1/(2\pi I\omega) \quad & [\mu + \nu(\omega/500)^2] \quad (\hat{S} \times \hat{G}) \\ & + [\gamma_{10} + \gamma_{13} (\hat{G} \cdot \hat{S})] \hat{F}_x \\ & + [\gamma_{20} + \gamma_{23} (\hat{G} \cdot \hat{S})] F_y \end{aligned}$$

The above equation, even though it is in vector form, is valid only when the derivative is taken in an inertial reference frame. Units are as follows

I: gram centimeters^2

ω: revolutions per second

Torque Coefficients: dyne centimeters

Thus:

Torque coefficient

is a pure number.

Experience shows that actual ESG drift may be "fitted" extremely well by the math model, but predicted less well. That is, the actual gyro drift may be represented at all times by a model of the above form, but the coefficients in the model are subject to change with time. This fact is very useful in simulating ESG operation. A "true" gyro may be drift simulated by using the above model with a set of "true" coefficients, while the compensation process is simulated by the same model with slightly different coefficients. The differences between the coefficients used in the two models are chosen to represent the expected changes in the coefficients from the time of gyro calibration to the time of drift prediction.

More complex models have been used to approximate ESG drift, but the model above contains all of the important terms, especially those which experience has shown to undergo significant change with time.

Rotor spin speed, the parameter in the model, is not constant in time. The gyro rotor slowly runs down from its original value. Even though the rotor contracts very slightly as its spin speed decreases, the principle moment, I, is taken to be constant in the model

The earth's gravity unit vector, $\hat{G}$, varies with time in an inertial frame. Also, the two ESG case fixed unit vectors, $\hat{F}_x$ and $\hat{F}_y$, vary with time, both because $\hat{S}$ itself varies slowly in an inertial frame and because the gimbal

APPENDIX B

DISCRETE KALMAN FILTER EQUATIONS SOLVED

Measured Variable Vector Equation:

$$\bar{y} = \begin{pmatrix} \delta\phi_m \\ \delta\theta_m \\ \delta\psi_m \end{pmatrix} \tag{1}$$

State Variable Vector Equation:

$$\bar{X} = \begin{pmatrix} \delta\phi \\ \delta\theta \\ \delta\psi \\ \delta p_L \\ \delta q_L \\ \delta r_L \end{pmatrix} \tag{2}$$

Measurement Geometry Matrix (M) Equations:

$$\delta\bar{y} = \frac{\partial}{\partial x}(\bar{y})\,\delta\bar{X} \tag{3}$$

or:

$$\delta\bar{y} \equiv M\,\delta\bar{X} \tag{4}$$

where:

$$M = \begin{bmatrix} 1 & 0 & 0 & 0 & 0 & 0 \\ 0 & 1 & 0 & 0 & 0 & 0 \\ 0 & 0 & 1 & 0 & 0 & 0 \end{bmatrix} \tag{5}$$

Transition Matrix (Φ) Equations:

$$\dot{\bar{X}} = A\,\bar{X} \tag{6}$$

where:

$$A \cong \begin{bmatrix} 0 & 0 & (-p s\psi - q c\psi) & (c\psi) & -s\psi & 0 \\ (p s\psi + q c\psi)(\tan\phi \sec\phi) & 0 & (p c\psi - q s\psi)\sec\phi & (s\psi \sec\phi) & c\psi \sec\phi & 0 \\ (q c\psi + p s\psi)(\sec^2\phi) & 0 & (p c\psi - q s\psi)\tan\phi & (s\psi \tan\phi) & c\psi \tan\phi & 1 \\ 0 & 0 & 0 & 0 & 0 & 0 \\ 0 & 0 & 0 & 0 & 0 & 0 \\ 0 & 0 & 0 & 0 & 0 & 0 \end{bmatrix} \tag{7}$$

$$\dot{\Phi} = A\,\Phi \tag{8}$$

$$\Phi(0) = [I] \tag{9}$$

Covariance Matrix (P) Propatation Equation:

$$P(t_k) = \Phi\, P(t_{k-1})\, \Phi^T + N \tag{10}$$

Weighting Matrix (K) Equation:

$$K = P M^T [M P M^T + Q]^{-1} \tag{11}$$

Covariance Matrix (P) Update Equations:

$$P_{new}(t_k) = P_{old}(t_k) - K M P_{old}(t_k) \tag{12}$$

State Vector Update Equation:

$$\bar{X}(t_k) = \bar{X}_{old}(t_k) + K\left[\bar{y}(t_k)\right] \qquad (13)$$

In the above equations, P is a 6 x 6 covariance matrix of state variable errors, Q is a 3 x 3 matrix of mean square measurement variable errors, K is a 6 x 3 matrix, Φ is a 6 x 6 matrix, M is a 3 x 6 matrix, and N is a 6 x 6 matrix. The N matrix (given in equation 10) is a matrix of approximate mean square errors which have been neglected in modeling the system (e.g., computation truncation and roundoff errors, etc.). It is further discussed in references 4, 5, and 6.

In addition to the above equations, the transformation between direction cosines and Euler angles was solved, as well as the inverse transformation from Euler angles to direction cosines. A pitch-roll-yaw rotation sequence was arbitrarily assumed for the transformations.